Fate of Para-Toluenesulfonamide (p-TSA) during Drinking Water Treatment and In-Situ Enhanced Remediation: Column Experiments, Field Study and Numerical Modelling

A dissertation

Submitted in Partial Fulfilment of the

Requirements for the degree of Doctor Rerum Naturalium

to the Department of Geosciences

of the Freie Universität Berlin

by

Raffaella Meffe

Berlin, January 2011

Supervisor: PD. Dr. Claus Kohfahl

Second examiner: Prof. Dr. Gudrun Massmann

Date of the viva voce/defense: 03.03.2011

Preface

The present study has been carried out in the framework of a cooperation between the Freie Universität of Berlin and the Berliner Wasserbetriebe (BWB). Financial support was provided by the University of Rome "La Sapienza", the Deutscher Akademischer Austauch Dienst (DAAD), the Freie Universität of Berlin and the BWB.

The research activities described in this thesis incorporate the following contributions from scientists, technicians and students:

- Data used in the simulations discussed in chapter 2 were produced by Dr. Doreen Richter as part of her Ph.D. work.
- The column experiment described in chapter 3 was designed by Prof. Dr. Gudrun Massmann and by Dr. Thomas Taute. The experimental set up was carried out by the technicians of the Freie Universität of Berlin.
- The column tracer experiment (chapter 3) was conducted with the help of Stephanie Warbein, diploma student at the Freie Universität of Berlin.
- Groundwater analyses were performed by the BWB and by the analytical laboratory of the Freie Universität of Berlin.
- Hydraulic data were provided by the BWB.
- A large fraction of the groundwater samples were collected by the technicians of the Fugro Consult GmbH and of the BWB.
- Flow model used for transport simulation in chapter 4 was developed by Dr. Enrico Hamann as part of his Ph.D. work.

This work was partly published in:

1. Chapter 2: Meffe, R., Kohfahl, C., Holzbecher, E., Massmann, G., Richter, D., Dünnbier, U., Pekdeger, A., 2010. *Modelling the removal of para-toluenesulfonamide (p-TSA) during rapid sand filtration used for drinking water treatment.* Water Research 44 (1), 205-213.
2. Chapter 3: Meffe, R., Massmann, G., Kohfahl, C., Taute, T., Richter, D., Dünnbier, U., Pekdeger, A. *Investigating the redox sensitivity of para-toluenesulfonamide (p-TSA) with a column study*. Environmental Earth Sciences.DOI: http://dx.doi.org/10.1007/s12665-011-1130-9.

3. Chapter 4: Meffe, R., Kohfahl, C., Hamann, E., Massmann, G., Dünnbier, U., Pekdeger, A. *Fate of para-toluenesulfonamide (p-TSA) in groundwater under anoxic conditions: Modelling results from a field site in Berlin (Germany).* Submitted to Science of the Total Environment.

I have been responsible for the development and the writing of the studies reported in these publications. Co-authors have played an advisory and supervisory role.

Summary

The industrial micropollutant para-toluenesulfonamide (p-TSA) has several applications. It is applied as plasticizer, as intermediate for pesticides and as fungicide in paints and coatings. p-TSA is also the primary degradation product of the common disinfectant Chloramine-T. Therefore, p-TSA has several potential sources in wastewater and can represent a serious problem in partly closed water cycles where groundwater is used for drinking water production. p-TSA was found to be ubiquitous in the Berlin wastewater, sewage water and groundwater. The highest concentrations (up to 30 μg L^{-1}) were encountered in the groundwater of the catchment area of a drinking water treatment plant (DWTP). The toxicity of p-TSA can be considered as moderate since it is toxic to algae but not to fishes and daphinids; however, dedicated tests are advised if in the future larger amounts of p-TSA are used in consumer products. Following the guidelines of the German Federal Environmental Protection Agency (UBA), the concentration limit for p-TSA in drinking water is 0.3 μg L^{-1}. Such a concentration is around 100 times lower than the maximum concentrations encountered in Berlin's groundwater. Motivated by the occurrence of high p-TSA concentrations in the groundwater used for drinking water production, a series of intensive investigations of the distribution and behaviour of p-TSA in different aquatic compartments started a few years ago. The present study is a continuation of these investigations and aims at providing further knowledge on several aspects of the contamination by p-TSA that are still not well understood.

Chapter 1 is a general introduction to the problem of groundwater contamination by sewage farms.

Chapter 2 documents a numerical modelling study using the finite element method to determine p-TSA degradation rate constants during rapid sand filtration. Data used for simulations were obtained by a previous column experiment carried out in the filter hall of the DWTP of Friedrichshagen. During the experiment, aerated abstracted groundwater was infiltrated through the column applying different infiltrations rates (from 2 to 6 m h^{-1}). Experimental breakthrough curves and depth profiles were modeled with the software Comsol Multiphysics 3.3. p-TSA degradation was simulated with first-order kinetics and Michaelis Menten kinetics. Simulation results showed that p-TSA was readily removed

during drinking water treatments. Degradation rate constants were temporally variant probably due to the adaption of microbes to the changes of infiltration rates. Higher degradation rate constants were observed close to the column inlet where probably a higher microbial activity could develop. Degradation rate were generally very high probably because the filter material had been in contact with the raw groundwater for decades and an adapted microbiology had developed.

Chapter 3 reports a laboratory column experiment using aquifer material and groundwater from the field site that was performed to investigate the potential removal of p-TSA by applying injection of oxygen. Initially, the column was operated under completely anoxic conditions. Successively, oxic conditions were simulated by adding compressed air to the experimental system. Results revealed that p-TSA was not removed under anoxic conditions, whereas it was fully removed under oxic conditions. The experimental results were modeled through a one dimensional reactive transport model that was set up using the Comsol Multiphysics 3.3 software. p-TSA degradation was simulated with first-order kinetics and the obtained degradation rate constants were 3 to 4 orders of magnitude lower than those obtained during rapid sand filtration. Experimental results clearly displayed that air or O_2 injections in the aquifer can be a successful strategy for p-TSA remediation.

Chapter 4 describes a field study investigating the distribution and persistence of p-TSA under natural aquifer conditions. p-TSA is considered not to be geochemically retarded and under anoxic conditions it should behave conservatively. To refine the current knowledge of p-TSA transport and degradation at the field scale, measurements of p-TSA and major ions were performed from the Berlin Water Company (BWB) at nine locations between 2005 and 2010. The measurements showed that p-TSA is retarded in the same manner as chloride (Cl^-) indicating hydraulic retardation due to low permeability layers where groundwater is immobile. To verify the non-reactive transport of p-TSA under field conditions, a vertical 2D transport model was set up with PMWIN 8, using the modules Modflow and MT3DMS. The immobile domains were considered applying the dual-domain mass transfer approach. The measured data for p-TSA and Cl^- concentrations were successfully reproduced, supporting the hypothesis that both compounds behave conservatively but that at the field site they are hydraulically retarded. Prognostic simulations with the calibrated 2D transport model revealed that without any remediation

measures the groundwater quality near the drinking well galleries will be affected by high p-TSA loads for more than a hundred years.

In chapter 5, the interpretation of available data concerning the effects of air/oxygen injections on p-TSA removal at the field site is provided. Injections of air and oxygen into the aquifer were performed by the Fugro Consult GmbH on behalf of the BWB. The injections aimed to develop a migration barrier for the ammonium contamination plume to remediate groundwater before arriving at the abstraction well galleries. As demonstrated in the previous chapters, the injections could be a suitable strategy also for the removal of p-TSA. The injections were performed by six injection tubes installed in a line perpendicular to the main groundwater flow direction. To sufficiently supply the aquifer with oxygen, injections were carried out at different depths. The groundwater quality was monitored using a series of monitoring wells located between and downgradient of the injection tubes. Data obtained during three years of active application of the remediation measure were analysed by giving particular attention to the effects of the injections on p-TSA and ammonium concentrations. p-TSA and ammonium appeared to behave similarly, indicating removal only in few monitoring wells. However, both substances were not degraded at the majority of the monitoring wells even under oxic conditions. This phenomenon may be related to antiseptic conditions as a result of elevated oxygen concentrations. A list of further potential reasons for the unsuccessful application of the remediation measure was given and some improvements of the system were suggested. For the interpretation of the p-TSA and ammonium field data, a one-dimensional reactive transport model was set up using the computer code PHREEQC-2. The model considers p-TSA degradation, nitrification, denitrification, pyrite oxidation and organic matter degradation. The resulting disagreements between measured and simulated data are mainly attributed to (i) three-dimensional effects controlling the oxygen distribution, (ii) transient flow conditions and (iii) reduced microbial activity associated with high oxygen concentrations not considered in the model.

Zusammenfassung

Die Verbindung para-Toluensulfonsäureamid (p-TSA) ist ein in der Industrie anfallender Spurenschadstoff mit verschiedenen Einsatzgebieten. P-TSA wird als Weichmacher, als Zwischenprodukt in der Pestizidherstellung, wie auch als Fungizid in Anstrichen und Farben verwendet. P-TSA ist zudem ein Hauptabbauprodukt des Desinfektionsmittels Chloramin-T. Demzufolge gelangt p-TSA aus mehreren Quellen in das Abwasser und kann in teilweise geschlossenen Wasserkreisläufen, insbesondere dort, wo Grundwasser zur Trinkwassergewinnung verwendet wird, ein ernsthaftes Problem darstellen. Es konnte festgestellt werden, dass p-TSA im Berliner Abwasser, Oberflächenwasser und Grundwasser ubiquitär auftritt. Die höchsten Konzentrationen (bis 30 µg L^{-1}) wurden im Grundwasser des Einzugsgebietes eines Wasserwerkes nachgewiesen. Bezüglich der Toxizität wird p-TSA als moderat eingestuft, da es auf Algen eine toxische Wirkung hat, jedoch nicht auf Fische und Daphnien; es sollten jedoch weitere geeignete Tests durchgeführt werden, falls in Zukunft größere Menge von p-TSA in Verbrauchsgütern verwendet werden. Nach den Leitlinien des deutschen Umweltbundesamtes (UBA) beträgt der Grenzwert für p-TSA im Trinkwasser 0,3 µg L^{-1}, und ist somit 100-mal niedriger als die maximale, im Berliner Grundwasser nachgewiesene Konzentration.

Aufgrund des Auftretens hoher p-TSA-Konzentrationen im Grundwasser, das auch zur Trinkwassergewinnung genutzt wird, begannen vor einigen Jahren eine Reihe intensiver Untersuchungen über die Verteilung und das Verhalten von p-TSA in verschiedenen aquatischen Kompartimenten.

Die vorliegende Studie ist eine Fortsetzung dieser Untersuchungen mit dem Ziel weitere Kenntnisse über die verschiedenen Aspekte der Kontamination von p-TSA zu liefern, die bisher kaum verstanden werden.

Kapitel 1 ist eine allgemeine Einführung in das Problem der Kontamination des Grundwassers durch die Rieselfeldbewirtschaftung.

Kapitel 2 dokumentiert eine numerische Modellierungsstudie unter Anwendung der Finite-Elemente-Methode, um p-TSA Abbauraten bei der Schnellsandfiltration zu bestimmen. Die für die Simulationen verwendeten Daten stammen aus einem vorangegangenen Säulenexperiment, das in der Filterhalle des Wasserwerks Friedrichshagen durchgeführt

wurde. Der Versuchsfilter wurde mit belüftetem Rohwasser unter Einsatz verschiedener Filtrationsgeschwindigkeiten (von 2 bis 6 m h^{-1}) betrieben. Experimentelle Durchbruchskurven und Tiefenprofile wurden mit der Software COMSOL Multiphysics 3.3 modelliert. Der p-TSA Abbau wurde mit einer Kinetik 1. Ordnung und der Michaelis Menten Kinetik simuliert. Die Ergebnisse der Simulation zeigen, dass p-TSA während der Trinkwasseraufbereitung abgebaut wird.

Die Abbaukonstanten variieren zeitlich, was wahrscheinlich auf die Anpassung der Mikroorganismen an die Veränderung der Filtrationsgeschwindigkeit zurückzuführen ist. Höhere Abbaukonstanten wurden im Bereich des Säulenzulaufes beobachtet, wo sich vermutlich eine höhere mikrobielle Aktivität entwickeln konnte.

Die Abbauraten waren im Allgemeinen sehr hoch. Dies lässt sich möglicherweise dadurch begründen, dass das verwendete Filtermaterial seit Jahrzehnten in Kontakt mit dem Rohwasser steht und sich dementsprechend eine angepasste Mikrobiologie entwickeln konnte.

Kapitel 3 beschreibt ein Säulenexperiment im Labormaßstab, bei dem mit Aquifermaterial und Grundwasser aus dem Untersuchungsgebiet gearbeitet wurde. Das Ziel der Untersuchung war die Ermittlung eines möglichen Abbaus von p-TSA durch die Injektion von Sauerstoff. Zu Beginn wurde die Säule unter vollständig anoxischen Bedingungen betrieben. Sukzessiv wurden oxische Bedingungen simuliert, indem dem System Druckluft zugeführt wurde.

Die Ergebnisse zeigen, dass p-TSA nicht unter anoxischen Bedingungen entfernt wird, wohingegen es unter oxischen Bedingungen vollständig abgebaut wird.

Die experimentell ermittelten Ergebnisse wurden mit einem eindimensionalen, reaktiven Transportmodell modelliert, welches mithilfe der COMSOL Multiphysics 3.3 Software aufgebaut wurde.

Der Abbau von p-TSA wurde mit einer Kinetik 1. Ordnung simuliert. Die daraus ermittelten Abbauratenkonstanten lagen drei bis vier Größenordnungen unter den Werten, die für die Schnellsandfiltration bestimmt wurden.

Die Ergebnisse des Experiments zeigen eindeutig, dass die Injektion von Luft oder Sauerstoff in den Grundwasserleiter eine erfolgreiche Strategie zur p-TSA Sanierung darstellen kann.

Kapitel 4 beschreibt eine Feldstudie zur Ausbreitung und Persistenz von p-TSA unter natürlichen Bedingungen im Grundwasserleiter. Es ist anzunehmen, dass p-TSA

geochemisch nicht retardiert wird und sich unter anoxischen Bedingungen konservativ verhält. Um den jetzigen Kenntnisstand zum Transport und Abbau von p-TSA auf Feldskala zu erweitern, wurden von der Berliner Wasserbetriebe (BWB) zwischen 2005 und 2010 an neun Standorten durchgeführte Messungen von p-TSA und den wichtigsten Ionen im Rahmen dieser Arbeit ausgewertet. Die Messergebnisse zeigen, dass p-TSA in der gleichen Weise wie Chlorid (Cl^-) retardiert wird. Dies deutet auf eine hydraulische Verzögerung hin, die durch schlecht durchlässige Schichten verursacht wird, in denen das Grundwasser immobil ist. Zur Verifizierung des nicht-reaktiven Transportes von p-TSA unter Feldbedingungen wurde mit PMWIN 8 anhand der Module MODFLOW und MT3DMS, ein vertikales 2D-Modell aufgebaut. Die immobilen Bereiche wurden mithilfe des Dual-Domain-Ansatzes berücksichtigt. Die gemessenen Werte der p-TSA und Cl^--Konzentrationen konnten erfolgreich reproduziert werden und unterstützen somit die Hypothese, dass sich beide Substanzen konservativ verhalten, im Untersuchungsgebiet jedoch hydraulisch retardiert werden. Prognostische Simulationen mit dem kalibrierten 2D-Modell zeigen, dass ohne Sanierungsmaßnahmen die Grundwasserqualität in der Nähe der Trinkwasserbrunnengalerien durch hohe p-TSA Frachten für über hundert Jahren beeinträchtigt wird.

Kapitel 5 interpretiert die bereits vorliegenden Daten zu Auswirkungen der Luft/Sauerstoff-Injektionen auf den p-TSA Abbau im Untersuchungsgebiet. Die Injektionen von Luft und Sauerstoff in den Grundwasserleiter wurden von der Fugro Consult GmbH im Auftrag der BWB durchgeführt, mit dem Ziel, eine Migrationsbarriere für die Schadstofffahnen des Ammonium zu entwickeln, um das Grundwasser vor dem Erreichen der Fördergalerien zu sanieren.. Wie in den vorangegangenen Kapiteln gezeigt wurde, könnten die Injektionen auch eine geeignete Strategie für die Entfernung von p-TSA darstellen. Die Injektionen wurden über sechs Injektionslanzen durchgeführt, die in einer Linie senkrecht zur Hauptfließrichtung des Grundwassers installiert wurden. Um eine ausreichende Versorgung des Grundwasserleiters mit Sauerstoff sicherzustellen, wurden die Injektionen in unterschiedlichen Tiefen durchgeführt.
Die Qualität des Grundwassers wird mithilfe mehrerer Messstellen kontrolliert, die sowohl zwischen den Injektionslanzen als auch in deren Abstrom installiert wurden. Die Daten, die in den drei Jahren der aktiven Anwendung der Sanierungsmaßnahme erhoben wurden, wurden mit besonderem Augenmerk auf die Auswirkungen der Injektionen auf die p-TSA- und Ammonium-Konzentrationen analysiert. p-TSA und Ammonium verhalten sich

ähnlich und deuten auf einen Abbau in nur wenigen Messstellen hin. Allerdings wurden beide Substanzen bei der Mehrzahl der Messstellen auch unter oxischen Bedingungen nicht abgebaut. Dieses Phänomen könnte eventuell auf das Vorliegen antiseptischer Bedingungen in Folge erhöhter Sauerstoff-Konzentrationen zurückzuführen sein. Eine Reihe weiterer potentieller Gründe für die erfolglose Anwendung der Sanierungsmaßnahme wird gegeben und einige Verbesserungen des Systems werden vorgeschlagen. Zur Interpretation der Messergebnisse des p-TSA-und Ammonium-Abbaus wurde ein eindimensionales reaktives Transportmodell mithilfe des Computer-Codes PHREEQC-2 erstellt. Das Modell berücksichtigt sowohl den p-TSA Abbau, als auch Nitrifikation, Denitrifikation, Pyritoxidation und den Abbau organischer Substanz. Resultierende Unstimmigkeiten zwischen den gemessenen und den simulierten Daten sind hauptsächlich zurückzuführen auf (i) dreidimensionale Effekte, die die Sauerstoff-Verteilung bestimmen, (ii) instationäre Strömungsverhältnisse und (iii) eine reduzierte mikrobielle Aktivität, die im Zusammenhang mit hohen Sauerstoffkonzentrationen steht, welche keine Berücksichtigung im Modell findet.

Table of Contents

1 Introduction

1.1 Groundwater Contamination by Sewage Farm Operation

During the last century, the irrigation of untreated wastewater directly into the soil has been a common practise worldwide (Hoffmann, 1999). Wastewater irrigation may cause changes in soil properties and accumulation of organic and inorganic contaminants (Blume et al., 1980) which may be mobilized towards groundwater (Hoffmann, 1999). Recent studies point to the occurrence of several organic contaminants in the soil and in groundwater below or downgradient of former sewage farms (Grunewald, 1994; Beckmann and Grunewald, 1995a; Abdel-Shafy et al., 2008). The presence of organic pollutants in groundwater is of particular concern when groundwater is used for drinking water production. In this context, the understanding of the fate, distribution and behaviour of the target compound is essential for a proper groundwater management.

Redox processes in groundwater play a crucial role in the fate and distribution of a large number of major organic pollutants (Bouwer and Zehnder, 1993). Most organic contaminants can be considered as electron donors since they can undergo oxidation as a result of microbial metabolism. Some of the breakdown intermediates may be assimilated as a carbon source for microbial growth. Functional groups (e.g. $–NH_2$, $-NO_2$ and $–SO_3$) may be used as nutrients or cleaved from the carbon skeleton when the compound is reduced or oxidized (Bouwer and Zehnder, 1993). Redox reactions can also occur inorganically, but many of them only proceed at significant rates when the reactions are microbially catalyzed (e.g. Appello and Postma, 1996). Recently, several organic pollutants have been shown to be redox sensitive, including pharmaceutically active substances (Massmann et al., 2006; Heberer et al., 2008; Massmann et al, 2008), pesticides (Tuxen et al., 2006), disinfection by-products (Pavelic et al., 2005; Reineke et al., 2008) and halogenated organic compounds (Bosma et al., 2006; Grünheid et al., 2005). Therefore, the redox conditions have to be considered as one of the key environmental variables of degradation processes affecting organic pollutants in groundwater.

Routine treatments at the drinking water treatment plants consist in aeration followed by coagulation and flocculation, sedimentation, rapid sand filtration and disinfection (EPA,

2000). These processes are usually sufficient to ensure high drinking water quality. However, especially when contaminated groundwater affects the catchment area of a drinking water treatment plant, in situ remediation activities should be considered. These technologies involve the introduction of appropriate nutrients and electron donors and/or acceptors into contaminated aquifers to stimulate microbial activity creating more favourable redox conditions. In situ air sparging (IAS) is among the more popular ones (Johnson et al., 2001). It consists of air or oxygen (O_2) gas injections to remove immiscible contaminants through volatilization or dissolved contaminants through enhanced biodegradation. IAS systems can be applied to eliminate contamination sources, to degrade dissolved contaminant plumes or to create a migration barrier for the displacement of the contamination plumes in the aquifer (Johnson et al., 2001). IAS, which was originally developed in Germany in 1985, has been applied successfully at several field sites for removal of petroleum hydrocarbon and chlorinated compounds (Bass et al., 2000). However, this technique involves processes which are so far not fully under control and therefore it often occurs that an IAS system fails to fulfill the expectations (Aivalioti et al., 2008).

1.2 Numerical Modelling

Numerical modelling has been proved to be a valuable tool in analysing physical and chemical processes controlling the geochemistry of the groundwater (Miotlinsky, 2008). The interpretation of data collected at the field site is often obscured by the intricate interaction of several physical and chemical phenomena. Reactive transport models can therefore provide an insight in the understanding of complex environmental systems. Several modelling approaches have been applied to describe microbial degradation processes of organic contaminants. The simplest approach neglects kinetics induced by microbial activity and assumes instantaneous chemical equilibrium (Borden et al., 1986; Marquis, 1994). This method considers that biochemical reactions are fast compared to the transport timescale. In other models, the microbial degradation is simulated by first-order kinetics in which the only factor affecting the degradation is the concentration of the substrate (Knudsen et al., 2000). Through the application of the first-order kinetics the dependency of the reaction rate between the organic compound and any other chemical or microbial population is neglected. As the concentration of the substrate increases, the

degradation rate does not increase indefinitely but rather reaches a maximum value. This behaviour is described by the Michaelis Menten kinetics which is used to model enzyme-substrate reactions (Park et al., 2001; Sato et al., 2002). Michaelis Menten kinetics can be extended to account for inhibition of the degradation operated by other organic or inorganic species. Finally, more elaborated models have been developed to account for microbial dynamics. Microbial growth and decay rate of a degrader population can be modelled by using a Monod-type kinetics (Höhener et al., 2006; Kim and Jaffe, 2008).

Gas-water mass transfer and transport of dissolved gas in saturated porous media are fundamental processes during IAS system application. Modelling approaches are frequently applied to obtain a deeper insight into the process of gas exchange between entrapped air bubbles and surrounding groundwater. The first models to be developed assumed a constant gas volume with equilibrium between gas and aqueous phase (Fry et al., 1997). Successively, this modelling approach was upgraded by introducing a kinetic term (Donaldson et al., 1998; Vulava et al., 2002). More recently, a kinetic approach considering changes in gas-phase composition, compound-specific transfer kinetics and changes in gas saturation during the transport of dissolved volatile compounds has been developed (Holocher et al., 2003; Balcke et al., 2007). However the complex interplay between gas dissolution, microbial O_2 uptake, groundwater flow and gas accumulation in the subsurface remains not fully understood and field operations are still largely carried out on empirical basis (Oswald et al., 2008). Most of the models integrated to the application of an IAS system deal with transport of dissolved gas without considering the transport of the gas-phase. Neglecting advective gas transport can have serious implications under certain conditions and more efforts are needed to include the gas spreading in the subsurface during injections.

1.3 Previous Studies at the Field Site

The study site is located north of Lake Müggelsee, in the eastern part of Berlin. The Münchehofe sewage farm (SF) is placed at about 3 km north of the lake and upgradient of the Friedrichshagen drinking water treatment plant (DWTP) (Fig. 3.2). For almost 70 years, untreated wastewaters were discharged on the irrigation fields of the Münchehofe SF. Due to the wastewater irrigation, the groundwater downgradient of the SF is

significantly contaminated by anthropogenic compounds (Heberer, 1995; Schenk, 1995; Heberer and Stan, 1997).

Since 1992, periodic geochemical and hydraulic monitoring has been performed by Fugro Consult GmbH and the Berlin Water Company (BWB). The monitoring aims are (i) to study the evolution of the contamination plume (ii) to optimize the pumping rate at the abstraction gallery of the DWTP, in order to avoid the abstraction of contaminated groundwater.

Due to the significant anthropogenic contamination of the groundwater in the catchment area of the Friedrichshagen DWTP, the development of a decontamination concept became necessary. To ensure high drinking water quality, part of the abstracted groundwater is currently pumped into a wastewater treatment plant (WWTP) where it is being treated. In addition, in situ groundwater decontamination studies were carried out with the support of the German Federal Ministry of Education and Research (Bundesministerium für Bildung und Forschung). The research project NIDESI ("Entwicklung eines gekoppelten Nitrifikations-/Denitrifikations-Verfahrens zur in situ Reinigung stark stickstoffbelasteter Grundwasserleiter", Ehbrecht and Luckner, 2000) and BIOXWAND ("Entwicklung und Erprobung einer Bio-Oxidationswand im Abstrom eines hoch mit Ammonium kontaminierten Grundwasserleiters", Ehbrecht and Luckner, 2004) were conceived for the development of an in situ oxidation barrier for the displacement of the ammonium (NH_4^+) contaminantion plume. NH_4^+ was one of the anthropogenic contaminants present at the field site in high concentrations. The operation of the oxidation barrier was also supported by numerical reactive transport simulations forecasting decontamination times (Horner et al., 2009). The evolution of the NH_4^+ contamination plume has also been studied using numerical transport models without considering in situ remediations (BWB, 2000; Hamann, 2009).

Analysis of organic pollutants carried out by the BWB in 2003 revealed the occurrence of three sulfonamides, identified as para-toluenesulfonamide (p-TSA), ortho-toluenesulfonamide (o-TSA) and benzenesulfonamide (BSA). These results triggered intensive studies of the behaviour of these three compounds in the Berlin water cycle.

1.4 Aims of the Study

The purpose of this study is to refine the current understanding of the behaviour of p-TSA under natural field conditions, during drinking water treatments and in situ remediation activities. Therefore, the fate of p-TSA was studied at laboratory- and field scale and results were interpreted based on different numerical modelling approaches.

The following specific issues were addressed by the present study:

1. What is the range of values of p-TSA degradation rate constants during drinking water treatments?

2. How do p-TSA degradation rate constants depend on the infiltration rates and microbial activity during drinking water treatments?

3. How can p-TSA drinking water treatments, through rapid sand filtration, be improved?

4. What is the fate of p-TSA under natural anoxic aquifer conditions?

5. Is p-TSA degradation properly enhanced by in situ O_2 injection and which are the determining processes for optimized remediation?

2 Modelling the Removal of p-TSA (para-toluenesulfonamide) during Rapid Sand Filtration used for Drinking Water Treatment

A finite element model was set up to determine degradation rate constants for p-TSA during rapid sand filtration (RSF). Data used for the model originated from a column experiment carried out in the filter hall of a drinking water treatment plant in Berlin (Germany). Aerated abstracted groundwater was passed through a 1.6 m long column-shaped experimental sand filter applying infiltration rates from 2-6 m h^{-1}. Model results were fitted to measured profiles and breakthrough curves of p-TSA for different infiltration rates using both first-order reaction kinetics and Michaelis Menten kinetics. Both approaches showed that degradation rates varied both in space and time. Higher degradation rates were observed in the upper part of the column, probably related to higher microbial activity in this zone. Measured and simulated breakthrough curves revealed an adaption phase with lower degradation rates after infiltration rates were changed, followed by an adapted phase with more elevated degradation rates. Irrespective of the mathematical approach and the infiltration rate, degradation rates were very high, probably owing to the fact that filter sands have been in operation for decades, receiving high p-TSA concentrations with the raw water.

R. Meffe, C. Kohfahl, E. Holzbecher, G. Massmann, D. Richter, U. Dünnbier, A. Pekdeger *Modelling the removal of para-toluenesulfonamide (p-TSA) during rapid sand filtration used for drinking water treatment.* Water Research 44 (1), 205-213, 2010.

http://dx.doi.org/10.1016/j.watres.2009.08.046

2.1 Introduction

The occurrence, fate and potential harms of organic pollutants in the aquatic environment have been an object of growing interest in recent years, as shown by the increasing number of studies in this field (Heberer, 2002a,b; Yu et al., 2006; Kim et al., 2007; Loos et al., 2007). The presence of organic pollutants in groundwater is of particular concern where the groundwater is used for drinking water production. The principal source of organic micropollutants in the aquatic environment is municipal wastewater, which is generally treated in wastewater treatment plants (WWTPs) before being discharged into surface water (Daughton and Ternes, 1999). In the past, untreated wastewater was often also irrigated on sewage irrigation farms, causing a significant anthropogenic contamination of the surrounding environment (Grunewald, 1994; Heberer and Stan, 1994; Beckmann and Grunewald, 1995a; Beckmann and Grunewald, 1995b; Abdel-Shafy et al., 2008). Various studies showed that residues of some organic pollutants from human and animal use are not fully eliminated during wastewater treatment and can be found in the aquatic environment (Heberer, 2002a; Heberer 2002b; Derksen et al., 2004). Wastewater-bound, poorly degradable compounds may enter the raw water for drinking water production via bank filtration, or the catchment area of a drinking water treatment plant (DWTP) may receive groundwater affected by former sewage irrigation.

The organic pollutant discussed in the following (para-toluenesulfonamide, p-TSA) originates from wastewater. It is applied as a plasticizer, an intermediate for pesticides and drugs, and is the primary degradation product of the common disinfectant Chloramine-T in water. Chloramine-T is used as an antimicrobial agent in the food industry to disinfect surfaces, instruments and machinery. This substance is also used as a therapeutic drug for bacterial gill diseases of fish species and for bacterial diseases of swine and poultry (Beljaars et al., 1994; Meinertz et al., 1999; Haneke, 2002; Gaikowski et al., 2004; Harris et al., 2004; Smail et al., 2004; Richter et al., 2007). According to the German Federal Environmental Agency (UBA), the tolerable concentration limit of p-TSA in drinking water is 0.3 $\mu g\ L^{-1}$ (Grummt and Dieter, 2006).

p-TSA was found to be ubiquitous in the aquatic environment in Berlin, the largest city of Germany (Richter et al., 2008a). It was detected in Berlin's untreated and treated wastewater, surface water, groundwater and raw water used for drinking water production

(Richter et al., 2008a). The highest concentrations of p-TSA (up to 38 µg L^{-1}) were encountered within the catchment area of a DWTP (Friedrichshagen) in the eastern part of the city. This DWTP is located downgradient of a former sewage irrigation farm, where untreated wastewater had been irrigated directly onto the soils until the 1980s, when the farm was closed. Though the concentrations of p-TSA in the raw water of this plant are considerably lower due to dilution with bank filtrate from Lake Müggelsee, an efficient removal during treatment is still necessary to reach the required limit of 0.3 µg L^{-1} in the final drinking water. Treatment at this DWTP involves aeration and rapid sand filtration (RSF) through open bed filters composed of biologically active sand (Richter et al., 2008b). Using an analytical method described in Richter et al. (2007), Richter et al. (2008b) investigated the behaviour of p-TSA during drinking water treatment with an experimental sand filter (column experiment), which provided the data used for the present modelling approach. Incubation experiments revealed that p-TSA degradation occurs as a result of microbial processes (Richter et al., 2008b). In addition, it appears to be largely limited to oxic conditions, explaining the persistence of p-TSA in the anoxic groundwater downgradient of the former sewage irrigation site (Richter et al., 2009). According to a laboratory experiment carried out by Richter et al. (2008b) sorption and retardation are negligible and can be excluded as a potential removal process. Their conclusion is also supported by data from a recently conducted, unpublished column study, in which p-TSA and a tracer were injected at the same time. p-TSA breakthrough occurred simultaneously with the tracer breakthrough at the outlet. Results of column studies are normally valid only for the specific experimental conditions, making comparison with other experiments and upscaling to field conditions difficult or impossible. Modelling refines and improves the interpretation of experimental studies by providing reaction rate constants which can be applied also to other sites and experimental condition. This holds true particularly where experimental conditions, such as influent concentrations, are highly variable and transient as in the present case, and it therefore becomes difficult to distinguish different effects.

In the literature different approaches were used to simulate microbially mediated reactions in column experiments. The simplest approach neglects kinetics induced by microbial activity and assumes instantaneous chemical equilibrium (e.g. Sabbagh et al., 2007). This method is appropriate if the microbial kinetics are fast compared to the transport timescale. Another group of models accounts for kinetics using zero or first-order reaction (Knudsen et al., 2000; Amondham et al., 2006) or Michaelis Menten kinetics (Bengtsson and

Carlsson, 2001a; Park et al., 2001; Sato et al., 2002). Both approaches are based on the concept of degradation constants, assuming that the microbial population does not change. Monod-type kinetics accounts also for microbial dynamics that describes growth dynamics (Höhener et al., 2006; Kim and Jaffe, 2008; Kinzelbach et al., 1991).

The role of microbiology in degradation has been investigated by numerical simulation for several organic compounds, such as antimicrobials (Rooklidge et al., 2005), hydrocarbons (Bengtsson and Carlsson, 2001b; Goedeke et al., 2008), chlorinated organic compounds (Bosma et al., 1988; Corapcioglu et al., 1991) and pesticides (Pang et al., 2005; Magga et al., 2008). However, no quantitative information applicable to other sites and conditions has been obtained yet for the sulfonamide p-TSA. Therefore, this paper provides a modelling framework for the simulation of the column experiment performed by Richter et al. (2008b), and the aim of this study was to (i) to determine the reaction rate constants defining microbial degradation of p-TSA, (ii) to explore and compare two different kinetic approaches to describe the degradation process and (iii) to investigate the dependence of microbial reaction rate constants on infiltration rates.

2.2 Methods

2.2.1 Column Experiment

The column experiment performed by Richter et al. (2008b) simulated rapid sand filtration during drinking water treatment in Berlin. The column was installed in the filter hall of the DWTP Friedrichshagen (Fig. 2.1) and was operated similarly to the real large rapid sand filters.

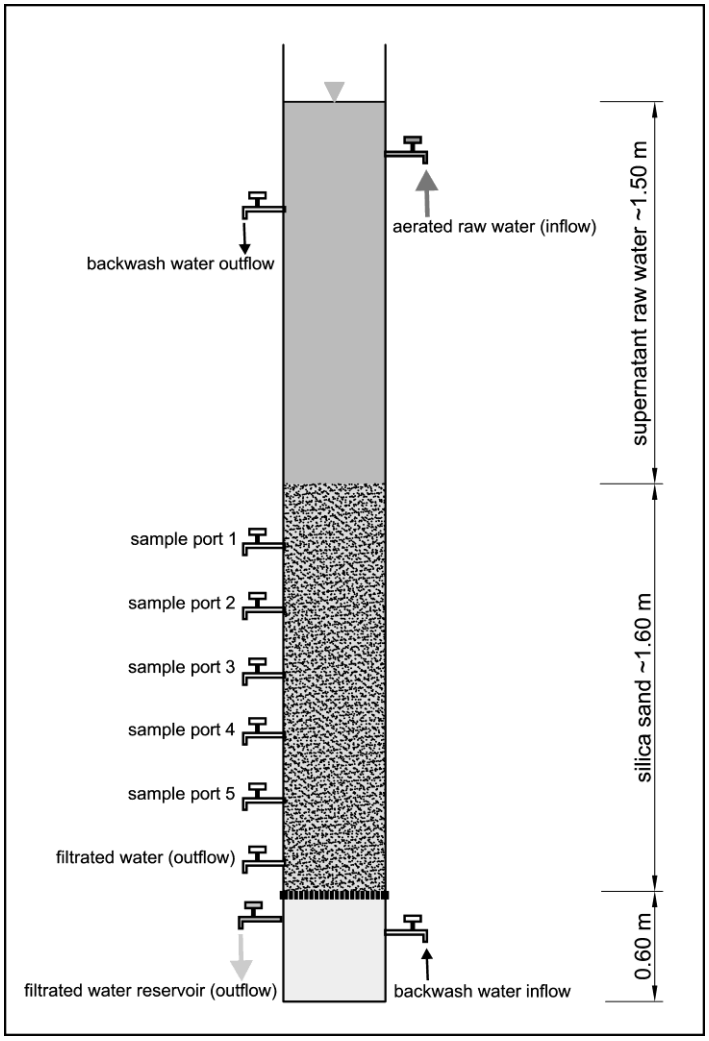

Figure 2.1 Experimental set up after Richter et al. (2008).

It was packed with the same silica sand that had been used for decades during RSF and had a length of 1.6 m, corresponding to the real filter length used during drinking water treatment at the DWTP Friedrichshagen. The silica sand had an effective porosity of 0.3, determined with the saturation method, and a uniformity coefficient (ratio d_{60} over d_{10}) of 1.33 (analysis carried out by the laboratories of Freie Universität Berlin). Sampling ports were installed every 0.25 m along the column (Fig. 2.1). The aerated raw water used during routine treatment was passed through the column. The infiltration rate was regulated via the effluent flow. After an initial regulation phase of about two weeks using an infiltration rate of 2 m h^{-1}, the functional capability of the experimental filter was determined by measuring the concentration of ammonium, iron and manganese, all efficiently removed in the column.

After the initial regulation phase the infiltration rate was raised in steps from 2 m h^{-1} to 6 m h^{-1} (Fig. 2.2). Results of 5 m h^{-1} are not presented here owing to technical problems during measurements. Considering a given porosity of 0.3, the corresponding residence times in the column range from 9.6 minutes for the infiltration rate of 3 m h^{-1} and 4.8 minutes for the infiltration rate of 6 m h^{-1}.

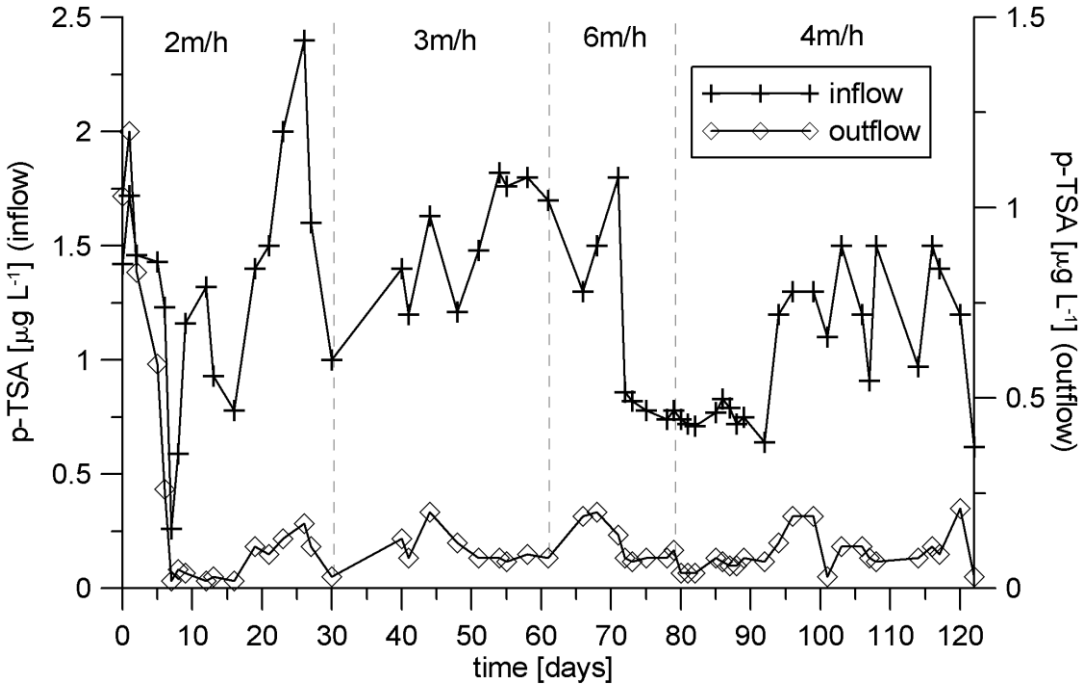

Figure 2.2 Measured inflow and outflow concentrations during the entire column experiment.

Backwashing of the sand with drinking water was performed every three to four days at an infiltration rate of 40 m h^{-1}. During the entire experiment 66 samples were collected both from the inlet and the outlet of the column at intervals between 1 and 3 days. Moreover, to obtain steady state concentration profiles the p-TSA sampled at the intermediate ports was analysed once for each infiltration rate after a minimum of 8 days of constant infiltration rate. The measurements at the outlet and at the sampling ports detected only the removal of p-TSA without accounting for the possibility of p-TSA transformation into an intermediate product. Therefore, the term "degradation" in the present paper refers to a microbial removal of p-TSA and not to a complete mineralization.

2.2.2 Model Set-up

Equations

The simulations were performed with Comsol Multiphysics 3.3 (COMSOL Multiphysics, Version 3.3, 2006), a multi-physics software tool for the solution of partial differential equations, which is based on the finite element method.

A transient one-dimensional solute transport model was set up based on the governing equations:

$$\theta_s \frac{\partial c}{\partial t} + \nabla \cdot \left[-\theta_s D_L \nabla c + uc \right] = R_L , \qquad \text{(eq. 2.1)}$$

$$D_L = \alpha_l v + \frac{Df}{\tau} \qquad \text{(eq. 2.2)}$$

where c (M L^{-3}) denotes the solute concentration in the liquid for the studied specie, θ_S is the porosity, D_L stands for hydrodynamic dispersion (L^2 T^{-1}), α_l is the dispersivity (L), v is the seepage velocity (L T^{-1}), Df is the molecular diffusion coefficient corrected for temperature and pressure (L^2 T^{-1}), τ is the tortuosity, u is the Darcy velocity (L T^{-1}), and R_L is the reaction term (M L^{-3} T^{-1}).

The first term of eq. 2.1 gives the time rate change in dissolved mass within the porous medium; the expression in brackets is the solute flux.

Physical parameters

Physical properties used in the model are listed in Table 2.1 and were assumed to be constant throughout the entire solution domain. The tortuosity was defined as the ratio of the real path length over the shortest path length and was approximated to $\pi/2$, assuming a circular shape of the silica grains.

Table 2.1 Input parameters of model simulations.

Input parameters	Value	Reference
Porosity	0.3	experimental data
Dispersivity (m)	0.01	Gelhar et al. (1985)
Tortuosity factor	1.57	$\pi/2$
Diffusion coefficient (m^2 s^{-1})	1 e-9	(Frederikse and Lide, 1997)
Infiltration rate (m h^{-1})	3. 4. 6	experimental set-up

Chemical parameters

The initial p-TSA concentration was set to 0.1 μg L^{-1}, and the measured concentrations of p-TSA at the column inlet were defined as transient inflow concentrations. Microbial degradation of p-TSA was simulated by (i) first-order kinetics and (ii) Michaelis Menten kinetics, both defined in the model by the reaction term of eq. 2.1. Monod kinetics was not applied due to the lack of input data required for this approach. First-order kinetics assumes that the only factor affecting degradation is the concentration of the substrate, without considering a maximum reaction rate. The reaction rate based on first-order kinetics is expressed by the following equation (Appello and Postma, 2007):

$$R_L = -\theta_s \lambda c \qquad \text{(eq. 2.3)}$$

where λ (T^{-1}) is the degradation rate constant. For the remaining parameters, refer to eq. 2.1.

The Michaelis Menten approach describes the dependence of the reaction velocity on the concentration considering a maximum reaction rate (Michaelis & Menten, 1913):

$$R_L = -\theta_s \frac{K_{\max} \cdot c}{k_s + c} \qquad \text{(eq. 2.4)}$$

where K_{max} is the maximum reaction rate (M T^{-1}), and k_s is the half-velocity concentration (M L^{-3}), also known as Michaelis Menten constant. For the remaining parameters, refer to eq. 2.1.

Following the results obtained from the analysis of the filter sludge samples carried out by Richter et al. (2008b), sorption and retardation were not taken into account. The simulations did not take the consumption of oxygen into account because the column experiment was conducted under completely oxic conditions. Hence, parameters are representative for oxic conditions only and are expected to be much lower during anoxic conditions.

Discretization

The column experiment was modelled by a 1.60 m long, one-dimensional solution domain discretized in 120 quadratic elements, corresponding to a degree of freedom of 241. Mesh refinement studies were carried out, and the simulations showed that the results are mesh-independent.

Calibration procedure

Forward modelling runs with the described model were performed for parameter estimation. Transport parameters were derived from the measurements or from the literature (Table 2.1), and only the degradation parameters were used as fitting parameters. Inverse modelling was performed manually, minimizing the difference between numerical and experimental values.

The mean square error was implemented as a measure of the fit. The difference between simulated and measured results is expressed by:

$$R = \frac{1}{m}\sqrt{\left(\sum_{n=1}^{m}(c_{meas} - c_{sim})^2\right)} \qquad \text{(eq. 2.5)}$$

where R is the least square residual, c_{meas} denotes the measured concentrations, c_{sim} is the simulated concentration. The sum in eq. 2.5 extends on all values from profiles and breakthrough curves. m is the number of measurements in the profiles and in the breakthrough curves. Note that a weighting factor was not used.

2.3 Results

2.3.1 Column Experiment

The depth profiles measured for infiltration rates of 3, 4 and 6 m h^{-1} showed that p-TSA was almost completely degraded after passage through the column (Fig. 2.3). Changes of initial concentrations during the experiment correspond to the variability of the inflowing raw water composition. Effluent concentrations show similar values for all infiltration rates. The measured steady state profiles revealed a strong decrease in concentration as far as a depth of 0.5 m, whereas in the lower part of the column only a minor decrease was observed.

The breakthrough curves resulting from the experiment showed a total reduction of > 89% p-TSA after passage through the filter for all infiltration rates tested (Richter et al., 2008b). A further outcome of breakthrough curve measurements is that variations in the concentration of the inflowing raw water are more attenuated at the outlet of the column after a minimum number of days with constant infiltration rates (Fig. 2.3). During the first days after a change in the infiltration rate, the attenuation of the breakthrough curves was weaker, indicating lower degradation rate constants during this period. In the following, the term “adaption phase” refers to the first period with lower degradation rates, and the subsequent period is named “adapted phase”. The length of the adaption phase ranged from 3 to 20 days (Table 2.2). The long duration of 20 days after the infiltration rate was reduced from 6 to 4 m h^{-1} may be attributed to strong changes of the inflow concentration in the same period (Fig. 2.3).

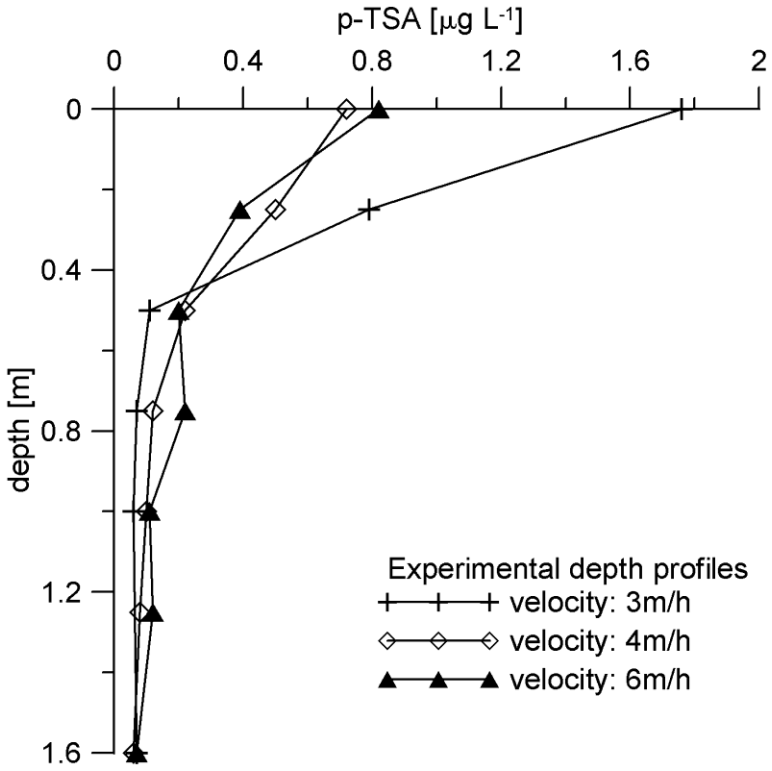

Figure 2.3 Measured steady state depth profiles.

Table 2.2 Values of fitted parameters of first-order kinetics and Michaelis Menten kinetics. Lambda values are given in s^{-1} and maximum reaction rates (K_{max}) in µg L^{-1} s^{-1}.

Velocity ($m\ h^{-1}$)	First-order kinetics				Quality of the fit (R)	Lenght adaption phase (day)
	Adaption phase		Adapted phase			
	upper part (λ_1)	lower part (λ_2)	upper part (λ_3)	lower part (λ_4)		
3	6.94E-03	2.89E-03	1.62E-02	1.60E-03	0.0256	9
4	8.68E-03	4.05E-03	1.04E-02	3.93E-03	0.0068	20
6	9.49E-03	5.90E-03	1.62E-02	4.98E-03	0.0056	3

Velocity ($m\ h^{-1}$)	Michaelis Menten kinetics				Quality of the fit (R)	Lenght adaption phase (day)
	Adaption phase		Adapted phase			
	upper part ($Kmax_1$)	lower part ($Kmax_2$)	upper part ($Kmax_3$)	lower part ($Kmax_4$)		
3	8.10E-03	1.50E-03	1.42E-02	4.63E-04	0.0074	9
4	6.37E-03	2.78E-03	1.16E-02	2.08E-03	0.0065	20
6	8.10E-03	5.67E-03	1.22E-02	2.31E-03	0.0346	3

2.3.2 Modelling

Measured breakthrough curves and steady state profiles of 3, 4 and 6 m h^{-1} were fitted by first-order kinetics and Michaelis Menten kinetics using λ, k_s and K_{max} respectively as fitting parameters.

In the initial simulation using first-order kinetics, only one temporary invariant degradation rate constant for p-TSA for the entire column was assumed, resulting in a single value of 5.55E-03 s^{-1} for λ. It was not possible to reproduce the measured data, neither the steady state profiles nor the analysed breakthrough curves as shown for 3 m h^{-1} in Fig. 2.4.

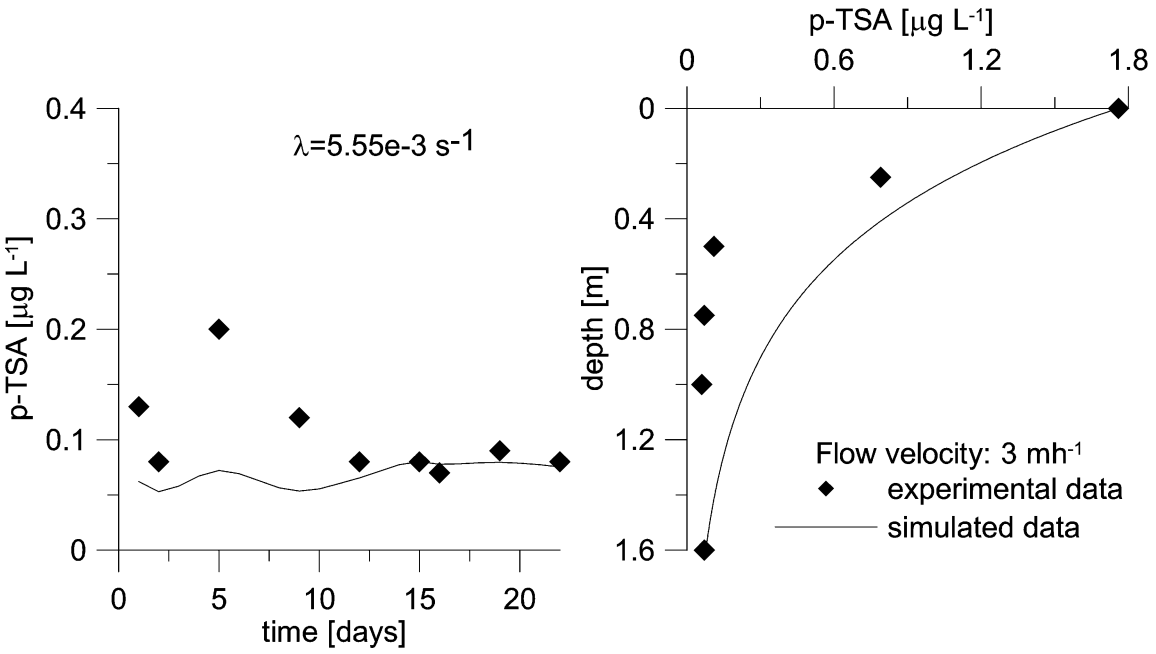

Figure 2.4 Measured and simulated p-TSA breakthrough curve and steady state profile using first-order kinetics for the infiltration rate of 3 m h^{-1}, considering one temporally invariant degradation constant λ for the entire solution domain.

To account for changes of degradation rate constants, the column was divided into an upper part of 0.5 m and a lower part of 1.1 m, allowing the attribution of higher and lower degradation rate constants, respectively. With regard to the temporal change of λ in the adaption phase and the adapted phase, one degradation rate constant for both time periods (adapted/adaption phase) in both parts of the column (upper/lower) was considered, resulting in four different values of λ. The parameter sets used to fit the different

infiltration rates are compiled in Table 2.2. The lengths of the defined adaption phases are derived from the experimental data and are documented in Fig. 2.5-2.7 and in Table 2.2.

No information about the microbiology of the sediment inside the column being available, K_{max} and k_s values for the two parts of the column were used as fitting parameters. The k_s value is specific for a microbial species, and K_{max} depends on the individual microbial activity and the number of individuums (Appelo and Postma, 2007). Changes of microbial species are not assumed here, and therefore only one k_s value was used for the simulation of all filtration rates. To identify the optimal k_s value, several simulations were run for the infiltration rate of 3 m h^{-1}. The value of k_s that provided the best fit for the experimental data (R = 0.0074) was 0.3 μg L^{-1} (Fig. 2.5). However, k_s values between 0.1 μg L^{-1} and 0.5 μg L^{-1} also reproduced the experimental data with sufficient agreement. After fixing the optimum k_s value, for each infiltration rate a different K_{max} was used to fit simulated to observed results and analogously to first-order kinetics, 4 maximum reaction rates (K_{max}) were attributed to the upper/lower column and to the adaption/adapted phase in the Michaelis Menten approach.

For all infiltration rates and both kinetic approaches, simulated and observed data are in good agreement, as illustrated in figures 2.5-2.7. In the case of the infiltration rate of 6 m h^{-1} (Fig. 2.7) the simulated peak is related to a strong increase of the inflow concentration at this time, as documented in Fig. 2.3.

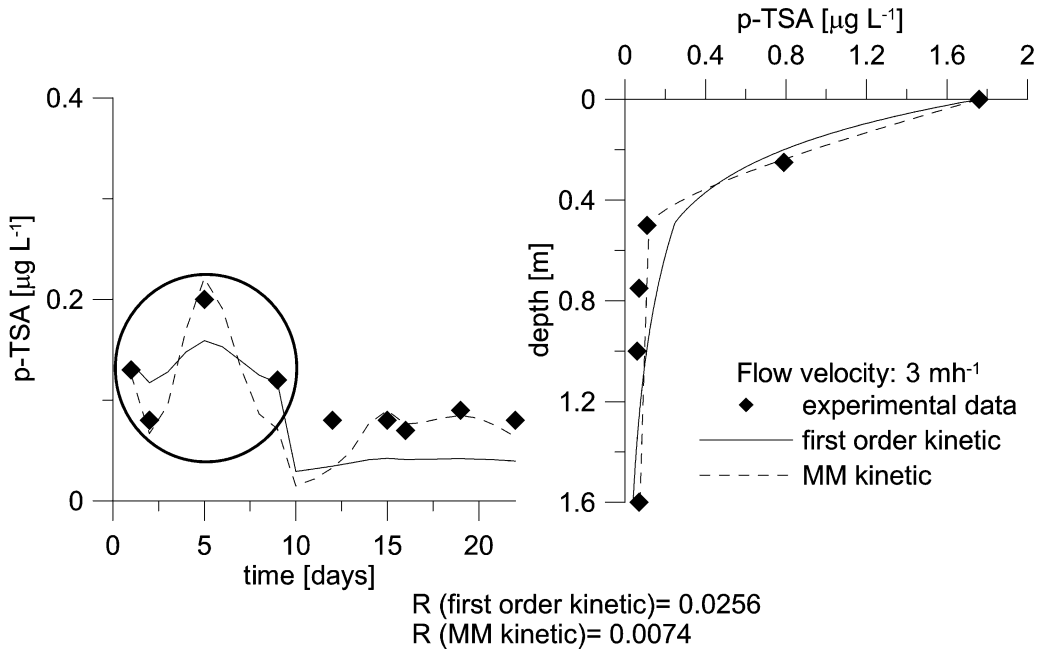

Figure 2.5 Measured and fitted concentrations of p-TSA using first-order kinetics and Michaelis Menten (MM) kinetics for the infiltration rate of 3 m h^{-1}, considering different values of degradation constants. The dashed circle indicates the adaption phase.

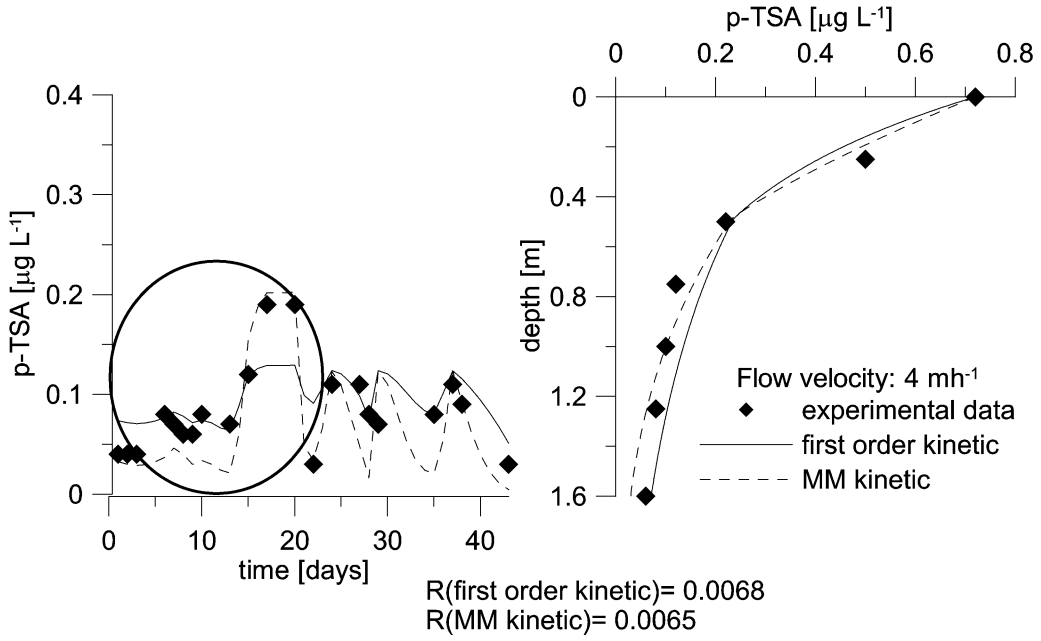

Figure 2.6 Measured and fitted concentrations of p-TSA using first-order kinetics and Michaelis Menten (MM) kinetics for the infiltration rate of 4 m h^{-1}, considering different values of degradation constants. The dashed circle indicates the adaption phase.

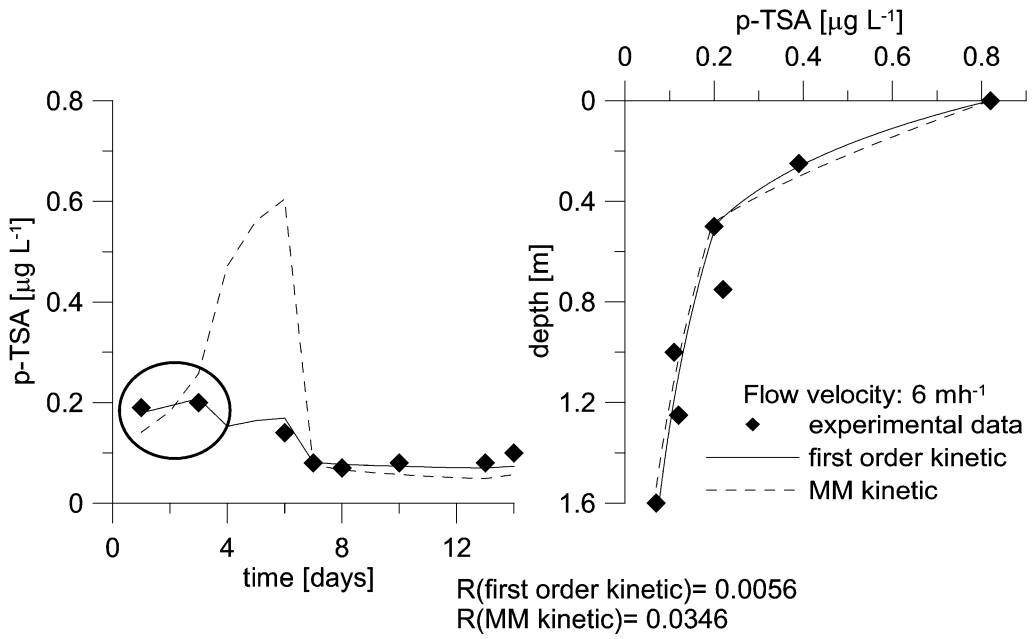

Figure 2.7 Measured and fitted concentrations of p-TSA using first-order kinetics and Michaelis Menten (MM) kinetics for the infiltration rate of 6 m h^{-1}, considering different values of degradation constants. The dashed circle indicates the adaption phase.

2.4 Sensitivity Study

The sensitivity study was performed to investigate the effects of λ and K_{max} on degradation, especially because no information on the microbiology within the column is available. The sensitivity study was carried out for two infiltration rates (3 and 6 m h^{-1}) and one range of parameter change (50 %) using the verified models (Table 2.3). The sensitivity of λ and K_{max} was calculated considering the steady state outflow concentration (c_{out}) as model dependent variable, and the adapted phase was analysed.

To exclude the effect of different inflow concentrations, a constant inflow concentration of 1.76 µg L^{-1} was used for all the simulations. Parameter sensitivity was tested for the upper part of the column because λ_3 and K_{max3} affect also the lower part and are supposed to have a major impact on steady state outflow concentrations.

To enable comparison of sensitivities between different parameters, sensitivities are normalized according to Bennett and Zheng (2002):

$$X_p = \frac{\partial c_{out}}{\partial P / P} \qquad \text{(eq. 2.6)}$$

where X_p is the normalized sensitivity, c_{out} is the steady state outflow concentration, and P represents the tested parameter (λ_3 or K_{max3}).

The outcome of the sensitivity study is presented in Table 2.3. The analysis showed a greater sensitivity to K_{max} than to λ for both infiltration rates, with the sensitivity of K_{max} being almost three times higher than the sensitivity of λ for the infiltration rate of 3 m h^{-1} and more than two times higher for the infiltration rate of 6 m h^{-1}.

As expected, the resulting data show a negative correlation between infiltration rate and parameter sensitivity, which is due to the dependence of parameter sensitivity on residence times.

Table 2.3 Sensitivity study. The first-order degradation rate constant values (λ) are given in s^{-1}, the maximum reaction rate values (K_{max}) in μg L^{-1} s^{-1} and the concentration in μg L^{-1}. The constant inflow concentration is 1.76 μg L^{-1}.

	Run 1D	Parameter	Value in the reference model	Value in the sensitivity model	% change in parameter	c_{out} value	Normalized sensitivity (X_p)
3m h^{-1}	Reference				0.00	0.075	
	1	λ_3	1.62E-02	8.10E-03	-50.00	0.280	0.410
	Reference				0.00	0.076	
	2	K_{max3}	1.42E-02	7.12E-03	-50.00	0.637	1.125
6m h^{-1}	Reference				0.00	0.166	
	3	λ_3	1.62E-02	8.10E-03	-50.00	0.328	0.324
	Reference				0.00	0.574	
	4	K_{max3}	1.22E-02	6.10E-03	-50.00	0.953	0.758

2.5 Discussion

Richter et al. (2008b) already presented a rough estimation of degradation rate constants for p-TSA during the column experiment obtained by simple graphical exponential fitting

of the steady state depth profiles without considering invariant inflow concentrations, changes in infiltration rate, and breakthrough curves. The approach was only rudimentary, similar to the initial simulation described above, where only one temporary invariant degradation rate constant for p-TSA for the entire column was used. The resulting degradation rate constants of Richter et al. (2008b) were around 6.3E-03 s^{-1}, but obtained fits were rather poor. Instead, in the present paper, the degradation rate constants were derived through the application of a model that considered both depth profiles as well as breakthrough curves simultaneously and accounted for the spatial and temporary variability of the parameters, thereby obtaining much better agreement between modeled and measured data and a refined understanding of the processes.

Fitted λ (and likewise K_{max}) values for p-TSA are very high, ranging from 10^{-3} (in the lower part of the column) and 10^{-2} s^{-1} (in the upper part of the column) during the adapted phase (Fig. 2.8). For comparison, values of degradation constants for other substances such as pesticides range between 10^{-6} s^{-1} for the insecticide acephate/orthene and 10^{-9} s^{-1} for the herbicide paraquat/Gramoxone (Howard, 2004). Mackay and Shiu (1992) determined half-lives of certain polycyclic aromatic hydrocarbons (PAHs) in the aquatic environments, resulting in degradation rate constants between 10^{-7} s^{-1} and 10^{-8} s^{-1}. We assume that a highly adapted microbial community causes the effective elimination because the sands used in the column have been in operation for decades and p-TSA concentrations in the raw water have been continuously high for a long time. This is supported by experiments performed by Richter et al. (2008b), who showed that microbial degradation only takes place in filter sands of DWTPs abstracting groundwater polluted with p-TSA. In incubation experiments where drinking water was spiked with p-TSA and backwash water from “unpolluted” sand filters, no degradation occurred.

Simulations with both approaches confirmed the assumption based on visual interpretation of the experimental data that the degradation rate constants of p-TSA vary in both time and space (Table 2.2 and Fig. 2.8). The degradation rate constants (and likewise K_{max}) between the upper and lower parts of the column showed a difference of up to one order of magnitude, which may be related to greater populations of microbes in the upper part of the column owing to the greater availability of nutrients close to the inlet of the column. The reason for the less efficient degradation of p-TSA in the adaption phase could be related to a reduced microbial activity following a change in infiltration rate, owing to the

change of ambient conditions. Note that the temporal changes of the degradation rate constants (and likewise K_{max}) were limited to the upper part of the column, leading to greater spatial differences during the adapted phase.

The infiltration rates were originally varied to determine the optimum operational infiltration rate for p-TSA degradation. Fig. 2.8 illustrates that no clear correlation exists between degradation rate constants (and likewise K_{max}) and infiltration rates.

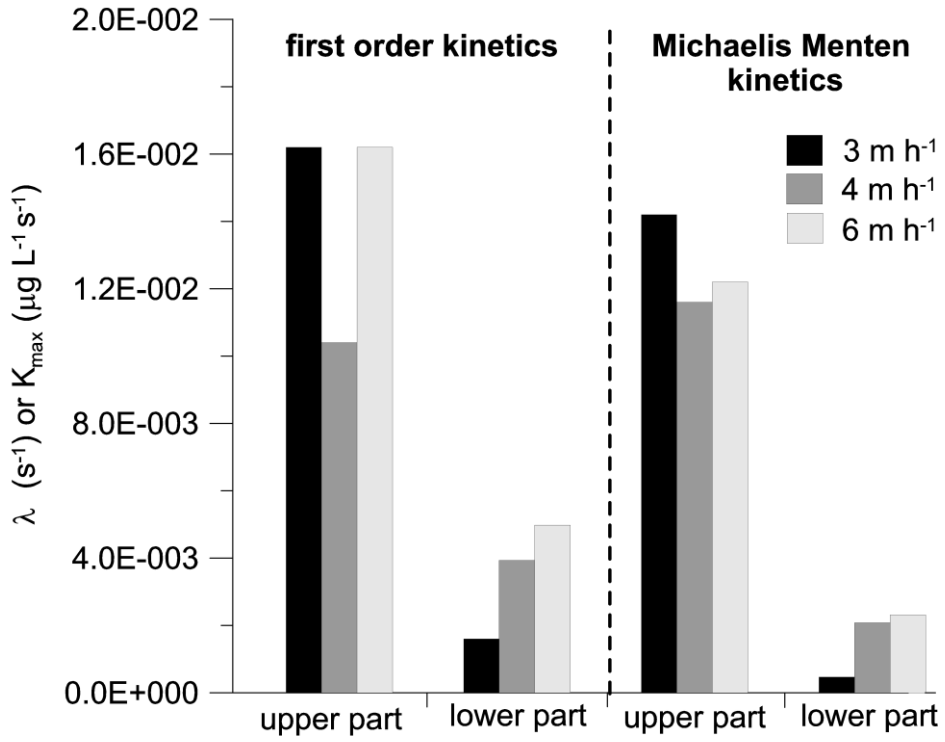

Figure 2.8 Fitted degradation rate constants in the adapted phase using first-order kinetics and Michaelis Menten kinetics for all three infiltration rates.

Fig. 2.9 shows the Michaelis Menten function (eq. 2.4) for parameter settings defined in the upper part of the column during the adaption (K_{max1}) and adapted (K_{max3}) phases for the infiltration rate of 3 m h^{-1}. The figure also includes the k_s value as well as the observed concentration range. The fact that the optimized k_s value falls within the range of natural concentrations results in high degradation rates already for low concentrations. For concentrations higher than 1 µg L^{-1}, the reaction rate R_L increases only in minor amounts.

Fig. 2.9 is also representative for the experimental conditions of the other infiltration rates because the values of K_{max} are in the same order of magnitude as the values of p-TSA concentration.

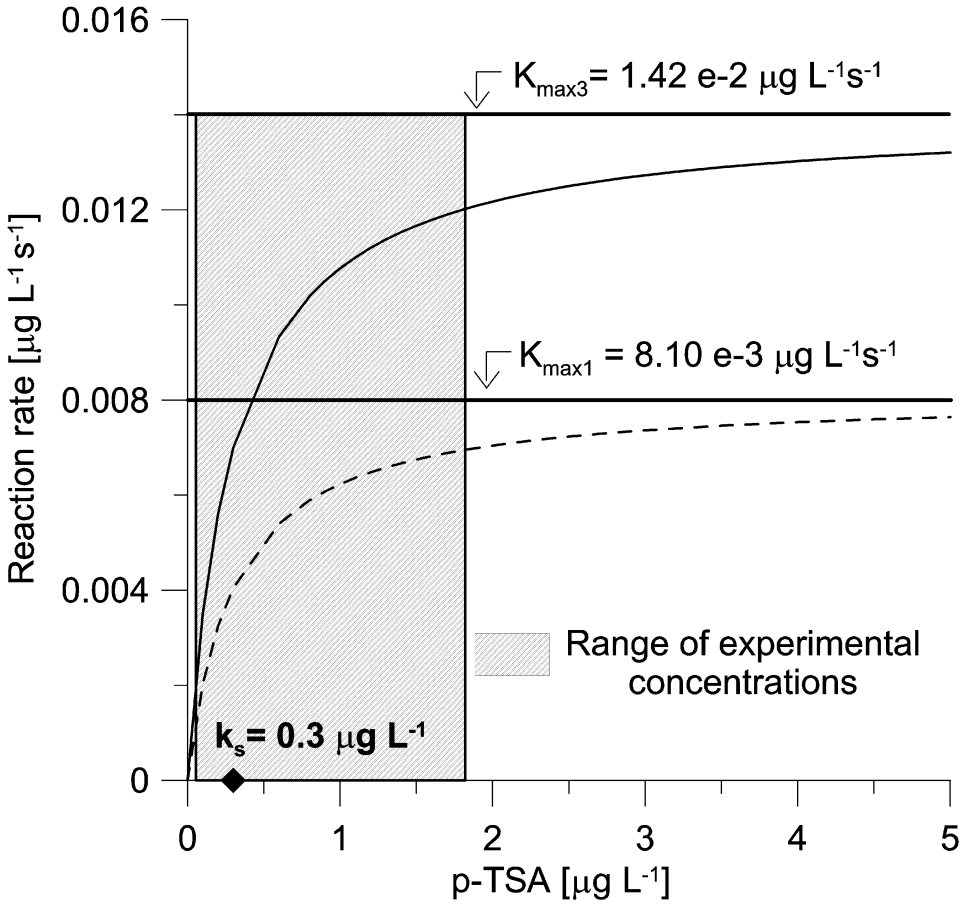

Figure 2.9 Applied Michaelis Menten function for the infiltration rate of 3 m h^{-1} and range of experimental concentrations.

The two kinetic approaches both support the concept of changing degradation constants in space and time and produce excellent fitting results. In general, the Michaelis Menten approach shows a higher capacity to reproduce fluctuations of the concentrations during this highly transient experiment. This holds true especially for the adaption phase, where fluctuating inflow concentrations are not attenuated until discharging at the outlet of the column.

2.6 Conclusions

- This research presents degradation rate constants for p-TSA removal during RSF, which were previously not available in the literature. The resulting values range between 10^{-3} and 10^{-2} s^{-1}.

- The model approaches, though simple, illustrate the usefulness of mathematical modelling to determine robust degradation parameters during drinking water treatment processes and can easily be applied to other sites and conditions.

- Results suggest higher microbial activities in the upper part than in the lower part of the column, where upper part refers to the sector of the column close to the inlet and lower part refers to the subsequent column sector. Microbial activity also appears to be temporally variable depending on the change of ambient conditions due to the transition between different infiltration rates.

- The degradation parameters showed only minor variations for different infiltration rates; therefore an optimal infiltration rate for the removal process could not be determined.

- Comparison of the two applied kinetic approaches showed that the Michaelis Menten approach is clearly more appropriate for reproducing highly transient experimental conditions than the more simplistic linear approach.

- Based on this research, some conclusions may be drawn for the design of treatment plants for p-TSA removal. First, maintenance of oxic conditions appears to be essential to guarantee these high degradation rates. Second, the study has demonstrated that the infiltration rate is not a relevant parameter to optimize future treatment strategies and to obtain more favourable degradation rates the infiltration rate should be maintained constant, avoiding the occurrence of the adaption phase with lower degradation efficiency. Finally, results suggested that the vertical thickness of the filter could be reduced to less than 1 m, because degradation at depths higher than 0.50 m almost vanishes.

3 Investigating the Redox Sensitivity of para-toluenesulfonamide (p-TSA) with a Column Study

The groundwater downstream of a former sewage irrigation farm in Berlin is contaminated with ammonium (NH_4^+) and para-toluenesulfonamide (p-TSA), besides other anthropogenic pollutants. In the field, in-situ removal of NH_4^+ by gaseous oxygen (O_2) and air injection is currently being tested. A laboratory column experiment using aquifer material and groundwater from the site was performed to determine whether this remediation technology is also feasible to reduce high p-TSA concentrations in the anoxic groundwater. First, the column was operated under anoxic conditions. Later, compressed air was introduced into the system to simulate oxic conditions. Samples were collected from the column outlet before and after the addition of compressed air. The experiment revealed that whereas p-TSA was not removed under anoxic conditions, it was almost fully eliminated under oxic conditions. Results were modeled using a transient one-dimensional solute transport model. The degradation rate constants for p-TSA increased from 2.8E-06 s^{-1} to 6.1E-05 s^{-1} as a result of microbial adaption to the change of redox conditions. Results show that oxygen injection into an anoxic aquifer is a successful strategy for p-TSA remediation.

R. Meffe, G. Massmann, C. Kohfahl, T. Taute, D. Richter, U. Dünnbier, A. Pekdeger *Investigating the redox sensitivity of para-toluenesulfonamide (p-TSA) with a column study.* Submitted to Environmental Earth Sciences.

http://dx.doi.org/10.1007/s12665-011-1130-9

3.1 Introduction

The majority of the world's population relies on groundwater for drinking, agricultural or industrial requirements (IAEA, 1998). In the last decades, particularly with the advent of industrialisation and population growth, the stresses on groundwater resources have increased. The problems associated with groundwater availability and deteriorating quality mainly originate from intentional or inadvertent disposal of waste in the ground (IAEA, 1998).

While the behaviour of macropollutants such nutrients, acids and organic matter in the aquatic environment is well known, knowledge is scarce about the effect and the behaviour of most trace pollutants, including organic micropollutants (Schwarzenbach et al., 2006). However, growing interest in the occurrence, fate and potential harmful effects of microrganic pollutants in groundwater is demonstrated by the increasing number of investigations on this topic (Lindsay et al., 2001; Batt and Aga, 2005; Grathwohl, 2006; Richter et al., 2007; Ternes, 2007; Ayotte, 2008; Soares et al., 2008).

Redox processes in groundwater play an important role in the fate and distribution of a large number of major organic pollutants (Bouwer and Zehnder, 1993). Recently, several organic micropollutants have also been shown or suspected to be redox sensitive, including pharmaceutically active substances (Ternes et al., 2004; Massmann et al., 2006; Heberer et al., 2008; Massmann et al., 2008; Pholchan et al., 2008), halogenated organic compounds (Bosma et al., 1996; Grünheid et al., 2005), pesticides (Patterson et al., 2002; Schwab et al., 2006; Tuxen et al., 2006) and disinfection by-products (Pavelic et al., 2005; Reineke et al., 2008). Hence, the redox conditions can be considered as one of the most important environmental key variables for the degradation processes affecting organic pollutants in groundwater.

Conventional groundwater decontamination methods often involve pump-and-treat technologies and have been widely investigated and optimised (e.g. Guan and Aral, 1999; Maskey et al., 2002; Espinoza et al., 2005). Beside these technologies, methods that rely on *in situ* enhancement of the microbial activity which creates more favourable redox conditions have been widely employed (Ulrich and Suflita, 2002; Stempvoort et al., 2007). These methods are based on the introduction of appropriate nutrients, electron donors

and/or electron acceptors into contaminated groundwater in order to stimulate microbial growth and enhance biodegradation processes (Bouwer, 1992).

para-toluenesulfonamide (p-TSA) (Fig. 3.1) is an industrial organic micropollutant which is applied as a plasticiser and an intermediate for pesticides and drugs, and it is the primary degradation product of the common antiseptic chloramine-T in water. Chloramine-T is used as an antimicrobial agent in the food industry to disinfect surfaces, instruments and machinery. This substance is also used as a therapeutic drug for bacterial gill diseases of fish species and for bacterial diseases of swine and poultry (Beljaars et al., 1994; Gaikowski et al., 2004; Haneke, 2002; Harris et al., 2004; Meinertz et al., 1999; Smail et al., 2004; Richter et al., 2007). p-TSA is slightly toxic to algae but non-toxic to fish and daphnids. Overall, its toxicity can be classified as moderate, and additional tests are recommended if large amounts of p-TSA are used in consumer products in the future (OECD, 1994). Few studies have investigated and quantified the fate of p-TSA in the hydrological cycle. Richter et al. (2008a) carried out research on the occurrence and behaviour of p-TSA in the Berlin water cycle. p-TSA was found to be ubiquitous in Berlin in wastewater, sewage water and groundwater. Highest concentrations of up to 38.0 $\mu g\ L^{-1}$ were encountered in an aquifer downstream of a former sewage farm in Berlin. Nonetheless, very little knowledge exists about p-TSA attenuation in groundwater. A redox dependency was suggested by Richter et al. (2008b), who carried out simple incubation experiments with anoxic groundwater, but degradation rate constants are so far unavailable.

This study investigates the potential of in-situ injection of O_2 into a contaminated anoxic aquifer in Berlin to enhance bioremediation of p-TSA. For this purpose, a column study simulating a change from anoxic to oxic conditions was carried out in the laboratory. The experimental setup attempted to mimic real field conditions by using an undisturbed sediment core and groundwater collected from the site whilst maintaining the natural hydrostatic pressure.

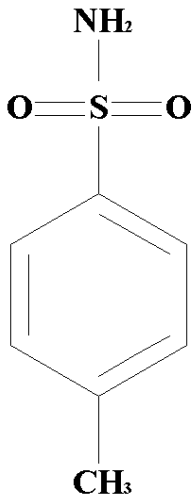

Figure 3.1 Chemical structure of p-TSA.

3.2 Site Description

The studied aquifer is located to the north of Lake Müggelsee, in the eastern part of Berlin (Fig. 3.2). The former Münchehofe sewage farm, which closed in the 1980s, operated for almost 70 years, and former irrigation fields are located upstream of a drinking water treatment plant (DWTP Friedrichshagen). At the study site there are various observation wells screened at different depths (from 3.5 m to 87.3 m below ground level) and several production well galleries of the nearby DWTP (Fig. 3.2, for details refer to Richter et al., 2009). Well galleries abstract variable proportions of ambient groundwater and infiltrated surface water (bank filtrate) from a lake (Müggelsee). Gallery A (Fig. 3.2) is not used for production and serves as hydraulic protection. The abstracted water is pumped directly to a wastewater treatment plant (Münchehofe).

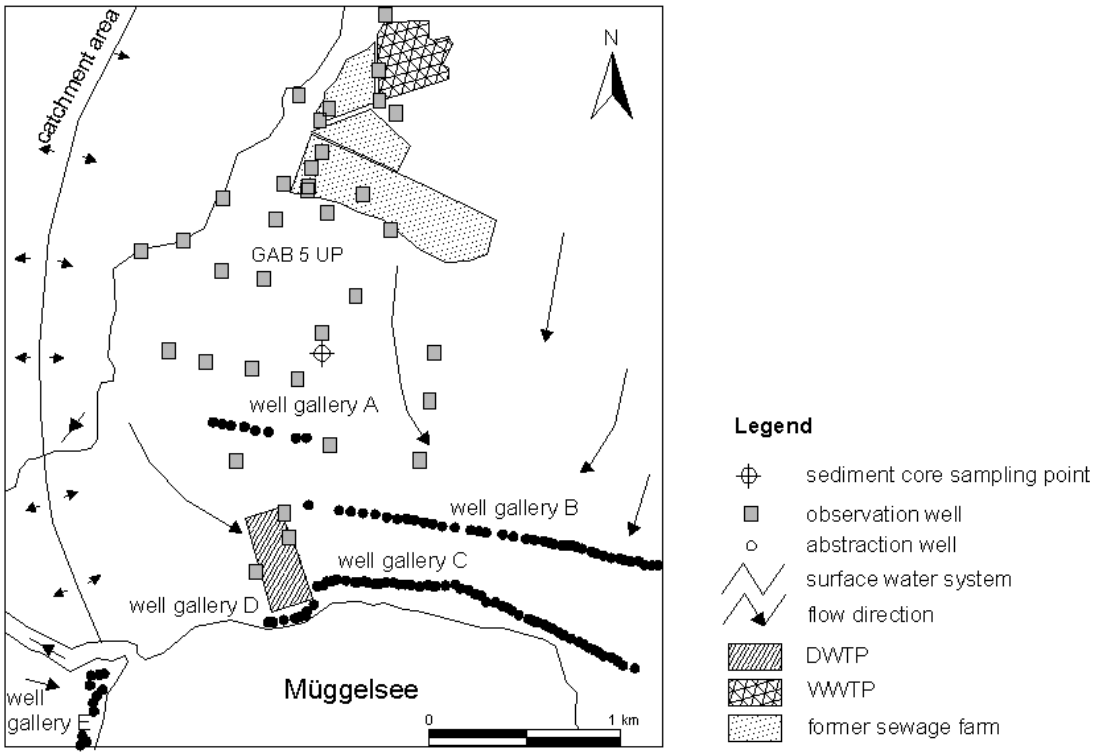

Figure 3.2 Map of the study site Machnow/KrummendammerHeide with location of drinking water treatment plants (DWTP), wastewater treatment plant (WWTP) and former sewage farm. Also shown is the western boundary of the catchment area of the DWTP Friedrichshagen, the observation wells, abstraction wells, the sampling point of the sediment core and stream lines (modified from Richter et al., 2009).

The aquifer of the area consists of porous, glaciofluvial and fluvial, mainly fine to medium-sized sand of the Pleistocene glaciations (Engelmann et al., 1992). Generally, the aquifer is not divided by aquitards since the glacial tills often encountered in the Berlin area are almost completely missing in the north of Lake Müggelsee. The aquifer is characterised by a medium hydraulic conductivity with a k_f value of about 1E-04 m s^{-1} and has a thickness of about 50 m (BWB, 2007). From the results of the sieve analysis the collected sediment can be classified as uniform medium size sand. The uniformity coefficient is 2.2 for the sediment at 33 m depth and 2.1 for the sediment at 34 m depth. The total organic carbon (TOC) content of the sediment in the column has an average value of 1000 mg kg^{-1}.

Even though the sewage farm was closed in the 1980s, the monitoring wells in the area continue to confirm high values of anthropogenic compounds such as NH_4^+ (between <0.04 and 89.0 mg L^{-1}), B (between <50.0 and 655.0 µg L^{-1}) and p-TSA (between <0.05

and 38.0 μg L^{-1}) in the groundwater (Richter et al., 2009). In 2004, the Berlin Water Company (BWB) started to explore the potential of enhanced bioremediation at the site to reduce NH_4^+ concentrations in the groundwater. For this purpose, injections of both gaseous O_2 and air are performed at a pilot plant through injection lances to enhance nitrification processes capable of removing NH_4^+ (Bioxwand, 2004).

Until summer 2009, p-TSA concentrations of the final drinking water have remained below the required limit of 0.3 μg L^{-1} because of dilution with bank filtered groundwater and because of p-TSA degradation during treatments (aeration and rapid sand filtration). However, high concentrations of p-TSA in the groundwater are undesirable and could cause problems in the future. Incubation experiments with groundwater from the site revealed that p-TSA degradation occurs under oxic conditions, mediated by an adapted microbiology present in the polluted water (Richter et al., 2008b). A column experiment simulating aerobic rapid sand filtration (RSF) showed a p-TSA removal of about 90 % during treatment at the respective DWTP within minutes (Richter et al., 2008b). Reactive transport modelling of the experimental results delivered degradation rate constants ranging between 1E-03 and 1E-02 s^{-1} (Meffe et al., 2010). These studies concur with the fact that p-TSA seemingly persists for decades in the anoxic aquifer. As suggested by Richter et al. (2009), we suspect that degradation is inhibited owing to the anoxic redox conditions of the groundwater. The O_2 injection into the aquifer to remove NH_4^+ from the groundwater may therefore also facilitate p-TSA removal. This remediation technology has proved to be feasible for other organic compounds such as BTEX (benzene, toluene, ethylbenzene and xylene) (Borden et al., 1997; Chapman et al., 1997) and MTBE (Salanitro et al., 2000; Wilson et al., 2002).

3.3 Methods

3.3.1 Sampling

A sediment core with a length of 1 m was collected at a depth of 33 m on 30 August 2006 during drilling of the observation well FRI 213 of the pilot plant at Machnow/Krummendammerheide (Fig. 3.2). The sample was stored at a temperature of 4 °C until the experimental setup was constructed.

The sampling campaign for groundwater was carried out on 19 May 2008. The samples were abstracted from the observation well GAB 5 UP (filter screen depth: 41.5 m to 47.5 m below ground) which showed the highest p-TSA concentration of the area (Richter et al., 2009, Fig. 3.2). The sampling was conducted in accordance with the official DVWK guidelines (1992). Filtration with 0.45 µm membrane filters was done immediately after sample retrieval for the analysis of cations and anions. Samples for cation analysis were preserved with concentrated nitric acid. Samples were stored at 4 °C, and full water analysis was performed one or two days after sampling. In addition, groundwater samples were filled in glass bottles, avoiding introduction of O_2, and stored in the freezer prior to analysis of organic micropollutants including p-TSA. Measurements for redox potential (Eh), pH, O_2, temperature and electrical conductivity (EC) were carried out in the field in a flow cell. Concentrations of hydrogen sulfide (HS^-), ammonium (NH_4^+) and nitrite (NO_2^-) were measured in the field using colorimetric field tests. Alkalinity was measured in the field by titration with hydrochloric acid.

For the column experiment, eight stainless steel tanks, previously sterilised by autoclavation for 15 minutes at 1 bar and 120 °C, were filled with nearly 15 litres of groundwater each under completely anoxic conditions. Before the sampling campaign, the stainless steel tanks were flooded with argon gas and kept at 2.4 bars. The groundwater was collected under pressure to prevent any hydrochemical changes caused by degassing. Not only the tanks but also the entire equipment for sampling was sterilised by autoclavation and with sodium hypochlorite to avoid microbiological contamination because experiments carried out by Richter et al. (2009) had shown that without sterilisation, p-TSA is biodegraded after a few days. The collected tanks were stored in a dark room at 11 °C corresponding to the temperature of the groundwater in the field. The sampling method was shown to be effective by Richter et al. (2009). p-TSA concentrations were measured in all sampled tanks from sub-samples collected using equipment sterilised with sodium hypochlorite.

3.3.2 Analytical Methods

The DOC measurements were performed with a DOC analyser. Cations in the water were determined with the Inductively Coupled Plasma Mass Spectrometer (ICP Perkin Elmer Otima 2100). Anions in water were measured by ion chromatography (Dionex DX 500).

The analytical method for p-TSA consists in solid-phase extraction followed by reverse-phase liquid chromatography (HPLC) coupled to tandem mass spectrometry detection (MS/MS). A detailed description of the analytical method is reported in Richter et al. (2007).

3.3.3 Experimental Design and Operation of the Column

The experiment was performed in a dark room with a temperature of 11°C (temperature of the groundwater at the site) using the undisturbed sediment core and groundwater collected from the field site as explained. The column was shortened to 0.76 m to remove loose and slightly disturbed sediment at the ends. The column study was performed maintaining pressure conditions above 2 bars to simulate realistic aquifer conditions. Therefore the entire design had to be performed using tubings of pressure resistant copper and the installation of probes and sensors was limited to maintain the pressure regime.

At the top and bottom of the polyvinyl chloride (PVC) liner (inner diameter 0.11 m, length 0.76 m), glass fibre filters were inserted to avoid loss of sediment and rubber O-ring seals to prevent water leakage. Finally, the column was connected to the tubing of the flow-through system and to a supporting structure. The tubing was made of pressure-resistant copper, impermeable to gas diffusion. A schematic representation of the column setup is shown in Fig. 3.3.

To preserve the field conditions and to avoid any atmospheric contact causing oxidation, the system was operated through a pressure gradient. The pressure was ensured by the connection of the collected pressurised tanks (Fig. 3.3, A) to the experimental setup through a damp valve, and it was measured by two manometers placed at the inlet and outlet of the column (Fig. 3.3, G1 and G2). The pressure gradient between the inlet (~2.4 bars) and the outlet (~2.2 bars) provided an upward flow. The pressure gradient was regulated manually by addition of argon gas to the connected tank (Fig. 3.3, A).

Two calibrated O_2 minisensors (optodes) (Presens, Fibox 3, 2 mm cable) were placed directly into the groundwater flow at the column inlet (Fig. 3.3, I1) and outlet (Fig. 3.3, I2). The optical O_2 measurement is based on the fluorescence-quenching effect of O_2. Modulated blue light is fed into an optical fibre with a fluorescent dye glued to its tip. The

fluorescent light is returned by the optical fibre and detected in the measuring device. In the presence of O_2 fluorescence is quenched, and on the basis of the intensity and lifetime of the fluorescence, the O_2 concentration can be detected (Hecht and Kölling, 2002).

The experimental system was also equipped with a small Plexiglass pre-column (inner diameter 0.08 m, length 0.22 m) located between the tank and the column inlet (Fig. 3.3, E); it was used for the addition of compressed air during the simulation of oxic conditions.

The system was set up in March 2007; the column was saturated and successively equilibrated for 6 months using groundwater collected in February 2007. A tracer test was conducted in December 2007, before the column experiment that simulated the behaviour of p-TSA started (no pre-column present). The p-TSA experiment was carried out over 26 days, starting on 11 July 2008. After 26 days, a leak developed in the pre-column and the experiment had to be stopped.

Initially, the column was operated under anoxic conditions, thereby avoiding any contact between the air and the groundwater. The flow rate was regulated at the outlet valve (Fig. 3.3, M) and by the pressure gradient. To simulate the change from anoxic to oxic conditions, compressed air was introduced in the pre-column (Fig. 3.3, E), generating an interface between air and groundwater where the O_2 could dissolve. The total volume of air introduced during the simulation of oxic conditions was about 0.05 m^3. To provide sufficient concentrations of dissolved O_2, the exchange at the air/groundwater interface (inside the Plexiglass pre-column; Fig. 3.3, E) was enhanced by a rotating magnetic stirrer. The O_2 concentrations were measured at the inlet and outlet optodes every 10 minutes.

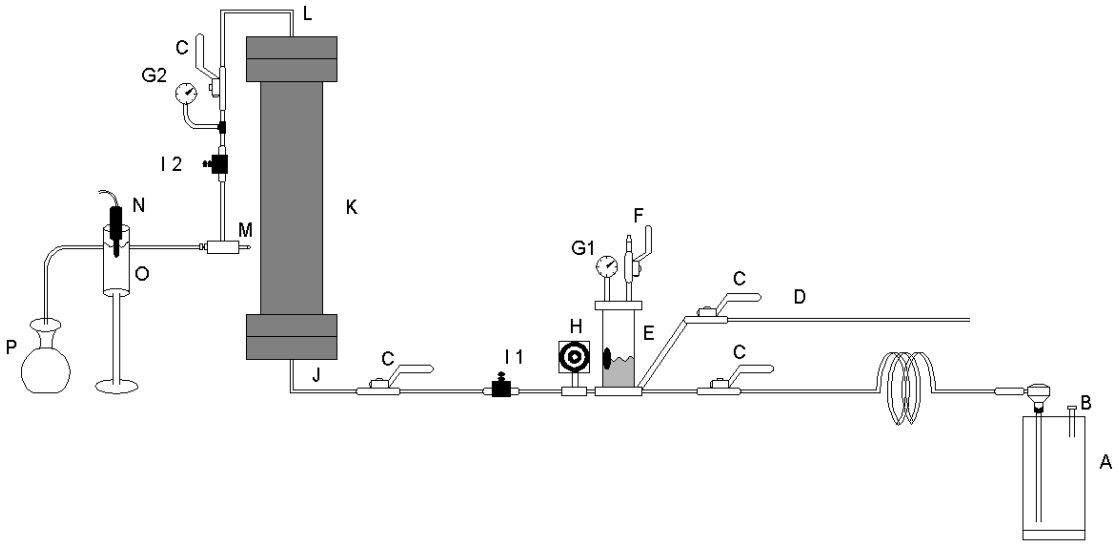

Figure 3.3 Schematic representation of the column experimental setup. *A*: connected tank; *B*: valve for argon addition; *C*: caps for controlling the flow; *D*: by-pass for tracer test; E: pre-column; *F*: cap for compressed air addition; *G* (1-2): manometers; *H*: magnetic stirrer with magnet; *I* (1-2): inlet and outlet optodes, respectively; *J*: column inlet; *K*: column; L: column outlet; *M*: outlet valve; *N*: EC probe; *O*: flow through cell; *P*: sample.

During the entire experiment 4 pressurised tanks were used (Nr. 9; 2; 4; 5). The tanks were sampled again before each installation, and the samples were frozen immediately and stored until analysis. Almost daily samples for p-TSA analysis were collected from the column outlet under both anoxic and oxic conditions using sterilised equipment.

3.3.4 Transport Parameter Estimation

A tracer test was conducted in order to determine the transport parameters. For this purpose 5 ml of a 50.0 g L^{-1} NaCl solution were quickly added to the column inlet via the by-pass (Fig. 3.3, D) (total mass of NaCl added: 0.24 g.).

Following the instantaneous pulse application, tracer concentrations were measured by an electrical conductivity (EC) probe (Fig. 3.3, N) placed in a flow-through cell at the outlet (Fig. 3.3, O). The background EC value was measured before the injection of NaCl. The TDS (Total Dissolved Solids) was calculated as follows:

$$TDS = (EC_m - EC_b) \cdot 0.755 \qquad \text{eq. 3.1}$$

where EC_m is the EC measured during the tracer experiment, EC_b is the background EC and *0.755* is the conversion factor estimated from the total recovery, assuming that a conservative tracer should have a mass recovery of nearly 100 %. The value of the conversion factor is in accordance with literature values provided by Wu- Seng (1993).

The elaboration of the tracer test data was performed using CXTFIT, an analytical 1D transport model developed for estimating transport parameters from laboratory or field tracer experiments (Toride et al., 1999). The CXTFIT code is based on analytical solutions of the transport equation:

$$\theta R \frac{\partial c}{\partial t} = D_L \frac{\partial^2 c}{\partial x^2} - u \frac{\partial c}{\partial x} - \theta R \lambda c \qquad \text{eq. 3.2}$$

where θ is the porosity, R is the retardation factor, D_L is the dispersion coefficient ($L^2\ T^{-1}$), u is the Darcy velocity ($L\ T^{-1}$), λ is the degradation rate constant (T^{-1}), c is the solute concentration ($M\ L^{-3}$).

Since the tracer concentration was measured at the column effluent, the concentration mode used for CXTFIT simulations was the flux-average concentration. For boundary conditions, a Dirac pulse representing an instantaneous tracer injection was applied assuming that the tracer injection period was negligible compared to the travel time. For a conservative tracer such as NaCl, the transport equation can be simplified by setting the retardation factor R= 1 and the degradation rate constant λ= 0, fitting only the transport parameters (dispersion coefficient and flow velocity expressed as u/θ). The simulation was done by inverse modelling.

3.3.5 Modelling p-TSA Degradation

To define the reaction rate constant of the p-TSA degradation in the groundwater under oxic conditions, a transient one-dimensional solute transport model was set up. The simulations were performed with Comsol Multiphysics 3.3 (COMSOL Multiphysics, Version 3.3, 2006), a multiphysics software tool based on the finite element method for the solution of partial differential equations. The governing equation is the transport equation (Eq. 3.1) in which the dispersion D_L is defined as:

$$D_L = \alpha_l v + \frac{Df}{\tau} \qquad \text{(eq. 3.3)}$$

α_l is the dispersivity (L), v is the seepage velocity (L T^{-1}), Df is the molecular diffusion coefficient corrected for temperature and pressure (L^2 T^{-1}), τ is the tortuosity.

Physical properties and discretization of the solution domain in the model are compiled in Table 3.1. Tortuosity was defined as the ratio of the real path length to the shortest path length and was approximated to $\pi/2$, assuming a circular shape of the sediment grains. The p-TSA concentration of tank 2 measured before the installation (34.4 µg L^{-1}) was used as a constant inflow boundary. Because the flow rate was not constant during the experiment, the simulations accounted for a transient Darcy velocity. The model also accounted for the propagation of O_2 in the column during the experiment. The O_2 propagation front, implemented through a Comsol transient function, was calculated as follows:

$$d_{O_2}^{(i)} = d_{O_2}^{(i-1)} + \left(\frac{C_{O_2}^{(i)} \cdot V_{H_2O}^{(i)}}{OD \cdot \rho_b \cdot V_s} \right) \cdot L \qquad \text{(eq. 3.4)}$$

where $d_{O_2}^{(i)}$ (L) is the O_2 penetration depth at time i, $C_{O_2}^{(i)}$ (M L^{-3}) and $V_{H_2O}^{(i)}$ (L^3) are the O_2 concentration and the volume of water entering the column during the interval between time i-1 and i, respectively. OD is the O_2 demand of the column sediment, ρ_b (M L^{-3}) is the bulk density of the sediment, V_s (L^3) is the sediment volume, and L (L) is the column length.

Microbial p-TSA degradation was simulated with first order kinetics (Appelo and Postma, 2007):

$$\theta \frac{\partial c}{\partial t} = -\theta \lambda c \qquad \text{(eq. 3.5)}$$

Forward simulations were performed using the degradation rate constant as a fitting parameter to reproduce p-TSA breakthrough measured at the column outlet. However, the degradation rate constant was not applied to the entire solution domain but only in the domain that was progressively occupied by O_2. Retardation was neglected according to findings by Richter et al. (2008b).

Table 3.1 Physical properties and solution domain discretization in the model.

	Parameter	Value	Reference
Solution domain (one-dimensional)	Solution domain extent (m)	0.76	from experiment
	Discretization in quadratic elements	120	
	Degree of freedom	240	
Physical properties	Tortuosity	1.57	$\pi/2$
	Dispersivity (m)	0.0034	from tracer exp.
	Porosity	0.46	from tracer exp.

3.4 Results and Discussion

3.4.1 Groundwater Quality

Groundwater collected from the centre of the p-TSA plume (GAP5UP, Fig. 3.2) has a pH of 7.04. O_2 is absent and therefore the value of Eh is low (-122 mV), indicating a strongly reducing environment. From the calculation of the total hardness the Ca-NH_4-HCO_3-SO_4 type groundwater can be classified as very hard. A summary of the groundwater composition is given in Table 3.2. Regarding NH_4^+, regular measurements at the site were around 62.0 mg L^{-1} (Richter et al., 2009). According to Berner (1981) the anoxic groundwater can be classified as post-oxic to sulfidic. Since the groundwater was collected in the contaminant plume derived from the former sewage farm irrigation, together with the high NH_4^+ concentrations, elevated concentrations of Cl^{-1}, SO_4^{2+} and DOC were encountered. The p-TSA concentration was 34.9 µg L^{-1} at the time of sampling. Median p-TSA concentrations from 5 sampling campaigns between April 2005 and April 2007 were 38.0 µg L^{-1}.

Table 3.2 Results from measurements of physical and chemical parameters of the groundwater collected at the field site.

Component	Unit	Value
pH	-	7.04
T	°C	11
EC	$\mu S\ cm^{-1}$	1053
Eh	mV	-122
O_2	$mg\ L^{-1}$	-
Na^+	$mg\ L^{-1}$	40
K^+	$mg\ L^{-1}$	21
Ca^{2+}	$mg\ L^{-1}$	111
Mg^{2+}	$mg\ L^{-1}$	11
Fe^{2+}	$mg\ L^{-1}$	1.9
Mn^{2+}	$mg\ L^{-1}$	0.4
Cl^-	$mg\ L^{-1}$	60
SO_4^{2-}	$mg\ L^{-1}$	186
NO_3^-	$mg\ L^{-1}$	0.2
PO_4^{3-}	$mg\ L^{-1}$	-
HCO_3^-	$mg\ L^{-1}$	430
NH_4^+	$mg\ L^{-1}$	62*
HS^-	$mg\ L^{-1}$	0.16
NO_2^-	$mg\ L^{-1}$	0.06
DOC	$mg\ L^{-1}$	6.2
p-TSA	μg L-1	34.9

3.4.2 Column Flow and Transport Parameters

Owing to the way the column was operated (by pressure gradient), the flow rate was not constant during the course of the experiment. The water flowing out of the column effluent caused a decrease of the system pressure and therefore a related decrease of the flow rate. To keep the flow rate as constant as possible, argon gas was added to the connected tank twice a day. Fig. 4a shows the flow rate during the entire experiment. During the simulation of anoxic and oxic conditions the average flow rates were 30 ml h^{-1} and 20 ml h^{-1}, respectively.

Inverse fitting of measured EC of the tracer experiment with CXTFIT provided mean values for flow velocity and for dispersion coefficient from which effective porosity and dispersivity values were obtained (0.46 and 0.0034 m, respectively). Since the porosity value is too high for a sediment collected at ~ 30 m depth, we suspect that the installation of the sediment core in the under-pressured system possibly led to a slight disturbance of the sediment. However, considering an effective porosity of 0.46 the calculated residence time during the anoxic conditions was 4.6 days. The residence time during the oxic conditions was 6.9 days. During the last 9 days of the experiment the flow rate decreased to an average value of 16.2 ml h^{-1} and therefore the groundwater residence time increased to 8.6 days.

3.4.3 Oxygen Concentrations in the Column

Fig. 3.4b shows inlet O_2 concentration in groundwater entering the column (at I1, Fig. 3.3) during the experiment, starting 6 days before the addition of compressed air via the pre-column (Fig. 3.3, E) when O_2 concentrations were 0 mg L^{-1}. The O_2 concentrations are expressed in percentage of air saturation and the measured over-saturation was due to the operational pressure (2.2 – 2.4 bars) that enabled a larger amount of O_2 to be dissolved in the water. O_2 detection started 30 minutes after the addition of compressed air. During the entire experiment, O_2 saturation was generally larger than 100 % of air saturation, with a maximum value of about 180 % air saturation corresponding to 47.0 mg L^{-1} of dissolved O_2. As Fig. 3.4b shows, the O_2 concentration was not constant. Fluctuations of the concentration were related to two main factors. Firstly, the pressure of the system tended to decrease with time, leading to a lowering of the water-table, i.e. the air/water interface in the pre-column (Fig. 3.3, E) until the pressure was restored by addition of argon to the connected tank. The second reason was probably the slow but progressive consumption of O_2 inside the pre-column. To maintain >100% air saturation, compressed air was added weekly, replacing the already existing air in the pre-column with new compressed air.

O_2 measurements were also performed in the column outlet (Fig. 3.3, I2), but O_2 was never detected. As expected, the O_2 introduced in the column was consumed by various reactions such as Fe^{2+} oxidation, nitrification, aerobic respiration and DOC degradation.

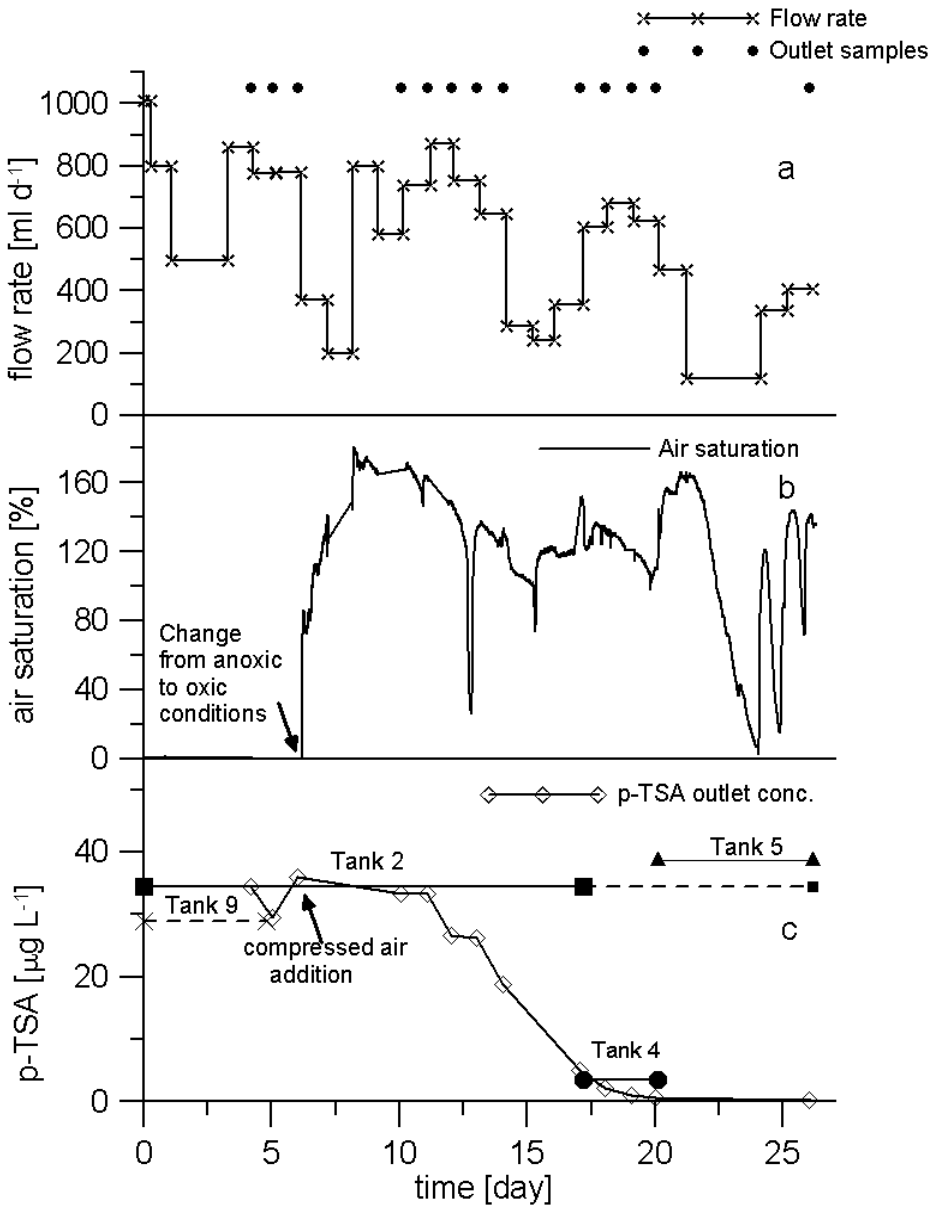

Figure 3.4 Results of the column experiment. (a) Flow rate during the experiment. Black dots indicate the collecting time of the samples from the column outlet. (b) O_2 concentration detected from the inlet optode. Concentrations are expressed as % air saturation. (c) p-TSA concentrations at the column outlet. Also plotted are p-TSA concentrations of the connected tanks indicating time of installation and removal. The dashed lines indicate the effective residence times of the groundwater for each connected tank.

3.4.4 p-TSA Degradation under Anoxic and Oxic Conditions

The sequential use of the four tanks (Nr. 2, 4, 5, 9) providing the inflow and its corresponding initial p-TSA concentrations are compiled in Table 3.3. According to the calculation of the column residence times, only the groundwater belonging to tanks 9 and 2 was sampled at the column outlet during the duration of the experiment, while groundwater

of tanks 4 and 5 did not reach the outlet within the 26 days documented in Fig. 3.4c. The low p-TSA concentration in tank 4 (2.7 μg L^{-1}) is probably related to previous aeration leading to degradation during the storage interval which is in agreement with results of Richter et al. (2009).

Fig. 3.4 shows p-TSA concentrations at the outlet during the entire experiment (see also Table 3.3). No p-TSA degradation was observed during anoxic conditions (previous to the addition of compressed air) and during the 4 days after the addition (Fig. 3.4c). During this period, the input concentrations of p-TSA varied between 29.0 μg L^{-1} (tank 9) and 34.4 μg L^{-1} (tank 2). The p-TSA concentration at the column outlet during the anoxic conditions ranged between 29.5 μg L-^{1} and 33.4 μg L^{-1}. Note that the column had already been equilibrated with groundwater from the site during several months before the beginning of the column experiment. In this period, sporadic samples were collected from the column inlet and outlet in June, October and December 2007. The measurements conducted on these previous samples revealed that p-TSA degradation did not occur at the absence of O_2 (Table 3.4).

Table 3.3 Outlet and inlet concentrations of p-TSA during column experiment. p-TSA concentration is expressed in μg L^{-1}.

Sample	Date	p-TSA
inlet-tank 9	27.05.2008	29.0
inlet-tank 2	11.07.2008	34.4
inlet-tank 4	21.07.2008	2.7
inlet-tank 5	21.07.2008	33.8
outlet----tank 9	15.07.2008	34.5
outlet----tank 9	16.07.2008	29.5
outlet----tank 2	17.07.2008	36.0
outlet----tank 2	21.07.2008	33.4
outlet----tank 2	22.07.2008	33.4
outlet----tank 2	23.07.2008	26.6
outlet----tank 2	24.07.2008	26.3
outlet----tank 2	25.07.2008	18.9
outlet----tank 2	28.07.2008	5.1
outlet----tank 2	29.07.2008	2.1
outlet----tank 2	30.07.2008	1.0
outlet----tank 2	31.07.2008	0.7
outlet----tank 2	06.08.2008	0.3

Table 3.4 Inlet and outlet p-TSA concentration during the column equilibration period.

Sample	Date	p-TSA
inlet	June 2007	31.1
outlet	June 2007	30.9
inlet	Oct. 2007	44.2
outlet	Oct. 2007	44.1
inlet	Dec. 2007	40.3
outlet	Dec. 2007	42.0

Six days after the change to oxic conditions, p-TSA concentrations started to decrease in the outlet, reaching a minimum concentration of 0.3 μg L^{-1} after 26 days (Fig.3.4c). Hence, 99 % of p-TSA was degraded at the end of the experiment and degradation was restricted to oxic conditions only.

Considering a residence time of 6.9 days at the start of the experiment (during oxic conditions), the curve indicates that roughly 50 % of p-TSA breaks through about 6.9 days after the system had been changed to oxic conditions. This behaviour resembles that of an ideal tracer added to the column for a given interval of time (continuous injection) followed by a tracer-free input. In the case of the present experiment, the time interval of the "tracer" application corresponds to the time in which the anoxic groundwater containing p-TSA was continuously entering the column, whereas no p-TSA input seemed to occur thereafter. Therefore, p-TSA must have been degraded very rapidly after conditions turned oxic. Degradation may have started already in the pre-column where concentrations of O_2 were generally above 30.0 mg L^{-1}. As detected by the inlet optode, the residence time from the pre-column to the the sediment column was about 40 minutes. Complete degradation of p-TSA in the water without sediment contact before entering the column is unlikely and contrasts with results from incubation experiments performed by Richter et al. (2009) which showed that p-TSA degradation in water under oxic conditions takes more than 15 days. Also, other authors such as Chapelle (2001) or Holm et al. (1992) reported that the majority of indigenous bacteria which control the degradation process are attached to sediment particles rather than being free in groundwater. p-TSA degradation in the gas phase of the pre-column can be excluded owing to the high solubility of p-TSA

(IUCLID; OECD,1994). Therefore, we conclude that p-TSA degradation occurred mainly within the first centimetres (0-15 cm) the column.

Since p-TSA degradation only takes place under oxic conditions, the part of the sediment which has been oxygenated during the entire experiment can be calculated based on sediment OD (see eq. 3.4). Batch experiments of similar sediments from the same location conducted by the Groundwater Research Institute GmbH Dresden (unpublished data) showed an OD of 200 mg kg^{-1} when the TOC content was 1000 mg kg^{-1}. Since sediments used in the column study had a similar TOC the OD value of 200 mg kg^{-1} was considered as realistic. Considering a sediment bulk density of 2.2 kg dm^{-3} (Horner et al., 2009), a porosity of 0.46 (result from tracer test) and an OD of 200 mg kg^{-1}, the amount of O_2 necessary to oxidize the column sediment is 1.72 g. Since the O_2 provided during the experiment was about 0.32 g, the penetration depth of the O_2 front at the end of the experiment was calculated to be 0.14 m. This allows the p-TSA degradation to be constrained within maximum 0.14 m from the column inlet. As described in eq. 4, the calculation of the transient propagation of the O_2 front during the experiment was carried out considering the daily flow rate, the O_2 concentration measured at the inlet optode every 10 minutes, and the sediment OD. The resulting transient function was applied in Comsol Multiphysics 3.3. Hence, during modelling simulations the degradation rate constant was activated only in the domain where O_2 could spread, while in the remaining part of the solution domain a non-reactive transport model was performed.

On the basis of this modelling approach the best fit of the measured breakthrough curve could be achieved by temporarily increasing degradation rate constants ranging from 2.8E-06 s^{-1} to 6.1E-05 s^{-1} with an intermediate value of 3.3E-05 s^{-1} (Fig. 3.5). The increasing value of the degradation rate constants during the experiment is probably due to the microbial adaption to the change of the redox conditions which has also been reported by other authors (e.g. Fiorenza and Ward, 1992; Meffe et al., 2010).

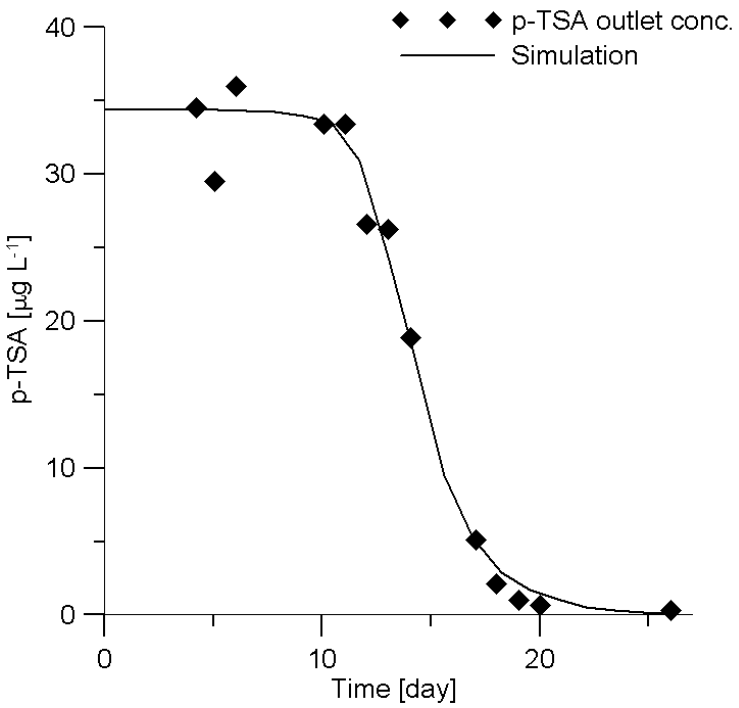

Figure 3.5 Measured and simulated p-TSA concentrations at the column outlet during the whole column experiment.

The magnitude of degradation rate constants differ considerably from results reported by Meffe et al. (2010), who investigated p-TSA degradation during aerated rapid sand filtration and obtained degradation rate constants between 10^{-3} and 10^{-2} s^{-1}. These more elevated degradation rate constants are most likely related to the lack of other electron donors in the sand filter compared to the aquifer material.

3.5 Summary and Conclusions

The present paper shows results of a column study carried out to investigate p-TSA degradation in an aquifer subject to oxygen injection. The following conclusions can be drawn from this study:

- p-TSA is not removed under anoxic conditions, confirming observations from the Berlin field site where p-TSA persists over decades in an anoxic aquifer.
- p-TSA degradation occurred only under oxic conditions. Modelling p-TSA degradation under these conditions resulted in degradation rate constants increasing

from 2.8E-06 to 6.1E-05 s^{-1} as a result of microbial adaption to the changing redox conditions

- p-TSA degradation rate constants in aquifer material are far below values obtained in a study on rapid sand filtration, most likely owing to the presence of electron donors and the differing sediment oxygen demand.

- O_2 (or air) injection as a remediation technology based on O_2 (or air) injection already trialed at the field site for reduction of NH_4^+ was proved to be a suitable strategy for p-TSA elimination.

- Results from this study yield valuable insights into *in-situ* p-TSA degradation and can be applied for future water management strategies at comparable field sites.

4 Fate of para-toluenesulfonamide (p-TSA) in Groundwater under Anoxic Conditions: Modelling Results from a Field Site in Berlin (Germany)

This article reports a combined field and modelling study to investigate the processes controlling the plume evolution of para-toluenesulfonamide (p-TSA) in anoxic groundwater in Berlin, Germany. The organic contaminant p-TSA originates from the industrial production process of plasticizers, pesticides, antiseptics and drugs and is of general environmental concern for urban water management. Previous laboratory studies revealed that p-TSA is degradable under oxic conditions, whereas it appears to behave conservatively in the absence of oxygen (O_2); however, its behaviour under field conditions has not been investigated until recently. p-TSA is ubiquitous in the aquatic environment of Berlin and presents high concentrations in an anoxic aquifer downgradient of a former sewage farm (SF), where groundwater is partly used for drinking water production. To obtain refined knowledge of p-TSA transport and degradation in aquifers at field scale, measurements of p-TSA were carried out at 9 locations between 2005 and 2010. Results showed that p-TSA is retarded in the same manner as chloride (Cl^-), indicating hydraulic retardation due to zones of immobile water. To verify the non-reactive transport behaviour under field conditions, a 2D transport model was setup, applying the dual-domain mass transfer approach. The distribution of Cl^- and p-TSA data from the site was reproduced well, supporting the hypothesis that both compounds behave conservatively being subjected to hydraulic retardation. Prognostic simulations showed that without any remediation measures, the groundwater quality near the drinking water well galleries will be affected by high p-TSA loads for more than a hundred years.

R. Meffe, C. Kohfahl, E. Hamann, G. Massmann, U. Dünnbier, A. Pekdeger

Fate of para-toluenesulfonamide (p-TSA) in groundwater under anoxic conditions: Modelling results from a field site in Berlin (Germany). Submitted to Science of the Total Environment.

4.1 Introduction

Wastewater irrigation

The contamination of the aquatic environment by anthropogenic organic compounds is a matter of great concern, and the increasing attention addressed to this topic is evidenced by numerous investigations (Lindsay et al., 2001, Loss et al., 2007, Soares et al., 2008). A major source of contaminants in urban groundwater is municipal wastewater (WW). Treated WW is discharged into the surface water system and may be introduced into aquifers under influenced conditions (bank filtration). In the past 150 years, the irrigation of untreated WW on sewage irrigation farms was a common practice in many parts of the world and an additional input path for contaminants (Heberer and Stan, 1994; Siebe and Fischer, 1996; Abdel-Shafy et al., 2008). In Berlin, untreated WW irrigation on sewage farms over unprotected aquifers was practised for more than one century until the 1980s, contaminating soils and downgradient groundwater with nutrients (N and P), heavy metals (Cu, Pb and Zn) and several organic contaminants (i.e., phenols) (Hoffmann et al., 2000; Scheytt et al., 2000).

p-TSA general aspects

The organic contaminant studied in the present paper is para-toluenesulfonamide (p-TSA). It originates from WW and is applied as a plasticizer and an intermediate for pesticides and drugs (OECD, 1994). p-TSA is the primary degradation product of the antiseptic chloramine-T in water. Chloramine-T is used as an antimicrobial agent in the food industry to disinfect surfaces, instruments and machines and also as a therapeutic drug for bacterial gill disease of fish and for bacterial diseases of swine and poultry (Beljaars et al., 1994; Meinertz et al., 1999; Haneke, 2002). p-TSA is slightly toxic to algae, but non-toxic to fish and daphnids (Haneke, 2002). Overall, its toxicity can be classified as moderate, and additional tests are recommended if large amounts of p-TSA are used in consumer products in the future (OECD, 1994). According to the German Federal Environmental Agency, the tolerable concentration limit in drinking water is 0.3 $\mu g\ L^{-1}$ (Grummt and Dieter, 2006).

Previous studies on p-TSA

p-TSA was found in WW, surface water, groundwater and raw water used for drinking water production in Berlin (Richter et al., 2008a), but only few studies have addressed p-TSA behaviour in groundwater. Previous studies including incubation and column experiments showed that p-TSA is degradable under oxic conditions, but appears to behave conservatively in the absence of oxygen (O_2) (Richter et al., 2008a, Meffe et al., 2010, Meffe et al., submitted 2010a). A large plume in the anoxic aquifer of the study area located upgradient of a drinking water treatment plant (DWTP) published by Richter et al. (2009) raised concerns because the concentration exceeded the recommended threshold value for drinking water (0.3 μg L^{-1}) by a factor of 100. According to a numerical study based on a conventional advection-dispersion 3D flow model carried out by Hamman (2009), p-TSA should have already been washed out during the past three decades under the given hydraulic conditions. Therefore, only hydraulic retardation would explain the elevated concentrations of p-TSA, assuming conservative behaviour that has not been verified at field scale until recently.

Therefore, a 2D transport model was set up to quantitatively evaluate the main processes controlling p-TSA transport under anoxic conditions at field scale. Available long-term chloride (Cl^-) data were used for calibration. The aims of the approach were (i) to explain the long-term presence of p-TSA in the groundwater, (ii) to verify the assumption that p-TSA behaves conservatively under anoxic conditions and (iii) to obtain a model with prognostic value to assess future p-TSA concentrations for water management issues.

4.2 Site Description

The study site is located south-east of Berlin, upgradient of Lake Müggelsee, and includes a former sewage farm (Münchehofe SF), a drinking water treatment plant (Friedrichshagen DTWP) with its well galleries, and a monitoring network of wells (Fig. 4.1). It is located in the Warsaw-Berlin glacial valley, bounded to the north by the Barnim plateau. The aquifer consists of Pleistocene glaciofluvial sands, which are not subdivided by aquitards owing to the lack of glacial tills in this area (Engelmann et al., 1992). The sands are about 50 m thick with an average hydraulic conductivity of 10^{-4} m s^{-1} (BWB, 2007). The aquifer

bottom corresponds to the top of the Holstein aquitard, showing local geological windows in the southern part that are associated with ascending deep groundwater (BWB, 1995).

Groundwater flow is nowadays anthropogenically influenced only by the DWTP well galleries; until 1976 it was also affected by the operation of Münchehofe SF. The main groundwater flow direction is from NNE to SSW with an average velocity of 0.3 m d^{-1} (Hamann, 2009). The former Münchehofe SF is located in the northern part of the site and covers an area of about 1.2 km^2. The Friedrichshagen DWTP is situated in the proximity of Lake Müggelsee shore and close to the well galleries B, C, D, E for raw water abstraction. Near Lake Müggelsee, bank filtration is caused by abstraction at the DWTP well galleries. The well gallery A located further inland serves as a warning protection gallery adverting the contamination plume. Between the Münchehofe SF and the Friedrichshagen DWTP, the groundwater quality at the field site is monitored by a dense network of 69 monitoring wells screened at different depths (between 3.5 m and 87.3 m below surface). In principle, the groundwater contamination at the site stems from irrigation of untreated WW at the former Münchehofe SF (BWB, 1992).

The beginning of the Münchehofe SF operation dates back to 1906, and the untreated WW irrigation continued without interruption until 1976. From 1955 onwards, WW volumes exceeded the sewage farm capacity owing to increased industrial activity. Continuous overload of the irrigation fields led to anoxic conditions in the unsaturated zone and decreased the remediation capacity of the sediments, resulting in high concentrations of contaminants such as ammonium (NH_4^+), dissolved organic carbon (DOC), and p-TSA (BWB, 1992). Starting in 1976, the irrigation fields were flooded with treated WW from a nearby wastewater treatment plant (Münchehofe WWTP). In addition, sludges used during treatments at the Münchehofe WWTP were deposited on the irrigation fields until 1991, the year in which the SF was definitively closed.

Previous studies in the past 10 years at the field site focused on investigation of the NH_4^+ plume, using field data and numerical reactive transport models to forecast the decontamination time and the feasibility of remediation activities (BWB, 2000, Hamann, 2009, Horner, 2009). Hamann (2009) applied a cation exchange approach to simulate the NH_4^+ plume evolution, predicting that NH_4^+ concentrations above 10 mg L^{-1} have to be expected at the DWTP well gallery B for more than 200 years. Horner et al. (2009) used a multireactive transport model to test the efficiency of in-situ enhanced bioremediation of

NH_4^+ tested at a pilot plant in an area located near the southern boundary of Münchehofe SF (Fig. 4.1). As already mentioned, Richter et al. (2009) described high p-TSA concentrations at the site. Since 2007, the Berlin Water Company (BWB) has performed O_2 gas injection in a subsection of the aquifer to test this remediation technology with regard to the removal of NH_4^+. Preliminary results showed that p-TSA and NH_4^+ concentrations decrease as a result of the O_2 injections.

Considering the dense hydrogeological information available, this area constitutes an outstanding location for studying the fate of p-TSA in groundwater under anoxic and oxic conditions at field scale, which has not been done before.

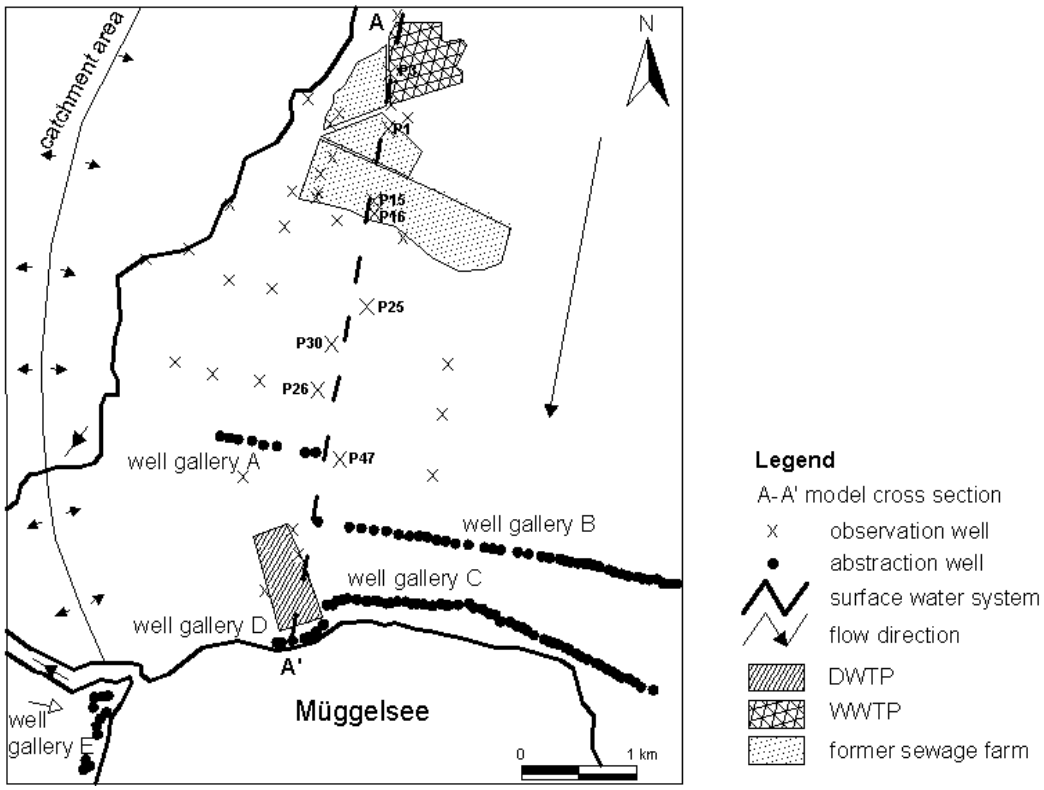

Figure 4.1 Map of the study site with location of the Friedrichshagen drinking water treatment plant (DWTP), and the wastewater treatment plant (WWTP) and former sewage farm Münchehofe. Also shown is the western boundary of the catchment area of the Friedrichshagen DWTP, the monitoring wells, abstraction wells, and stream lines. The line A-A' indicates the transect along which the 2D transport model was performed (modified from Richter et al., 2009). The monitoring wells used for model calibration are indicated with their acronyms.

4.3 Material and Methods

4.3.1 p-TSA Sampling and Analysis

Sampling network and frequency

p-TSA sampling at the field site started in 2005, when an analytical method for p-TSA detection in groundwater was first developed (Richter et al., 2007). Sampling and analyses were performed by BWB at least twice a year at the monitoring wells and once a month at well galleries A and B located along transect A-A' (Fig. 4.1). p-TSA data at the field site generally consist of 10 measurements at the monitoring wells, with the exception of monitoring well P30 MP, located approximately 1000 m downgradient from Münchehofe SF, where 4 p-TSA measurements were performed. At the well galleries A and B, p-TSA measurements were conducted more frequently than in the monitoring well, and therefore the data set is much larger. Cl^- data were obtained from previous studies since 1919 at the well gallery A and since 1994 at the monitoring wells.

Sampling method and analytics

For each sampling well and sampling campaign, 250 ml of groundwater were filled in glass bottles, avoiding introduction of O_2, and stored in the refrigerator at 4 ºC. p-TSA sample extraction and analysis were performed within two days after sampling. Sterilization of the sampling equipment was unnecessary, as shown by trials performed by Richter et al. (2008b).

The analytical method is based on sample preparation by solid-phase extraction followed by liquid chromatography (HPLC) separation coupled to tandem mass spectrometry (MS/MS) (Richter et al., 2007).

Data interpolation

To obtain concentration distributions of Cl^- and p-TSA along transect A-A', field data of the sampling campaign carried out in March 2010 (no. of measurements: 22) were interpolated using the modified Sheppard's method with Surfer 8 (Golden Software Inc., 2002).

4.3.2 Numerical Modelling

Modelling software

A vertical 2D model was set up with PMWIN 8 (Chiang and Kinzelbach, 2001), using the modules Modflow (McDonald and Harbaugh, 1998) for flow simulation and MT3DMS (Zheng and Wang, 1999) for solute transport simulations. MT3DMS uses the output hydraulic heads and cell by cell flow data computed by Modflow to establish the flow field to carry out the transport simulation.

Spatial discretization

Discretization, model setup and input parameters are compiled in Table 4.1. The vertical 2D transport model is orientated along the main groundwater flow direction (NNE-SSW); it has a longitudinal extension of 4600 m and a vertical thickness of 50 m, determined by the top of the Holstein aquitard which represents the lower boundary condition (Fig. 4.1). The solution domain was divided into 83 columns and 10 layers, each about 5 m thick (Table 4.1). The mesh in the inner part of the solution domain (columns 10-116) was refined to minimize the influence of the boundaries on the flow field. In this model region, the grid spacing is 50 m in the x-direction. In the remaining model domain, the resolution of the model grid was 100 m in the x-direction. Flow was calculated for a normalized width of 1 m. The base of the model corresponds to the top of the Holstein layer, which is underlain by sediments with considerably reduced hydraulic conductivities. The base of the model was assumed to be impermeable.

Table 4.1 Physical and chemical parameters used in the MT3DMS simulation.

	Parameter		Value
Physical Parameters	Longitudinal Extension (m)		4600
	Mesh Discretization	columns	83
		layers	10
	Model Thickness (m)		~ 50

	Parameter		Value
Initial conditions	Initial Cl^- concentration (mg L^{-1})	Co_{Cl}	16(1)
	Initial p-TSA concentration (μg L^{-1})	$Co_{p\text{-}TSA}$	0
	Cl^- input concentration (mg L^{-1})	C_{Cl}	240

	Cell	Type	Value
Transport Conditions **Boundary**	***for Cl- simulation***		
	column 1 *(northern boundary)* (mg L^{-1})	Dirichlet	16(1)
	column 83 *(southern boundary)* (mg L^{-1})	Dirichlet	16(1)
	for p-TSA simulation		
	column 1 (northern boundary) (μg L^{-1})	Dirichlet	0
	column 83 (southern boundary) (μg L^{-1})	Dirichlet	0

Calibration Parameters	dispersivity	α_L
	mobile porosity	θ_m
	immobile porosity	θ_{im}
	mass transfer rate coef.	β
	p-TSA input conc.	$C_{p\text{-}TSA}$

Flow parameters and boundary conditions

The 2D vertical transport model developed in this study used the flow parameter distribution and boundary conditions of the 2D flow model of Hamann (2009), which has been calibrated for hydraulic heads and for Cl^- and NH_4^+ concentrations at the well gallery A. The flow model was able to reproduce the measured heads and concentrations. The values assigned for hydraulic conductivity vary between 5.21E-05 and 1.73E-03 m s^{-1} (Table 4.1). The upstream boundary was defined as a constant head boundary, using the

average value of the hydraulic heads measured at the monitoring wells located in the northern part of the model region (Table 4.1). A constant head boundary was also defined in the upper cell of the southern boundary, which corresponds to the level of Lake Müggelsee (Table 4.1).

Sources and sinks / temporal discretization

A time invariant value of 150 mm y^{-1} estimated from the annual precipitation (SenStadt, 2007) was applied for the natural recharge by precipitation to the upper layer of the model domain.

The simulation time covered a period from 1906 (when Münchehofe SF started to operate) to 2016. The total simulation time was discretized in 64 stress periods of variable extent in accordance with the available data. To predict the p-TSA plume evolution at the DWTP well gallery B, the simulation time was extended to 129 years, until the year 2145, therefore 26 five-year stress periods were added. The WW irrigation was simulated with the recharge package of Modflow. The amount of irrigated WW was extremely variable and was defined for each stress period on the basis of measurements performed by BWB (1992). Pumping rates of the well galleries were specified at the corresponding model cells for each stress period, using the well package of Modflow in accordance with unpublished BWB data.

Transport parameters and boundary conditions

For the solute transport simulation, a Dirichlet type boundary was defined for Cl^- and p-TSA in the northernmost cells for the entire model thickness (Table 4.1). The same Dirichlet boundary condition was applied in the cells immediately downgradient of the well gallery B, assuming that the groundwater pumped at well gallery B is mainly the bank filtrate of Lake Müggelsee and not affected by contamination from Münchehofe SF. With this option, the extent of the transport model and the computation time decreased.

Since no reliable initial Cl^- and p-TSA concentrations of the groundwater at the field site were available, the specified initial concentrations were derived from measurements done in the nearest uncontaminated area (Table 4.1) (BWB, 1992). Assuming that Cl^- concentration in the irrigated WW did not change, a constant Cl^- concentration of

240 mg L^{-1} was applied following Henze et al. (1995), using the recharge package of MT3DMS in the part of the solution domain that corresponds to the irrigation fields of Münchehofe SF (columns 16-37). The Cl^- contamination source was activated for the entire period of SF operation (from 1906 to 1991). The same procedure was followed for p-TSA transport simulation, but p-TSA input via sewage irrigation was activated for the period from 1916 to 1976. 1916 was used as the starting year because chloramine-T, the primary p-TSA source, was discovered in 1916 (Haneke, 2002). After 1976, treated WW was irrigated on the SF irrigation fields. Since WW treatment involves aerobic reaction steps, p-TSA is largely removed during WW treatment and the input was assumed to be negligible (Richter et al., 2008a). Therefore, p-TSA concentrations in the irrigated WW were used as calibration parameters (Table 4.1).

The longitudinal dispersivity (α_l, where $D= \alpha_l v_i$) was considered to be uniform in the whole solution domain and was calibrated during modelling procedure. The ratio of the vertical dispersivity (α_v) to α_l was set at 0.01. Finally, also the effective porosity (θ) in the advection-dispersion approach was calibrated to obtain a reasonable simulation result.

Dual-domain mass transfer approach

To account for the hydraulic retardation indicated by the field data, the advection-dispersion approach was successively upgraded by the dual-domain mass transfer approach. The dual-domain mass transfer approach assumes that a porous medium is conceptually divided into two overlapping domains: a mobile domain, in which transport is dominated by advection, and an immobile domain, in which transport occurs essentially by molecular diffusion. Solute exchange between the two domains is characterized by a mass transfer relationship driven by a concentration difference between the two domains. Several authors described the dual-domain method and demonstrated that it is helpful to simulate transport in heterogeneous media (van Genuchten and Wierenga, 1977; Haselow and Greenkorn, 1991; Hamm and Bidaux, 1996).

The governing equation for the dual-domain mass transfer model can be written as (Feehley et al., 2000):

$$\theta_m \frac{\partial C_m^k}{\partial t} + \theta_{im} \frac{\partial C_{im}^k}{\partial t} = \theta_m \frac{\partial}{\partial x_i}\left(D_{ij} \frac{\partial C_m^k}{\partial x_j} \right) - \theta_m \frac{\partial}{\partial x_i}\left(v_i C^k\right) + q_s C_s^k \qquad \text{(eq. 4.1)}$$

$$\theta_{im} \frac{\partial C_{im}^k}{\partial t} = \beta \cdot \left(C_m^k - C_{im}^k\right) \qquad \text{(eq. 4.2)}$$

where θ_m is the porosity of the mobile domain, θ_{im} is the porosity of the immobile domain, C_m^k (M L^{-3}) and C_{im}^k (M L^{-3}) are the solute concentrations of the species *k* in the mobile and in the immobile domain, respectively, t is the time (T), $x_{i,j}$ is the distance along the Cartesian axis (L), D_{ij} is the hydrodynamic dispersion and diffusion coefficient (L^2 T^{-1}), v_i is the pore water velocity (M T^{-1}), q_s is the source/sink term (T^{-1}), β is the first-order mass transfer rate coefficient between the mobile and the immobile domains. As β increases, the dual-domain mass transfer model becomes a single domain model with a porosity approaching the total porosity of the porous medium. When β is very small, the right-hand side of Eq. 4.2 approaches zero and the model is reduced again to a single domain model with a porosity that is the effective porosity. β can be determined by laboratory experiments or through trial-and-error model calibration (Feehley, 2000).

In the solution domain, where dual-domain mass transfer approach was applied, θ_m, θ_{im} and β were set time and space invariant and used as calibration parameters.

4.4 Results and Discussion

4.4.1 Cl^- and p-TSA Field Data

Cl^- and p-TSA concentration along the cross section A-A' are given in Fig. 4.2. High concentrations of Cl^- and p-TSA can be encountered throughout the entire aquifer between Münchehofe SF and the DWTP well gallery.

Both Cl^- and p-TSA show similar distribution patterns characterized by increasing concentrations with flow direction and a vertical distribution with maximum concentrations at intermediate depths. The lowest levels of Cl^- and p-TSA in the entire aquifer occur (i) close to the northern boundary owing to uncontaminated groundwater

inflow and (ii) in the upper 10 m of the aquifer below Münchehofe SF owing to natural groundwater recharge. Here, the concentrations vary between 7 and 20 mg L^{-1} for Cl^- and between 0.1 and 1 µg L^{-1} for p-TSA. A further similarity is that Cl^- and p-TSA concentrations remain elevated below the central and southern part of the SF at depths between 15 and 40 m below surface, although WW irrigation at Münchehofe SF stopped in 1976.

Differences of the concentration patterns can be observed below P26 at about 40 m depth where elevated Cl^- concentrations (about 110 mg L^{-1}) are due to intrusion of deeper groundwater through a geological window of the Holstein aquitard that hydraulically connects the studied aquifer with the deep saltwater-bearing aquifer below (BWB, 1995). The rising groundwater influences also the Cl^- concentration at the downstream monitoring well P47 (at a depth of about 30 m) and at the well gallery B (at a depth of about 35 m) with concentrations of 80-90 mg L^{-1} above the average Cl^- content in the remaining aquifer (40-50 mg L^{-1}). This phenomenon only affects the deeper part of the downstream aquifer, which is of minor relevance for the objective of this study and was therefore not considered in the simulations.

Hamann (2009) stated that Cl^- should have been washed out of the aquifer below the Münchehofe SF 20 years after its definitive closure, assuming conservative transport and a mean Darcy velocity of 0.3 m d^{-1} in a homogeneous aquifer. The question is how to explain the retarded transport of Cl^- and therefore p-TSA, assuming the conservative behaviour of both components, as indicated by the similarity of their distribution patterns. We state that the persisting elevated concentrations in the entire aquifer and in particular the high concentrations of both the species below the SF can be explained by the occurrence of domains with immobile water phases caused by low permeable layers which lead to “hydraulic retardation” that delays the solute transport. This is supported by several representative boreholes performed by the BWB between 1996 and 1998 below the south-western boundary of the SF, pointing to a strong local heterogeneity of the aquifer below the SF, which is subdivided here by silty and fine sand layers at different depths (BWB, 1992).

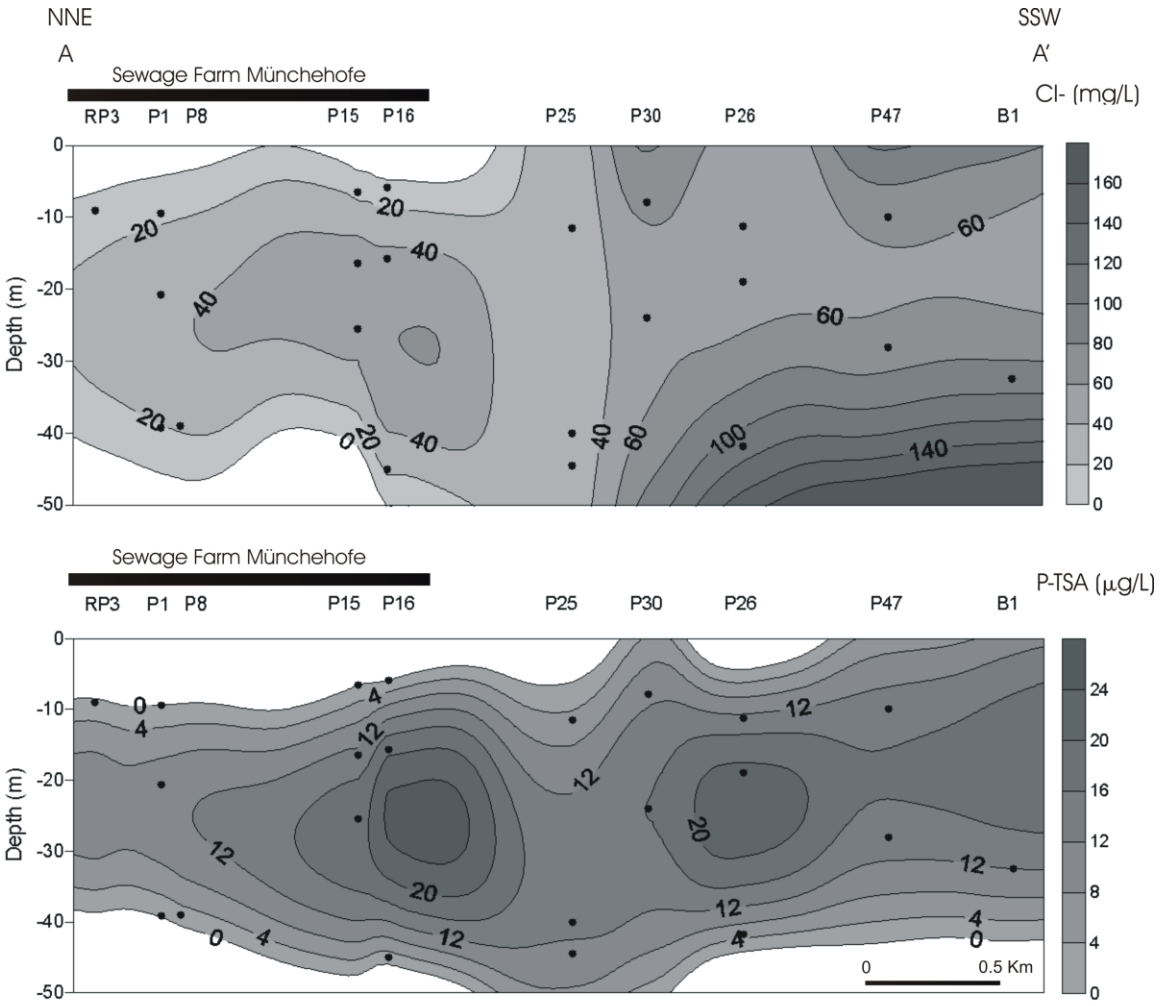

Figure 4.2 Cl^- and p-TSA distribution in the aquifer along the transect A-A' resulting from measurements performed in March 2010. The isolines of concentration were interpolated using the modified Sheppard's method. The black dots in the maps indicate the points where measurements were performed.

4.4.2 Modelling

Model calibration

In the first simulation, a standard advection-dispersion approach was used to fit the measured breakthrough curve of Cl^- at the well gallery A, using porosity (θ) and longitudinal dispersivity, (α_l) as calibration parameters. Results showed that the measured tailing of Cl^- following the breakthrough could not be reproduced by the standard advection-dispersion approach (Fig. 4.3)

As discussed above, high concentrations of Cl^- and p-TSA below Münchehofe SF can be explained by the occurrence of low permeability layers in which transport is driven by

molecular diffusion. The strong heterogeneity of the area below the SF is probably due to proximity to the edge of the glacial valley. Therefore, the standard advection-dispersion approach was upgraded by a dual-domain mass transfer approach that accounts for these aquifer heterogeneities below the Münchehofe SF. The parameters θ_m, θ_{im} and β were used as additional calibration parameters. Simulation results yield a satisfactory fit of the Cl^- breakthrough at the well gallery A and of the Cl^- tailing phase at the intermediate monitoring wells. The best fit of measured Cl^- data was obtained with the parameter combination given in Table 4.2, and the calibration results are shown in Fig. 4.3. As discussed above, a concentration of 240 mg L^{-1} Cl was defined for the irrigated WW following Henze et al. (1995). The value of α_l in the calibrated model (100 m) is in the range of reasonable values for the simulated aquifer scale (Gelhar et al., 1985). The value of β, which may vary temporarily under transient conditions (Jørgensen et al., 2004), was approximated by an average value. At the MADE (Macrodispersion Experiment) site, Feenhley et al. (2000) found values of β ranging between 0.0005 and 0.001 d^{-1} for high and low aquifer heterogeneity, respectively. Hence, the value of β resulting from this study (0.00003 d^{-1}) – which is an order of magnitude lower than those obtained by Feehley et al. (2000) – indicates a strong aquifer heterogeneity below the Münchehofe SF.

The calibration procedure applying different values for calibration parameters showed that β has a larger impact on the simulation results than θ_{im}.

Table 4.2 Parameter data set for calibration of the transport model.

Calibration Parameters		Value
dispersivity (m)	α_L	100
mobile porosity (DD)	θ_m	0.2
immobile porosity (DD)	θ_{im}	0.3
mass transfer rate coef. (d^{-1}) (DD)	β	3.0E-05
effective porosity (AD)	θ	0.2
p-TSA input conc. (mg L^{-1})	$C_{p\text{-}TSA}$	0.1

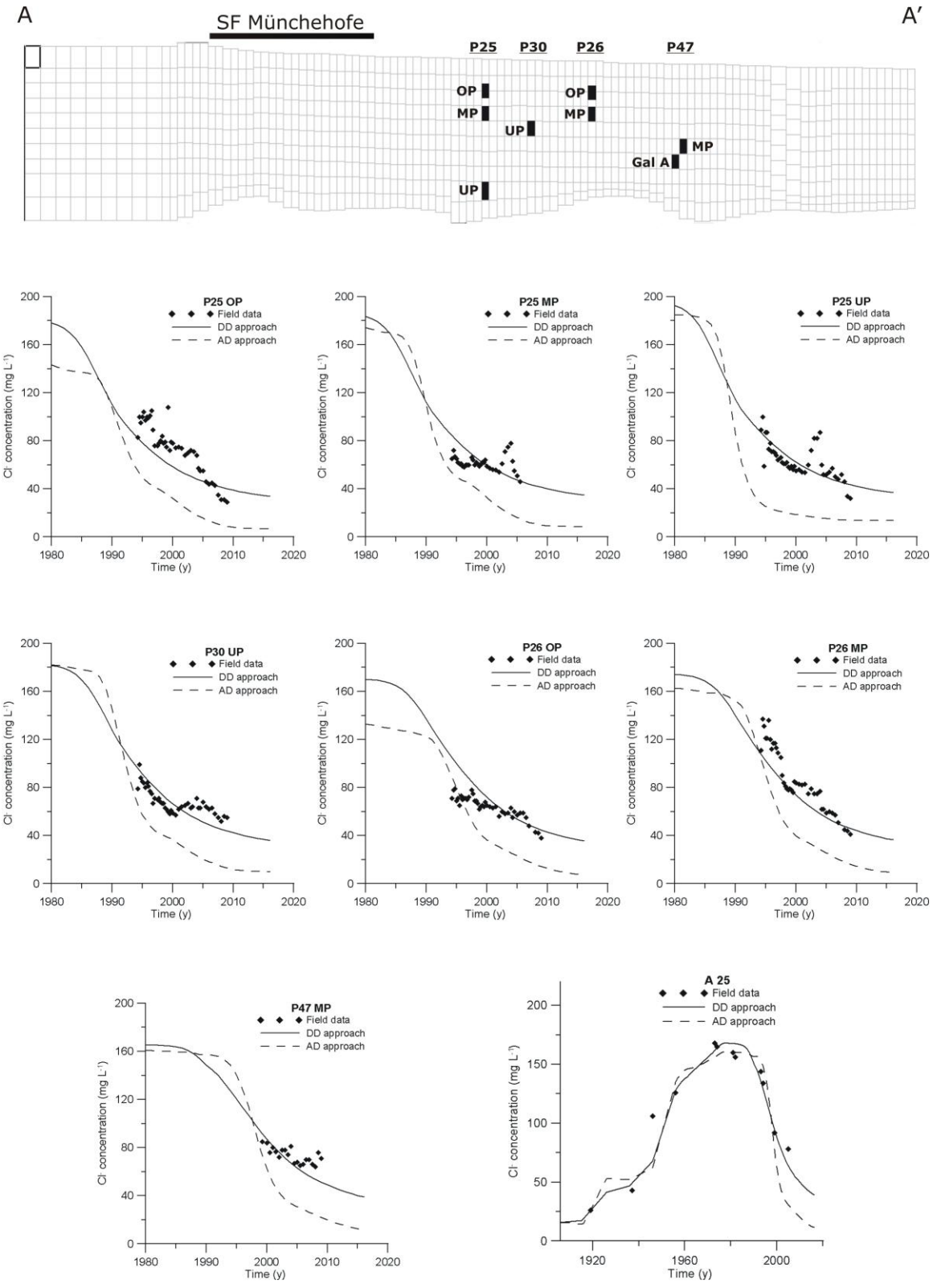

Figure 4.3 Simulation results for Cl^-. The solid line represents simulation results obtained applying the dual-domain mass transfer approach (DD approach), and the dashed line represents simulation results obtained by applying the standard advection-dispersion approach (AD approach). The image in the upper part of the figure is the cross section of the model solution domain with the intermediate monitoring wells and the well gallery A.

p-TSA transport simulation

p-TSA plume propagation in the aquifer was simulated with the transport model calibrated against Cl^- breakthrough curves. The values of β and θ_{im}, calibrated during Cl^- transport simulation, were maintained fixed, like all the other transport parameters. Unknown p-TSA input concentrations ($C_{p\text{-}TSA}$) in the irrigated WW were estimated on the basis of concentrations observed at the study site since 2005 and were used to fit p-TSA breakthrough curves. A technical report by Haneke (2002) described how chloramine-T was used intensively in Germany during the second world war, but no information on the specific amount is available. Although the p-TSA load of irrigated WW may have changed over time, it was assumed that temporal variations were considerably attenuated by mixing and dispersion, after having passed the unsaturated zone. Therefore, the unknown input concentrations were approximated by a time constant concentration which has to be considered as an average value.

The best fit of field data resulted from the application of an average p-TSA concentration of 0.1 mg L^{-1} in the irrigated WW (Fig. 4.4). Comparison with p-TSA concentrations of WW at other field sites is not possible since no data on p-TSA concentration during SF contamination are available in the literature so far. However, a concentration of 0.1 mg L^{-1} seems to be a reasonable value considering that in other areas of the same aquifer some monitoring wells currently reveal p-TSA concentrations of up to 0.04 mg L^{-1}. The simulations were able to reproduce the range of p-TSA concentrations in almost all the monitoring wells, confirming the reliability of the model. The temporal variability of measured concentrations may be related to transient input p-TSA concentrations ($C_{p\text{-}TSA}$) not considered in the model. Results show that the model is able to reproduce transient concentrations of two components at 4 different locations and in different depths.

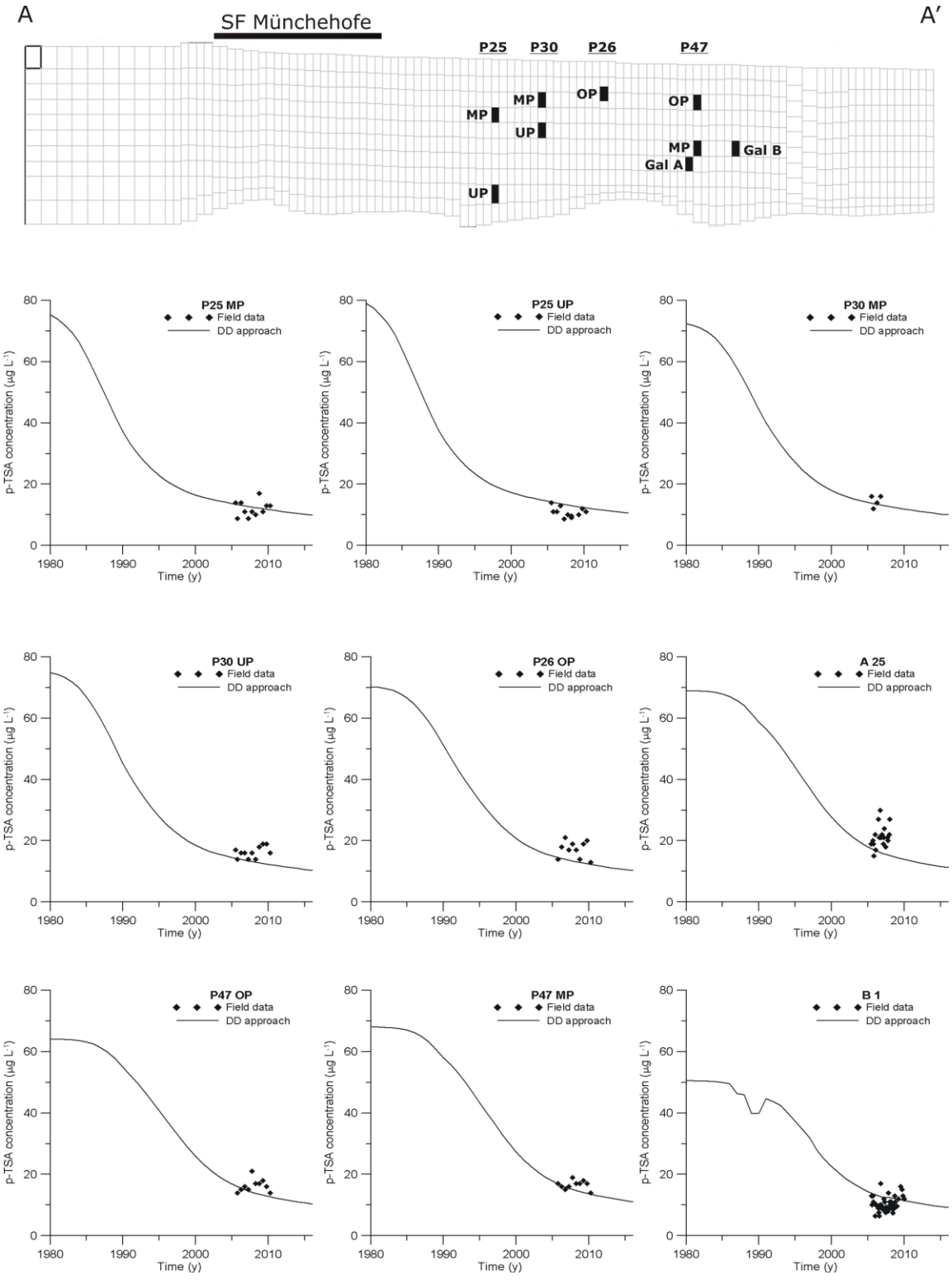

Figure 4.4 Simulation results for p-TSA obtained by applying the dual-domain mass transfer approach (DD approach). The image in the upper part of the figure is the cross section of the model solution domain with the intermediate monitoring wells and the well galleries A and B.

Predictive simulations

After a satisfactory fit of present p-TSA concentration was achieved at the field site, a predictive simulation was performed to investigate the evolution of p-TSA concentrations at the abstraction well gallery B. The simulation time of the former transport model was increased by 129 years (until 2145). The new simulation was carried out, assuming that all the sink and source terms applied in the flow simulation such as recharge by precipitation and well pumping rates will remain constant during the whole additional period of simulation and equal to those of the last time-step of the previous simulation.

Fig. 4.5 shows the predicted p-TSA concentrations at the abstraction well gallery B (well 1). It becomes evident that the p-TSA concentration will exceed the drinking water limit established by the German Federal Environmental Agency (0.3 $\mu g\ L^{-1}$) for the next 131 years (until 2141) if no aquifer remediation activities are applied. The predictive simulation shows that pollution due to untreated sewage irrigation entering unprotected aquifers – as was practised in large areas throughout Berlin and many other places worldwide (Xu et al., 2010, Li et al., 2009) – will continue to be problematic under anoxic conditions for a very long period of time. The tailing of compounds that should have been washed out of the system according to the conventional advection-dispersion model can be explained with the dual-domain mass transfer approach. Therefore, the present example illustrates that aquifer heterogeneities cannot be neglected and low permability zones may serve as sources of contaminants decades after the original contamination source was eliminated. This is particularly important when deciding on the possibility of applying a remediation technology at the field site. Underestimating the aquifer decontamination time would lead to a wrong decision.

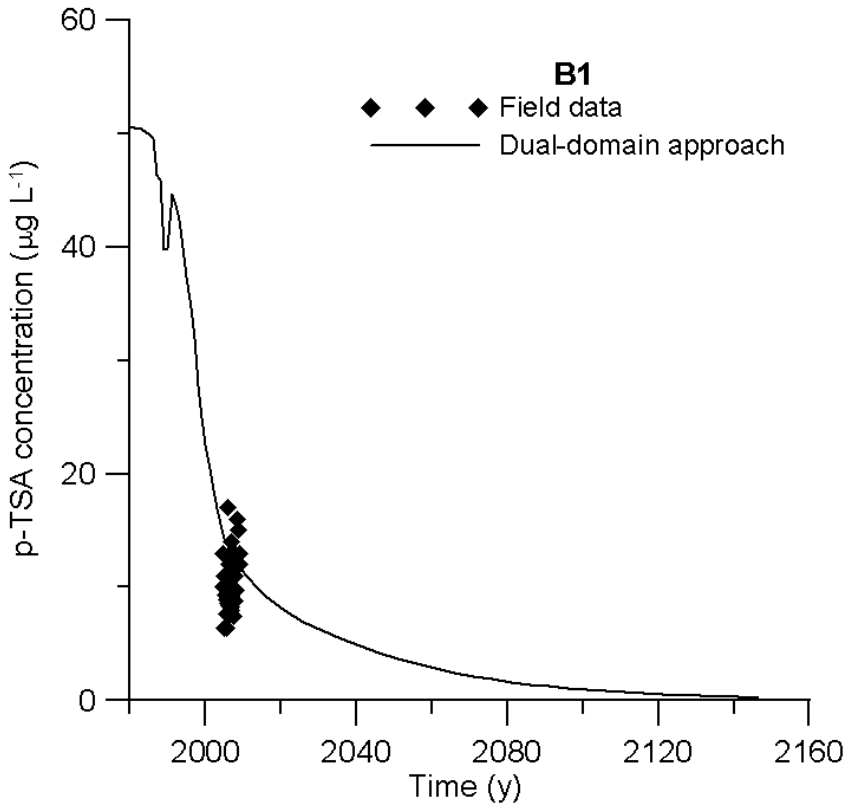

Figure 4.5 Results of the predictive simulation for p-TSA at the abstraction well gallery B.

4.5 Conclusion

The major findings obtained by the present study are:

- Field data processing showed that Cl^- and p-TSA concentrations in the studied aquifer have a similar distribution pattern, suggesting that p-TSA behaves like a conservative component under anoxic conditions.
- Conservative transport behaviour of p-TSA at field scale was verified by non-reactive model simulations under anoxic condions.
- The dual-domain mass transfer approach enabled present p-TSA concentrations in monitoring and abstraction wells to be reproduced, illustrating how immobile water phases in heterogeneous aquifers can lead to hydraulic retardation of otherwise conservative compounds.
- A reliable model was set up to perfom predictive simulations of future p-TSA loads for drinking water management and remediation issues.

5 Application of the In Situ Air Sparging Technique

5.1 Introduction

In-situ air sparging (IAS) is one of the most popular remediation techniques for the treatment of groundwater contaminated by volatile and non-volatile compounds. IAS consists of air or oxygen (O_2) gas injections to remediate groundwater by removing trapped immiscible contaminants through volatilization as well as dissolved contaminants through enhanced biodegradation (Johnson et al., 2001). When IAS is aimed to remove volatile contaminants, the technique is integrated with a soil vapor extraction (SVE) system (Johnson et al., 2001). When IAS is intended to remediate contaminants dissolved in groundwater, the air/O_2 injection rates have to be able to maintain a well-oxygenated treatment zone by reducing the volatilization rates so that an SVE system is not anymore necessary. This last operation mode is often called by practitioners "biosparging" to emphasize the fact that the system aims to enhance the biodegradation of the contaminants supplying through low injection rates the optimal amount of O_2 into the aquifer (Johnson et al., 2001). The IAS system can be implemented to: i) treat contamination source zone; ii) remediate dissolved contamination plumes; iii) provide barriers to prevent dissolved contaminant plume migration. A schematic design of a standard IAS system is represented in Fig. 5.1.

IAS was first applied in Germany in 1985 (Brown, 1994) and, was successively implemented in the United States in 1989 (Schaffner and Juneau, 1995). IAS has been successfully carried out at several field sites to remediate petroleum hydrocarbon (Marley et al., 1992; Reddy et al., 1995; Johnston et al., 1998) and chlorinated compounds (Bass and Brown, 1995; Bass et al., 2000). However, IAS is a relatively new technology which is affected by processes that have so far not been fully controlled (Aivalioti et al., 2008). Since the mid-1990s, several research activities have been carried out to gain a better comprehension of IAS performance. This effort is attested by the increasing number of investigations on air flow visualization and characterization, mass transfer studies in physical models, pilot testing, design issues and performance monitoring approaches (Johnson et al., 2001). However, it appears that valuable knowledge obtained from these

studies has yet to be integrated into practice (Johnson et al., 2001). Therefore, predictions on the capability of IAS to remove a specific contaminant suffer from many uncertainties characterizing this remediation technology.

Since 2007, the Berlin Water Company (BWB) is applying an IAS system using air and O_2 gas to a limited portion of the studied aquifer to test if this remediation technology is able to remove ammonium (NH_4^+) which was found in the aquifer with concentration up to 80 mg L^{-1}. Since p-TSA appears to be redox sensitive (Richter et al., 2008b; Meffe et al., 2010; Meffe et al., submitted 2010a), air/O_2 injections in the aquifer could be a suitable strategy for removing from the groundwater also p-TSA.

In the following sections the IAS system will be described and the results obtained from three years of its application will be presented and discussed. A multi component reactive transport model was set up to investigate the hydro-geochemical changes caused by the O_2 injections and to carry out prognostic studies. The results of the modelling will be given and discussed.

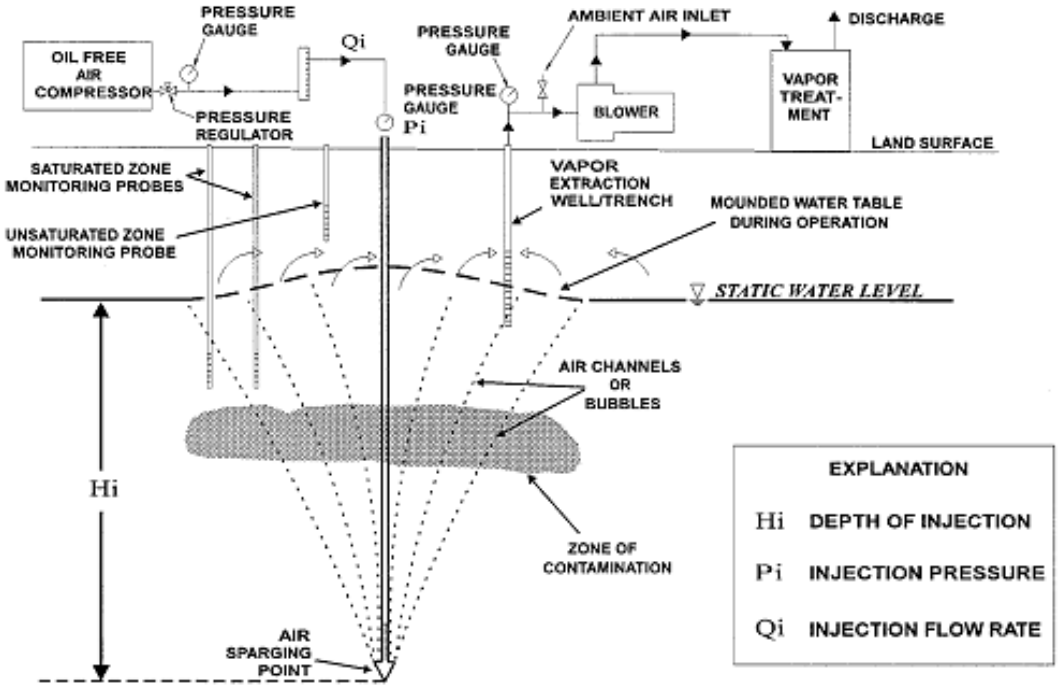

Figure 5.1 Schematic design of a standard in situ air sparging (IAS) system (from Suthersan, 1999).

5.2 Field site

5.2.1 Geological and Hydrogeological Setting

A correct procedure for the development of an IAS system includes a detailed characterization of the subsurface from a geological perspective. In fact, the effectiveness of an IAS system depends on the gas distribution in the aquifer which is strongly related to the heterogeneities of the porous media (Tsai, 2008). A reliable conceptual model for the gas distribution in the subsurface is not only used for feasibility assessments but also for IAS design since it helps to identify the minimal spacing between injection wells.

Therefore, the BWB carried out an extensive geological characterization of the aquifer at the field site (Fig. 5.3). Fig. 5.2 shows the geological section of the aquifer where the IAS system was implemented. The unconfined aquifer which has a thickness of approximately 50 m consists of coarse, medium and fine sands of the Pleistocene glaciations (Engelmann et al., 1992). The hydraulic conductivity varies between 1E-05 and 1.5E-03 m s^{-1}. The bottom of the aquifer corresponds to the top of the Holstein aquitard. The layering is mainly sub-horizontal. On the basis of the sediment characteristics, the aquifer can be divided into five depositional sediment units of approximately 10 m of thickness. At the site, these units were called with the following acronyms: OP, MP1, MP2, MP3, UP (Sensatec, 2009). A detailed description of the depositional sediment units is given in Table 5.1. The top and the bottom of the unit MP1 and the bottom of the unit MP3 are characterized by low permeability layers of silty and clayey sediments that extend laterally for two thirds of the cross section. These layers probably represent barriers for the vertical gas flow towards ground surface during the injections (Sensatec, 2009).

The water table of the unconfined aquifer varies between 3.5 m and 5 m below ground surface. The fluctuation depends on the metereological conditions and on the abstraction rates at the well galleries of the drinking water treatment plant (DWTP) of Friedrichshagen located south-west and south of the remediation site (gallery A and B). The groundwater gradient has an average value of about 1.5 ‰ directed mainly toward south-west (Sensatec, 2009).

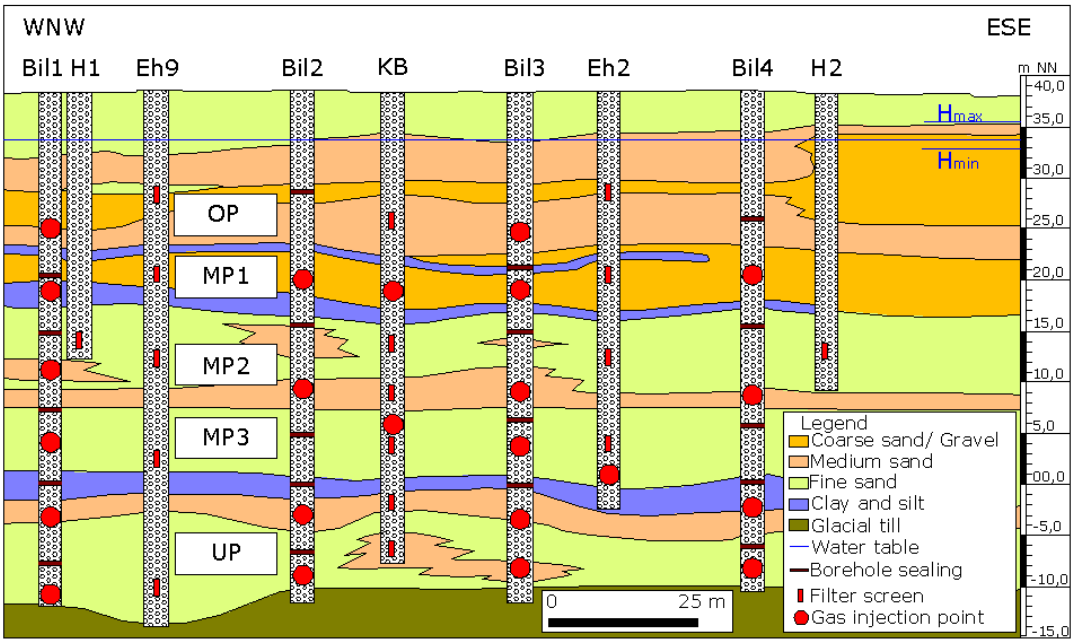

Figure 5.2 Geological section of the aquifer portion where the IAS system was applied. The figure also shows some technical elements of the IAS system. Hmax and Hmin indicate the maximum and minimum level of the water table, respectively (modified from Sensatec, 2009).

Table 5.1. Description of the five depositional sediment units.

Unit	Thickness	Sediment	Hydraulic conductivity (m s^{-1})
OP	10-13 m	Coarse and medium sand	1.00E-04
MP1	6-7 m	Coarse sand	1.50E-03
MP2	8-11 m	Fine and medium sand	6.00E-04
MP3	7-11 m	Fine sand	7.00E-04
UP	7-14 m	Fine sand interbedded with discountinuous pockets of coarse sand	1.00E-05

5.2.2 Pre-remediation Groundwater Quality

The groundwater temperature at the field site is approximately 11 ºC and the pH ranges between 7.2 and 7.7. The measured electrical conductivity (EC) and redox potential (Eh) vary between 900-1130 μS cm^{-1} and 10-140 mV, respectively. Dissolved oxygen (DO) levels are usually lower than 1.4 mg L^{-1} (BWB monitoring reports, unpublished).

Due to wastewater irrigation at the former Münchehofe sewage farm, high concentration of NH_4^+, p-TSA, sulfate (SO_4^{2-}) and dissolved organic carbon (DOC) were detected in the groundwater. However, the concentration distribution of these anthropogenic contaminants differs among the five vertical depositional sediment units. Highest concentrations were found at depth between 15 and 40 m below ground surface in the units MP1, MP2 and MP3. The distribution of these contaminants in the aquifer is influenced by the high hydraulic conductivity of the units MP. Therefore, in this portion of the aquifer NH_4^+ concentration varies between 8.5 and 29.4 mg L^{-1}; p-TSA concentration ranges between 4.4 and 20 μg L^{-1}; SO_4^{2-} was found with concentrations varying between 67 and 158 mg L^{-1} and finally, DOC concentration ranges between 3.5 and 5.4 mg L^{-1} (BWB monitoring reports, unpublished).

The shallower and the deeper depositional soil units, OP and UP are characterized by lower concentrations of NH_4^+, p-TSA, SO_4^{2-} and DOC (BWB monitoring reports, unpublished).

5.2.3 IAS System Design and Operation

The IAS system constructed by the BWB aims to remove dissolved and adsorbed chemicals reluctant to volatilization (low Henry's constant), such as NH_4^+ and p-TSA. Therefore, a SVE system for the extraction of the soil vapor was not required. Since July 2007, the air/O_2 gas injections have been performed along a 100 m transect perpendicular to the main groundwater flow direction. The IAS system is located in the middle of the p-TSA contamination plume where p-TSA concentrations range between 10 and 20 μg L^{-1} (Fig. 5.3, A). The injections are intended to create a contaminant migration barrier that prevents further downgradient migration of the contamination plumes. The IAS consists of 6 injection wells (BIL1, BIL2, BIL3, BIL4, KB and Eh9) placed at variable distances

among each other (from 13 to 29 m), the injections are performed at different depths through the aquifer (from 18 m to 40 m below ground surface) to provide well oxygenated zones (Fig. 5.2). Each well is characterized by several injection lances placed at different depths. The injection lances are surrounded by a gravel filter of a length between 0.5 and 2 m that acts as a cushion on the injected gas. Gas lances located in the same wells are separated by a clay seal. The annular space above the upper injection lance is filled with a suspension of bentonite or troptogel that prevents the flowing up of the gas along the well. The tubes for gas injection are pressure-resistant polyamide and polyethylene tubes with an inner diameter of 2-4 mm and an external diameter of 4-6 mm (BIOXWAND, 2004).

As initial step, a series of injection rates and injection modes were applied to optimize the IAS system design. From July 2007 to July 2009, injection wells were operated intermittently and alternately to investigate air/O_2 gas distribution, air/O_2 gas storage of the aquifer, air/O_2 gas dissolution rates and the upward movement of the gas towards the ground surface. During this period of time, injection rates from 0.24 to 2.5 $Nm^3\ h^{-1}$ were tested. The injection pressure varied between 2 to 4.9 bars (depending on the injection depth).

Since August 2009, only pure O_2 gas has been injected using a pulsed operation in almost all injection wells contemporarily. The pulsed cycles were time variant. From August 2009 until mid-December 2009, the O_2 gas injections were performed with a pulsed cycle of 4h on and 4h off. From mid-December 2009 until the end of January 2010, the pulsed cycle was 1h on and 2h off. Finally, since February 2010 the injections have been performed with a pulsed mode of 1h on and 5h off.

Monitoring wells were constructed between and downgradient of the injection wells to measure the physical and chemical parameters influenced by IAS operation. Monitoring wells are shown in the figure 5.3,B. The downgradient monitoring wells are located at interval of about 25 and 50 m from the injection transect. The monitoring wells at the injection transect are placed at variable distance from the sparging wells (from 5 to 13 m). At about 50 m upgradient of the remediation site, the well Eh1 monitors the characteristics of the groundwater entering the reactive barrier. The monitoring wells contain multiple micro pressure pumps (MPP of the Company IMW Innovative Messtechnick Weiss, Tübingen) which are hydraulically separated by tube-packers. The valves of the pumps

work without interference allowing the sampling of groundwater belonging to different depositional sediment units (Sensatec, 2009). Each MPP was equipped with an Eh-sensor.

Groundwater sampling for the analysis of temperature, electrical conductivity (EC), redox potential (Eh), cations and anions, dissolved O_2 and pH was carried out every two months. Groundwater was sampled by pumping after constant values of EC and Eh had been established. Measurements for pH, temperature and EC were carried out in the field. Groundwater samples were filtered immediately after sample retrieval for analysis of cations and anions using 0.45 μm membrane filters. Samples for cation analysis were preserved with concentrated nitric acid. In most cases alkalinity of filtered samples was determined in the field by titration with HCl (0.1 M), otherwise alkalinity samples were collected in glass bottles which were carefully filled without any air entrapment for analysis in the laboratory of the BWB. pH, temperature, EC and Eh were measured by means of a flow through cell.

The concentrations of the major ions were measured with standard methods (DIN EN 11885-E22 and DIN EN ISO 10304-1/2). Dissolved O_2 was determined by the electrochemical probe method (DIN EN 25814-G22). NH_4^+ was detected using the standard method DIN 38406-E5. p-TSA concentration was measured approximately every two months only at the monitoring wells H1 and H2 located at the borders of the injection transect (Fig. 5.3, B). The remaining monitoring wells were sampled for p-TSA analysis only sporadically. The reason for this poor groundwater sampling for p-TSA analysis is probably due to the fact that initially the IAS system was conceived to remediate only NH_4^+ and therefore a dedicated sampling strategy for p-TSA monitoring was not initially planned. The method for p-TSA detection was developed by Richter et al. (2007).

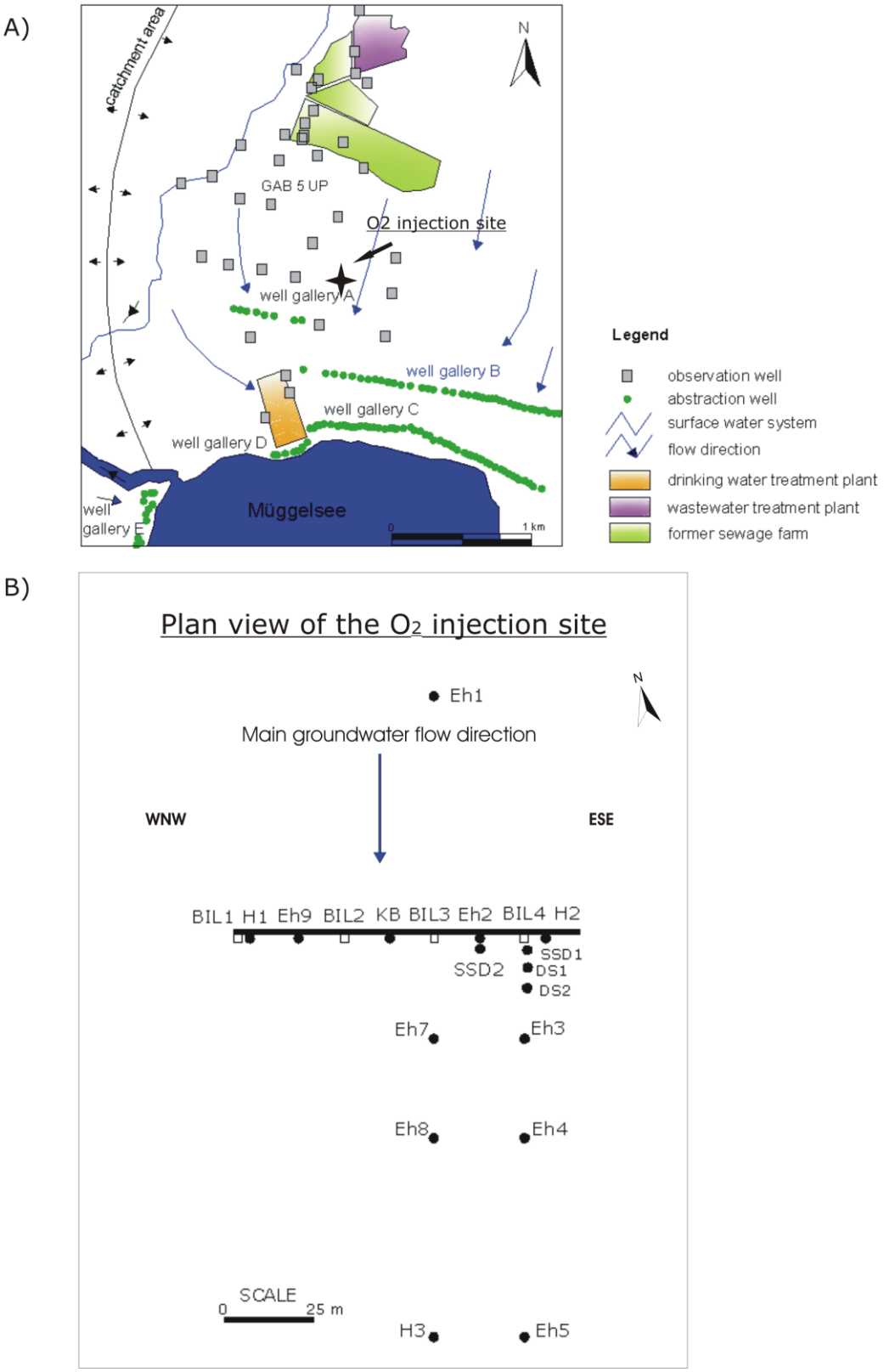

Figure 5.3 A) Map of the study area (modified from Richter et al., 2009; B) Plan view of the IAS design. The black circles represent the monitoring wells; the white squares indicate the injection wells. An exception is represented by the wells named KB and Eh9 which are contemporarily injection and monitoring wells.

5.2.4 Fate of the Injected O_2 Gas

As the injected gas moves through the saturated subsurface, O_2 is dissolved in the groundwater. Part of the injected gas remains in the pore space as trapped gas bubbles that may reduce the hydraulic conductivity of the aquifer. Through mass transfer kinetics processes between gas phase and groundwater, additional O_2 is delivered in the aqueous phase.

O_2 dissolved in groundwater is expected to be consumed by several reactions with electron donors of the aquifer matrix and of groundwater. The main expected reactions are:

- Pyrite oxidation;
- Nitrification;
- p-TSA degradation.

Pyrite Oxidation

$$FeS_2 + \frac{15}{4}O_2 + \frac{7}{2}H_2O \rightarrow Fe(OH)_3 + 2SO_4^{2-} + 4H^+$$ (From Appelo and Postma, 2007)

Pyrite was found in the aquifer with concentration up to 187 mg kg^{-1} of dry soil. Pyrite oxidation is an important O_2 consuming reaction. The reaction is driven by bacteria that generate their energy by oxidizing ferrous iron (Fe^{2+}) to ferric iron (Fe^{3+}) using O_2. The Fe^{3+} then attacks pyrite with the formation of SO_4^{2-} and Fe^{2+} which is then utilized back by bacteria.

Nitrification

$$NH_4^+ + 2O_2 \rightarrow NO_3^- + 2H^+ + H_2O$$ (From Schultz and Zabel, 2006)

In the presence of O_2, NH_4^+ is converted first into NO_2^- by bacteria belonging to the genera *Nitrosoma* and successively the NO_2^- is converted into NO_3^- by bacteria of the genus *Nitrobacter*.

p-TSA degradation

Van Haperen et al. (2001) studied the degradation of p-TSA in activated sludge where the bacteria *Pseudomonas sp*. was isolated. These bacteria grew on p-TSA in a chemostat with release of SO_4^{2-} and NH_4^+. The transient appearance of the metabolites 4-hydroxymethylbenzenesulphonamide and 4-carboxybenzenesulphonamide indicated that the oxidation of the methyl group is the initial "attack" in the biodegradation pathway (Van Haperen et al., 2001). According to Van Haperen et al. (2001), p-TSA was completely mineralized. Therefore, following these results and assuming that under oxic aquifer conditions the oxidation reaction has an efficiency of 50 %, the following reaction can be hypothesized:

$$C_7H_9NO_2S + 3.7O_2 + H_2O \rightarrow 0.7C_5H_7O_2N + 3.5CO_2 + 0.3NH_4^+ + SO_4^{2-} + 4.9H^+$$

with $C_5H_7O_2N$ representing the microbial structure (Barry et al., 2002).

However, it has to be specified that since p-TSA concentration is of the order of the $\mu g\,L^{-1}$ the chemistry of the groundwater is not really influenced by the reaction products and the O_2 consumption by p-TSA degradation can be assumed to be negligible.

5.3 Performance of the IAS System

Results from three years of IAS system application will be presented in this section. Particular attention will be given to the response of p-TSA and NH_4^+ to the continuous O_2 injections performed since August 2009.

5.3.1 Dissolved O_2 Concentration

Dissolved O_2 concentration of the groundwater at the field site was regularly monitored (approximately every two months). As already described, the initial phase of the remediation activity consisted in discontinuous injection trials to understand O_2 gas distribution and storage in the aquifer aiming at an appropriate O_2 injection design. During this period, a small O_2 concentration increase could be observed only in some areas close to the activated injection wells. Since August 2009, O_2 has been continuously injected at

several injection wells generating a considerable increase of O_2 concentration in the aquifer. Figure 5.4 shows the dissolved O_2 concentration at the injection transect in February 2010 (Fig. 5.4, A), April 2010 (Fig. 5.4, B) and June 2010 (Fig. 5.4, C) that were obtained by data interpolation with the modified Sheppard's method. As can be noted, the O_2 concentration was not homogeneously distributed, the central part of the injection transect presented lower O_2 concentration with values that varied between 1.1 and 25.6 mg L^{-1}. In contrast, the aquifer at the transect's borders appeared to be better supplied by the injections, with dissolved O_2 concentrations up to more than 90 mg L^{-1}. This may be related to preferential channeling of O_2 through more permeable areas. The high values of dissolved O_2 concentrations are due to the use of pure O_2 gas during the injections.

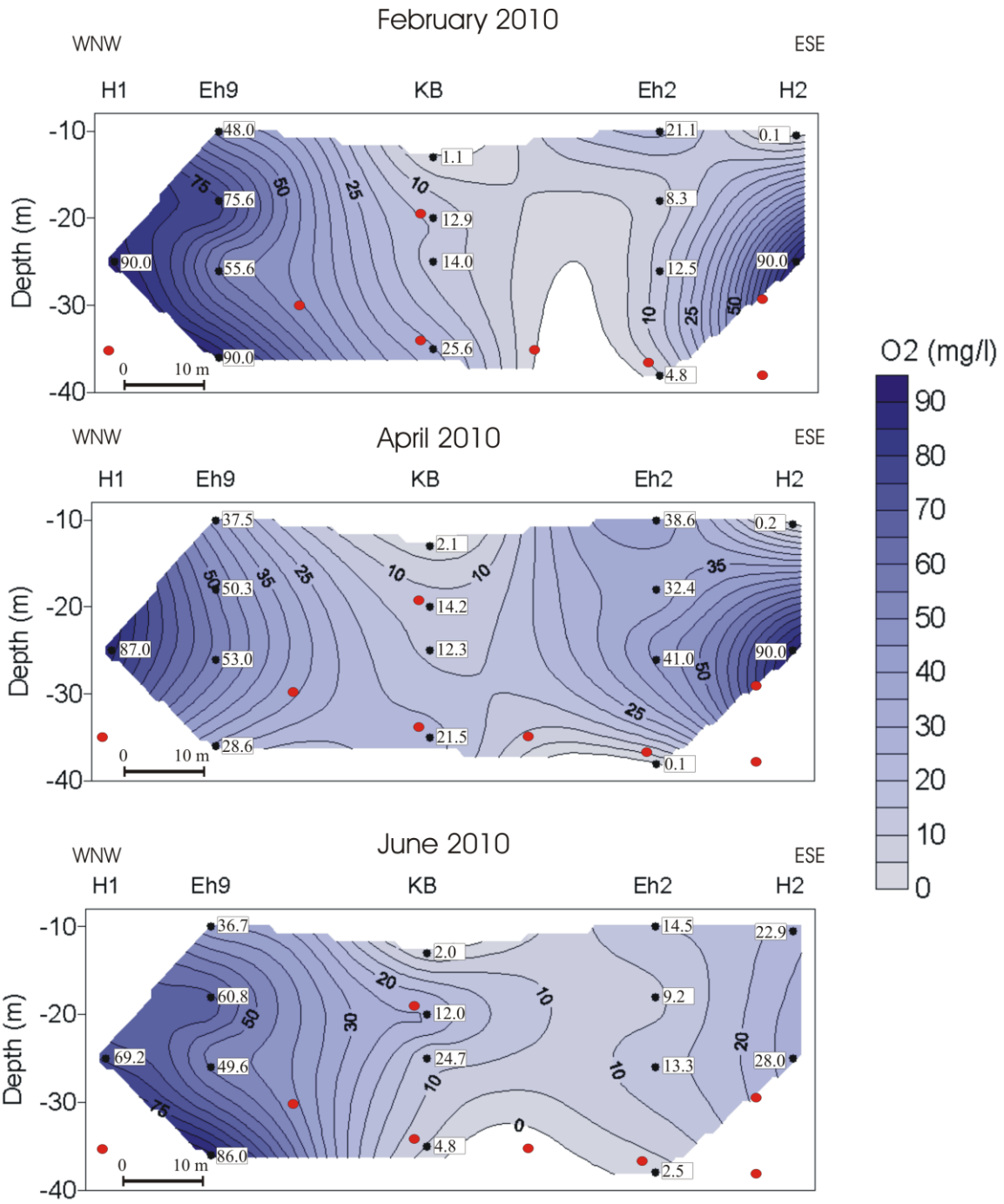

Figure 5.4 Dissolved O_2 distribution in the groundwater at the injection transect (see Fig. 5.3 A-B). The black dots indicate the observation points. The black numbers on white background represent dissolved O_2 concentrations (expressed in mg L^{-1}) considered for the interpolation. The red circles indicate the activated O_2 injection points. The interpolation was carried out only in the area where O_2 measurements were available using a blank file.

Downgradient of the remediation site, considerable dissolved O_2 concentration between 10 and 30 mg L^{-1}, were measured at the monitoring wells DS1 and DS2 placed at about 8 and 16 m from the transect, respectively (Fig. 5.3, B). An exception is the monitoring well Eh7

at about 25 m downgradient of the transect (Fig. 5.3, B); here dissolved O_2 concentration were exceptionally high, around 40-60 mg L^{-1}, through almost all the aquifer depth (Fig. 5.5). According to the observations described above, these high O_2 concentrations are also related to the presence of preferential transport channels for O_2 gas. This implies an heterogeneous O_2 distribution and localized high O_2 concentrations away from the injection wells.

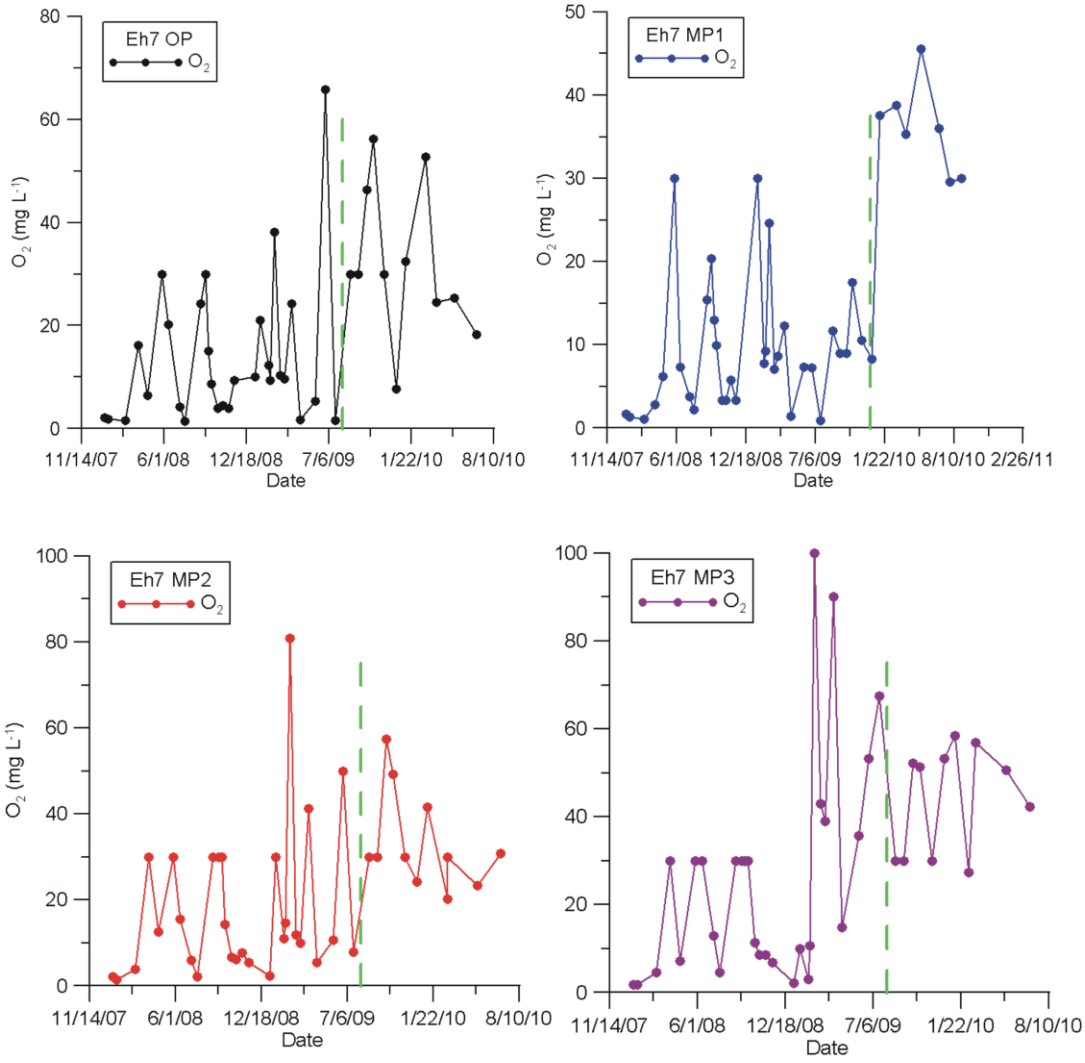

Figure 5.5 Dissolved O_2 concentrations at the monitoring well Eh7 at different depths OP, MP1, MP2 and MP3 (see Fig. 5.2). The green dashed line indicates the starting of the continuous O_2 gas injection.

Further downstream of the monitoring well Eh7, O_2 could only be observed occasionally in small concentrations (< 2 mg L^{-1}). The absence of dissolved O_2 downgradient of the

remedation site is due to O_2 consumption by electron donors of the groundwater and of the aquifer matrix.

5.3.2 p-TSA Concentration

At the field site, partial p-TSA removal was observed only in a few monitoring wells, whereas at the majority of the observation points no p-TSA degradation was detected. Fig. 5.6 shows p-TSA, dissolved O_2 and NH_4^+ concentrations at monitoring wells where p-TSA removal could be encountered. The dashed green line indicates the beginning of continuous O_2 injections for the development of a coherent oxidation barrier. Initial p-TSA concentration varied between 12 and 15 $\mu g\ L^{-1}$ depending on the monitoring well and on the monitored depth. Figure 5.6 shows that at the beginning of the continuous O_2 gas injections, O_2 concentration in groundwater started to increase, and consequently p-TSA concentration at these wells started to decrease. However, p-TSA is never completely removed. This is in contrast with the observation of Richter et al. (2008b), Meffe et al. (2010) and Meffe et al. (submitted 2010a) which suggest an almost complete degradation of p-TSA in the presence of O_2. At the well Eh9 MP3 and KB MP2u placed along the injection transect, p-TSA concentration only decreased down to value around 3-4 $\mu g\ L^{-1}$ even in the presence of a considerable amount of dissolved O_2. The removal of p-TSA at these two monitoring wells was of about 33 %.

However, p-TSA concentration in the majority of the monitoring wells did not show any clear evidence of degradation due to O_2 gas injections. Fig. 5.7 shows p-TSA and dissolved O_2 concentrations in some of the unaffected wells, chosen as representative examples. p-TSA concentration of the groundwater monitored at these wells did not decrease, even in the presence of high O_2 concentrations. Note however that the monitoring wells H1 MP2 and H2 MP2, screened at depth of unit MP2 (Fig. 5.2), showed a strong variation of p-TSA concentration.

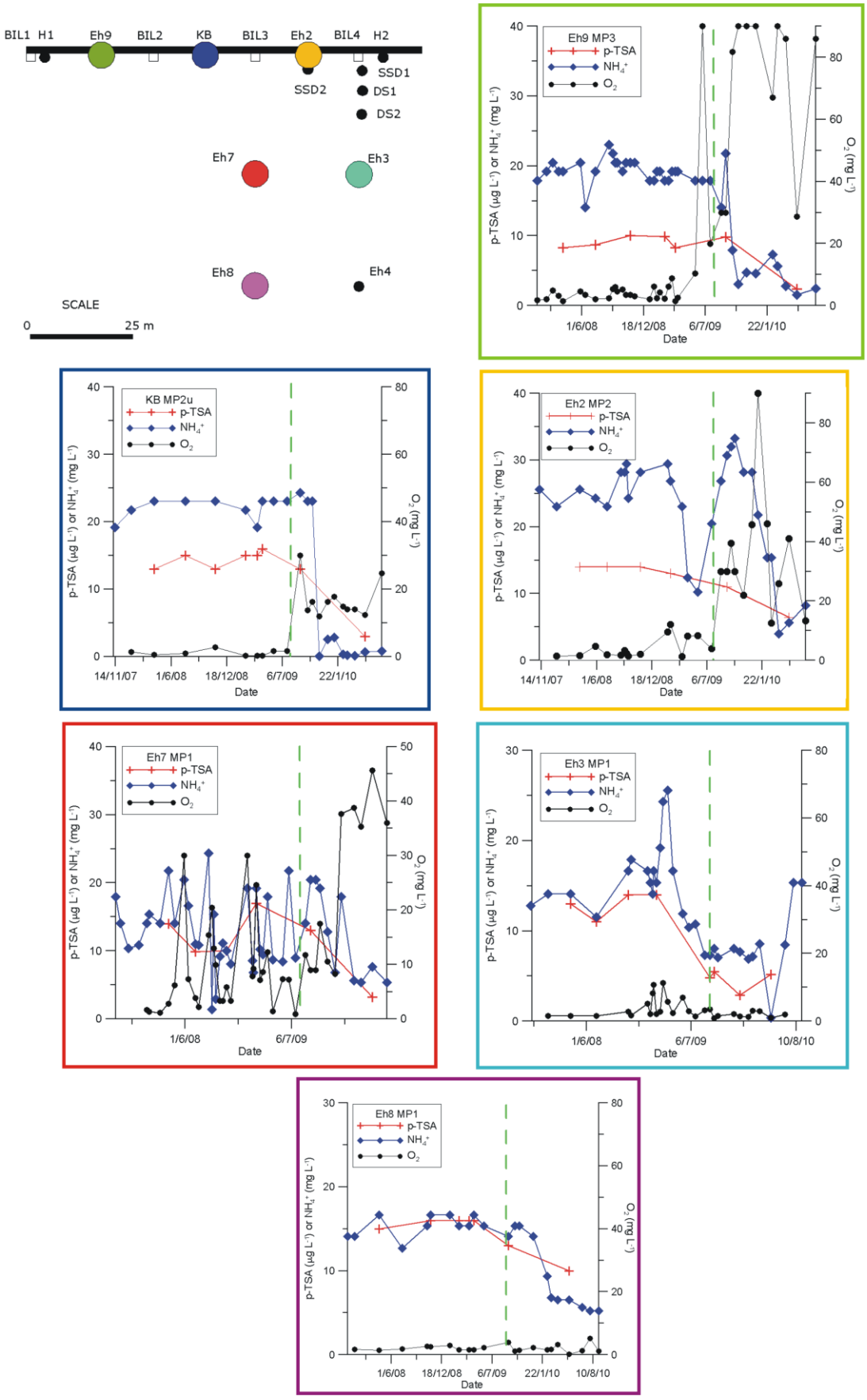

Figure 5.6 Monitoring points at the injection transect and downgradient showing removal of p-TSA and NH_4^+ as well as the concentrations of dissolved O_2. The green dashed line indicates the starting of the continuous O_2 gas injection.

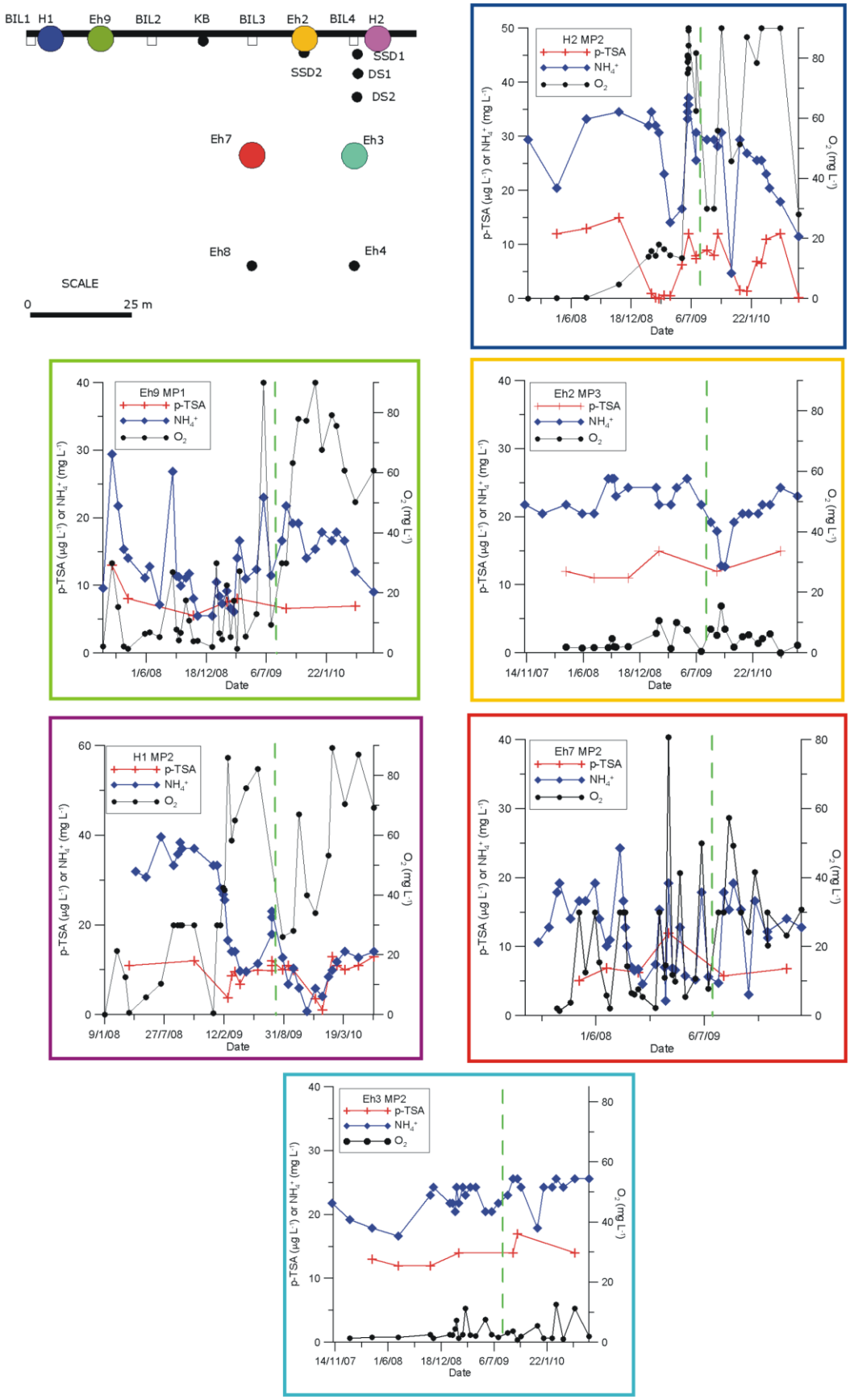

Figure 5.7 Monitoring points at the injection transect and downgradient showing the absence of p-TSA and NH_4^+ removal as well as the concentrations of dissolved O_2. The green dashed line indicates the starting of the continuous O_2 gas injection.

p-TSA degradation appeared to occur mainly in the soil depositional unit MP1, at about 20 m of depth. Here, p-TSA removal was observed at the wells located at the injection transect (Eh2 MP1 and KB MP1u) and at the downgradient monitoring wells (Eh7 MP1, Eh3 MP1and Eh8 MP1). The O_2 injection was performed through the well KB in the unit MP1 (Fig. 5.4) which is delimited by two layers of low permeability at its bottom and top (Fig. 5.2). These layers are supposed to act as a barrier for the vertical gas flow enhancing the horizontal gas propagation and the gas channels with the consequent formation of a more uniformly oxygenated area.

5.3.3 NH_4^+ Concentrations

NH_4^+ had similar behaviour to p-TSA during the operation of the IAS system. Indeed, it was removed in the same wells where p-TSA degradation was detected (Fig. 5.6). Subsequent to NH_4^+ removal in the oxic domain, NO_3^- was produced in stoichiometric amount before being consumed when entering the downgradient anoxic domain. However analogous to p-TSA, nitrification did not occur in the majority of the monitoring wells even in the presence of dissolved O_2 (Fig. 5.7). Contrary to what was observed for p-TSA, monitoring wells H1 MP2 and H2 MP2 (Fig. 5.7) showed a general decreasing trend of NH_4^+ concentration from the beginning of IAS application (July 2007). However since August 2009, an unexpected strong variation in NH_4^+ concentration was observed.

5.4 Numerical Model

To better interpret the controversial results obtained by the application of the IAS system, a preliminary attempt of a numerical reactive transport modeling was performed using the computer code PHREEQC-2 (Parkhurst and Appelo, 1999). The aim of this study was to investigate the hydro-geochemical changes caused by the O_2 injection at the monitoring wells Eh2 MP1, Eh7 MP1 and Eh8 MP1 once continuous O_2 gas injections started to be applied in August 2009.

5.4.1 Physical Parameters of the Model

The line along which the 1D model was performed is represented by the red dotted line in Fig. 5.8. The 1D solution domain has a length of 201 m and is defined by a series of 41 cells. The cell length is 5 m, except for the first cell which measures 1 m (Table 5.2). According to unpublished reports from Sensatec (2009), the groundwater velocity is approximately 0.5 m d^{-1} and was inserted in the model through time discretization simulating two pore volume exchange (Table 5.2). Remaining transport parameters and flow boundary conditions are reported in Table 5.2.

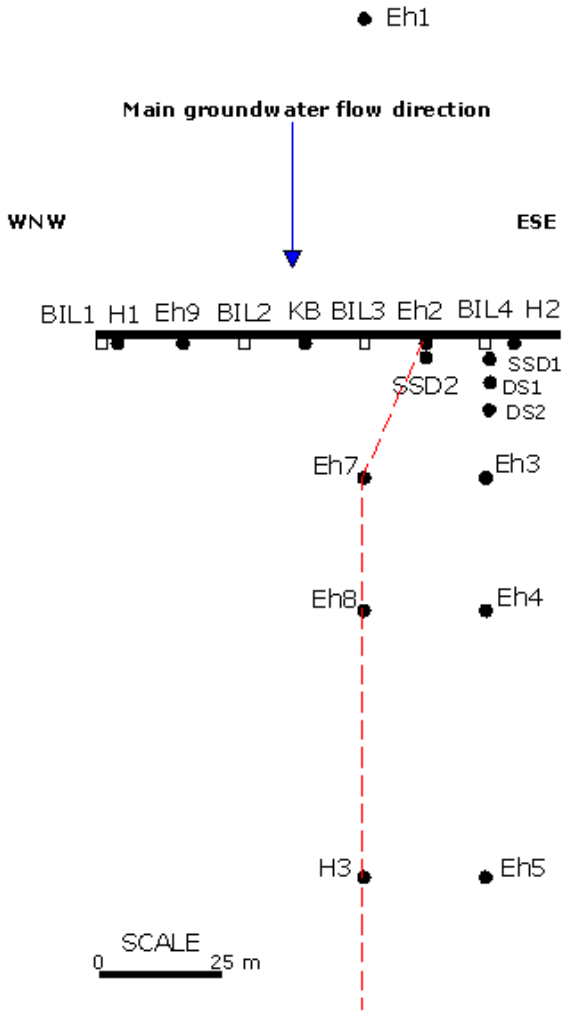

Figure 5.8 The red dotted line corresponds to the solution domain of the model. It extends further, in direction south-east-south, up to a distance of 200 m from the oxidation barrier. The black circles represent the monitoring wells; the white squares indicate the injection wells. An exception is represented by the wells named KB and Eh9 which are contemporarily injection and monitoring wells.

Table 5.2 Discretization, flow and transport parameters used in the model.

Parameter		Value	Unit
Grid spacing	cell 1	1	m
	cell 2-41	5	m
Model length		201	m
Inlet boundary		const. flux	
Outlet boundary		const. flux	
Dispersivity [a]		5	m
Diffusion coefficient [b]		1.00E-09	$m^2\ s^{-1}$
Nr. Shifts		82	
Time step		9.8	d

[a] from Gelhar et al. (1985)
[b] from Frederikse and Lide (1997)

5.4.2 Chemical Parameters of the Model

Groundwater and matrix composition

The composition of the groundwater entering the simulated system is based on measurements performed at the observation well Eh1 MP1 (about 50 m upgradient of the injection transect) in February 2009. Due to the lack of data prior to the remediation activity, the initial groundwater composition was assumed to be equal to that of the entering groundwater (Table 5.3).

Table 5.3 Entering and initial groundwater composition.

Aqueous component	Measured (mg/l)	Equilibrated (mg/l)
pH	7.6	7.12
pe		1.6
NH_4^+	21.8	21.8
Ca^{2+}	126	126
Mg^{2+}	12.8	12.8
Na^+	45	45
K^+	14.9	14.9
Fe^{2+}	4.9	4.7
Fe^{3+}	0.1	2.75E-04
Mn^{2+}	0.63	0.49
SO_4^{2-}	140	140
Cl^-	75	116.5
O_2	0	0
HCO_3^-	339	289
CH_4	0	0
NO_3^-	0	0
NO_2^-	0	0
p-TSA (in $\mu g\ L^{-1}$)	15	15
DOC	5.2	5.2

The solid matrix concentrations were taken from Horner et al. (2009) and are given in Table 5.4. Before running the model, groundwater analysis and solid matrix were equilibrated using PHREEQC-2 (Appendix A1) and Cl^- was allowed to achieve electroneutrality during the simulations.

Table 5.4 Matrix composition used in the model (From Horner et al., 2009).

Component	Value (mol L^{-1})
Cation exchange capacity	0.011
Total organic carbon	0.147
Calcite	1.56
Pyrite	0.014
Ferrihydrite	0
Rhodochrosite	0

5.4.3 Reaction Network

Based on previous investigations conducted by Horner et al. (2009) in an IAS pilot site located approximately 1 km north of the present IAS system, the processes listed in Table 5.5 were considered as relevant for the field site. The presence of dissolved O_2 induces p-TSA degradation, nitrification, aerobic respiration and pyrite oxidation. The nitrification produces NO_3^- which is consumed under anoxic conditions (absence of O_2) by autotrophic and heterotrophic denitrification. Reactions involving pyrite oxidation are mainly responsible for groundwater acidification. At the field site, acidification is buffered by calcite dissolution (Horner et al., 2009). Calcite buffering was incorporated by imposing thermodynamic equilibrium between calcite and groundwater.

p-TSA is considered not to be retarded by adsorption (Richter et al., 2008b; Meffe et al., submitted 2010b) whereas NH_4^+ is retarded by cation exchange (Horner et al., 2009). As mentioned above, the simulation considers only the period of continuous O_2 gas injections. Therefore, in the simulation, the injection was implemented by defining a fixed O_2 partial pressure of 0.2 atm in the first cell, in equilibrium with groundwater. Note that this approach is a simplification of the real processes governing O_2 gas dissolution in the saturated zone. However, this approximation was considered as viable since O_2 is constantly supplied at the injection transect. Successively, mathematical formulations for p-TSA degradation, nitrification, aerobic respiration, autotrophic and heterotrophic denitrification and pyrite oxidation were implemented, as available in the literature (Table 5.6). The remaining reactions, such as precipitation/dissolution of minerals and gas dissolution, were formulated as thermodynamic equilibrium.

Table 5.5 Reaction network (except for p-TSA, the reaction network was taken from Horner et al., 2009).

Process	Reaction formulations
p-TSA aerobic degradation	$C_7H_9NO_2S + 3.7O_2 + H_2O \rightarrow 0.7C_5H_7O_2N + 3.5CO_2 + 0.3NH_4^+ + SO_4^{2-} + 4.9H^+$
Nitrification	$NH_4^+ + 2O_2 \rightarrow NO_3^- + 2H^+ + H_2O$
Pyrite oxidation	$FeS_2 + 3.75O_2 + 3.5H_2O \rightarrow Fe(OH)_3 + 2SO_4^{2-} + 4H^+$
Autotrophic denitrification	$5FeS_2 + 15NO_3^- + 10H_2O \rightarrow 5Fe(OH)_3 + 2SO_4^{2-} + 4H^+$
Aerobic respiration	$CH_2O + O_2 \rightarrow HCO_3^- + H^+$
Heterotrophic denitrification	$CH_2O + 4NO_3^- \rightarrow 5HCO_3^- + 2N_2 + H^+ + 2H_2O$
Supply of organic carbon	$CH_2O_{particle} \leftrightarrow CH_2O_{dissolved}$
Calcite dissolution	$CaCO_3 + H^+ \leftrightarrow Ca^{2+} + HCO_3^-$
Ion exchange	$Ca^{2+} + 2NaX \leftrightarrow CaX_2 + 2Na^+$
	$Mg^{2+} + 2NaX \leftrightarrow MgX_2 + 2Na^+$
	$K^+ + NaX + \leftrightarrow KX + Na^+$
	$NH_4^+ + NaX \leftrightarrow NH_4X + Na^+$
	$Fe^{2+} + 2NaX \leftrightarrow FeX_2 + 2Na^+$

Table 5.6 Mathematical formulations of reaction kinetics.

Process	Mathematical formulations
p-TSA aerobic degradation	$\frac{\partial_{p-TSA}}{\partial t} = K_{\max} \frac{C_{p-TSA}}{C_{p-TSA} + k_{m,p-TSA}} \cdot \frac{C_{O2}}{C_{O2} + k_{m,O2}}$
Nitrification	$\frac{\partial C_{NH4+}}{\partial t} = K_{NH4+} \frac{C_{NH4+}}{C_{NH4+} + K_{m,NH4+}} \cdot \frac{C_{O2}}{C_{O2} + k_{m,O2}}$
DOC degradation	$\frac{\partial_{DOC}}{\partial t} = \left(K_{O2} \cdot \frac{C_{O2}}{C_{O2} + k_{m,O2}} + K_{NO3-} \cdot \frac{C_{NO3-}}{C_{NO3-} + k_{m,NO3-}} \cdot \frac{I_{O2}}{I_{O2} + C_{O2}} \right) \cdot C_{DOC}$
Pyrite oxidation	$\frac{\partial C_{Pyrite}}{\partial t} = \left(C_{O2}^{0.5} + f2 \cdot C_{NO3-}^{0.5} \right) \cdot C_{H+}^{-0.11} \cdot \left(10^{-10.19} \cdot \left(\frac{A_{Pyrite}}{V} \right) \right) \cdot \left(\frac{C_{Pyrite}}{Co_{Pyrite}} \right)^{0.67}$
DOC supply from matrix	$\frac{\partial C_{POC}}{\partial t} = k_{sol} \cdot C_{POC} \cdot \left(C_{sat,DOC} - C_{DOC} \right)$

The applied reactive kinetic parameters are given in Table 5.7. Some of these parameters are derived from the literature, whereas others were calibrated to fit the measured data. Resulting simulated concentrations were monitored at the cell 1 (Eh2 MP1), cell 6 (Eh7 MP1) and cell 11 (Eh8 MP1).

Table 5.7 Reactive kinetic parameters used in the model.

Process	Kinetic parameter	Label	Value	Unit	Reference
p-TSA degrad.	max. react. rate (t<=32d)	K_{max}	3.80E-15	mol L^{-1} s^{-1}	calibrated
	max. react. rate (t>32d)	K_{max}	2.50E-14	mol L^{-1} s^{-1}	calibrated
	Monod constant p-TSA	$k_{m,p\text{-}TSA}$	1.75E-09	mol L^{-1}	1
	Monod constant O_2	$k_{m,O2}$	3.00E-06	mol L^{-1}	2
Nitrification	max. react. rate	K_{NH4+}	3.00E-10	mol L^{-1} s^{-1}	calibrated
	Monod constant NH_4^+	$k_{m,NH4+}$	1.00E-06	mol L^{-1}	3
	Monod constant O_2	$k_{m,O2}$	1.00E-06	mol L^{-1}	3
	time lag	t_{lag}	50	d	calibrated
DOC degrad.	max. react. rate O_2	K_{O2}	1.16E-09	mol L^{-1} s^{-1}	4
	max. react. rate NO_3^-	K_{NO3-}	1.16E-09	mol L^{-1} s^{-1}	4
	Monod constant O_2	$k_{m,O2}$	1.00E-06	mol L^{-1}	4
	Monod constant NO_3^-	$k_{m,NO3-}$	1.00E-06	mol L^{-1}	4
	Inhibition factor	I_{O2}	1.00E-06	mol L^{-1}	4
Pyrite oxidation	reactive surface param.	Apyrite/V	10	dm^{-1}	5
DOC supply	Solubility	$C_{sat,DOC}$	5.00E-04	mol L^{-1}	6
	solution rate constant	k_{sol}	1.16E-10	s^{-1}	6

1) Meffe et al., 2010; 2) Schäfer et al., 1998; 3) Serapiglia, 2002; 4) Nidesi, 2000; 5) Prommer and Stuyfzand, 2004; 6) Horner, 2005a,b.

5.4.4 Model Results

The PHREEQC-2 input file for the simulation is given in Appendix A2. Modelling results were compared to data measured at the three monitoring wells, Eh2 MP1, Eh7 MP1 and Eh8 MP1 (Fig. 5.3, B and Fig. 5.8) where the IAS system had a clear effect on the field data. The evaluation of the fit quality is based on visual comparison between field data and simulation results.

Dissolved O_2 simulation

Fig. 5.9 shows simulated and measured dissolved O_2 concentrations at the three monitoring wells. At the well Eh2 MP1, the horizontal line of the simulated O_2 concentration represents the fixed O_2 partial pressure of 0.2 atm in the first cell in equilibrium with

groundwater, leading to a constant dissolved O_2 concentration of approximately 35 mg L^{-1}. Field data measured at the well Eh2 MP1 reveal an irregular variation of dissolved O_2 concentration which may be related to O_2 consumption by oxidation processes or to variable injection rates. At the monitoring well Eh7 MP1 the measurements reveal high concentrations of dissolved O_2 (from 9.0 to 46.0 mg L^{-1}), whereas the model yields only a small peak of dissolved O_2 during a short period of about 40 days. This small peak of O_2 is due to the time lag defined for nitrification allowing the dissolved O_2 to spread about 25 m downgradient of the injection transect without being consumed by nitrification.

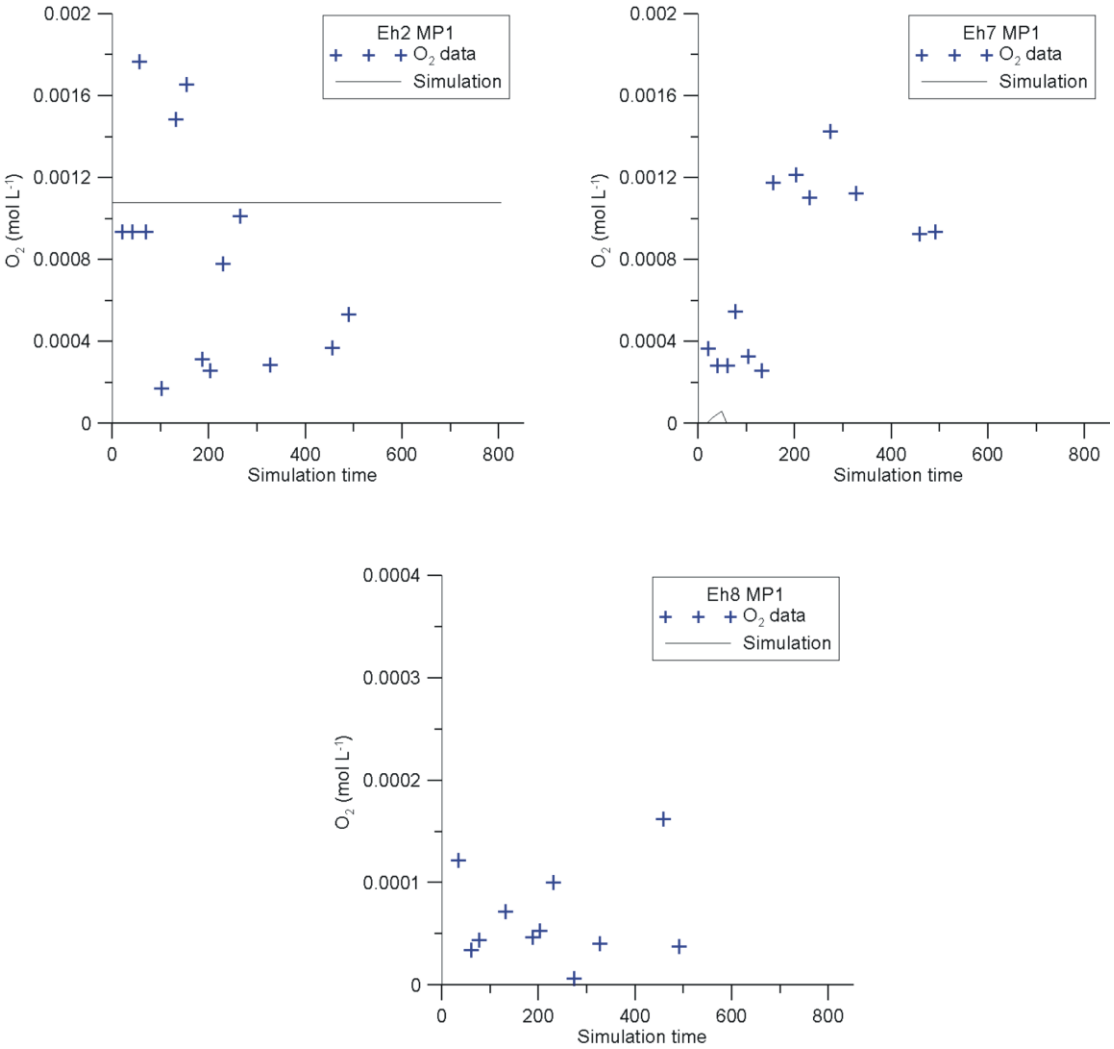

Figure 5.9 Measured and simulated dissolved O_2 concentrations at the monitoring wells Eh2 MP1, Eh7 MP1 and Eh8 MP1.

Once the nitrification process starts, the simulated O_2 front moves backwards.

Measured dissolved O_2 concentrations at the well Eh8 MP1 vary between 0.2 to 3.0 mg L^{-1}, with the exception of a single measurement which shows a concentration of 5.2 mg L^{-1}. Such field data are probably related to O_2 contamination during groundwater sampling. At this well, due to nitrification, pyrite oxidation and organic matter degradation, the model generates completely anoxic conditions, in agreement with the field data.

p-TSA simulation

Simulation results for p-TSA are represented as breakthrough curves in Fig. 5.10. As can be noted, the amount of p-TSA data is rather poor with only three measurements in approximately one year. This scarce monitoring for p-TSA characterized all the observation wells excepting wells H1 MP2 and H2 MP2 which could not be considered in the modelling due to large data fluctuations.

In spite of the limited size of the dataset, simulations were performed as an attempt to reproduce the observed p-TSA concentration. The best fit was obtained by using the parameter combination in Table 5.7. The maximum reaction rate (K_{max}) had to be increased after 32 days from 3.8E-15 to 2.5E-14 mol L^{-1} s^{-1} indicating a possible microbial adaption to the new redox conditions. The obtained K_{max} were comparable to those obtained by Meffe et al. (submitted 2010a) through modelling of a column experiment simulating O_2 injections.

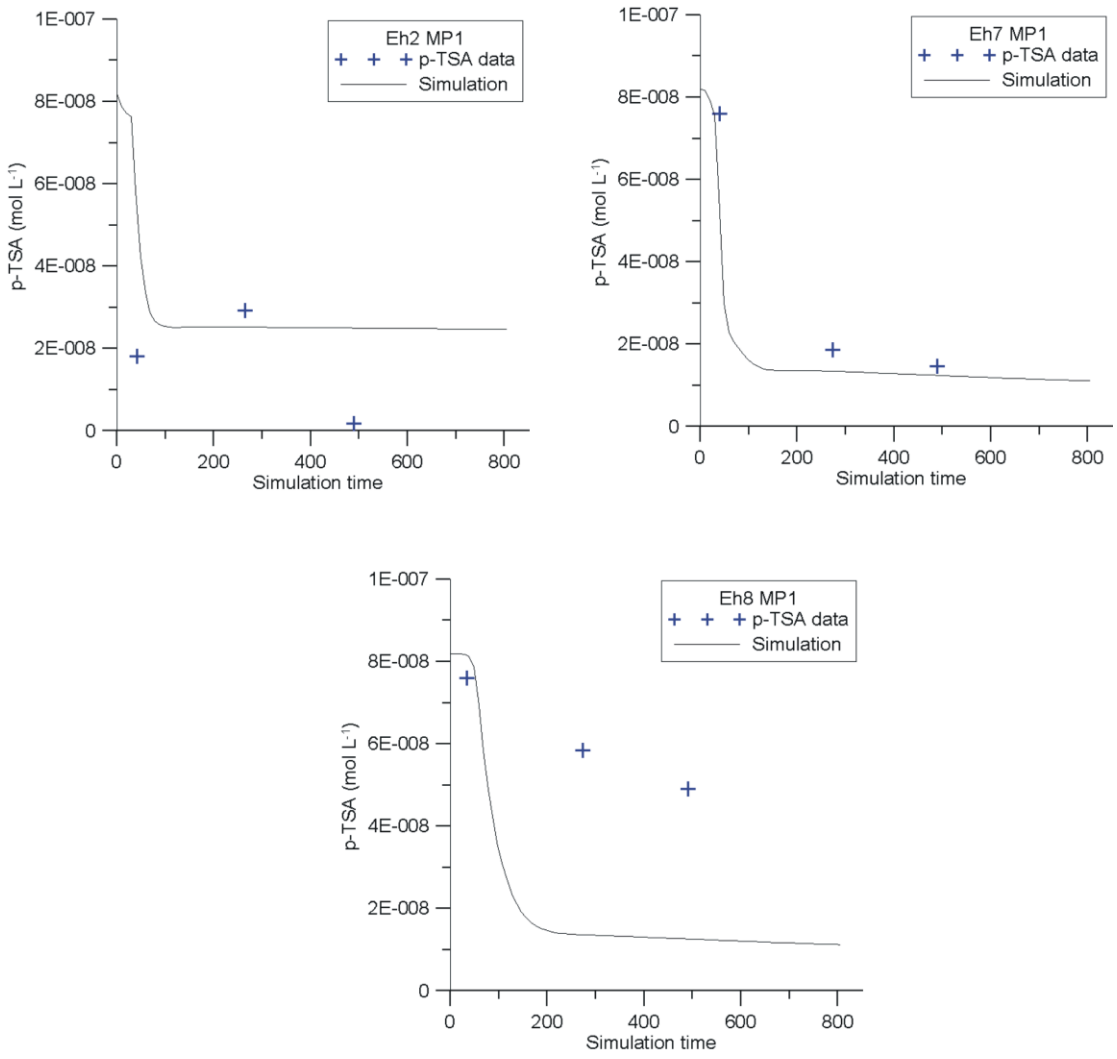

Figure 5.10 Measured and simulated p-TSA concentrations at the monitoring wells Eh2 MP1, Eh7 MP1 and Eh8 MP1.

As can be seen in Fig. 5.10, the results of the simulations at the wells Eh2 MP1 and Eh7 MP1 are qualitatively in agreement with field data whereas for Eh8 MP1 simulated concentrations are far below the measured p-TSA concentrations.

NH_4^+ simulation

Nitrification is activated in the simulation after a time lag of 50 days. The choice of 50 days was based on the measured data which show no NH_4^+ removal during this interval of time. The time lag is a manifestation of the microbial adaption to the change of redox

conditions. The same nitrification time lag was used by Horner et al. (2009) during modelling of an injection pilot site in the same aquifer. During the time lag, simulated NH_4^+ concentrations slightly increase as a result of NH_4^+ desorption from the ion exchanger (Horner et al., 2009) (Fig. 5.11). As soon as nitrification starts, NH_4^+ concentrations decrease until they reach, at the injection transect (cell 1 of the model), a quasi-steady state concentration of about 7 mg L^{-1}. Simulation results are in good agreement with observed data at the monitoring wells Eh2 MP1 and Eh7 MP2 (Fig. 5.11). Instead, the fit at the monitoring well Eh8 MP1 shows a difference with respect to field data in the initial NH_4^+ concentration in groundwater.

NO_3^- simulation

Figure 5.12 shows simulation results for NO_3^-. NO_3^- is produced by the nitrification in the oxic domain and is consumed by denitrification in the anoxic domain. The fits of NO_3^- data observed at the well Eh2 MP1 and Eh7 MP1 are satisfactory. At the monitoring well Eh8 MP1 the simulation always underestimates the measured NO_3^- concentration.

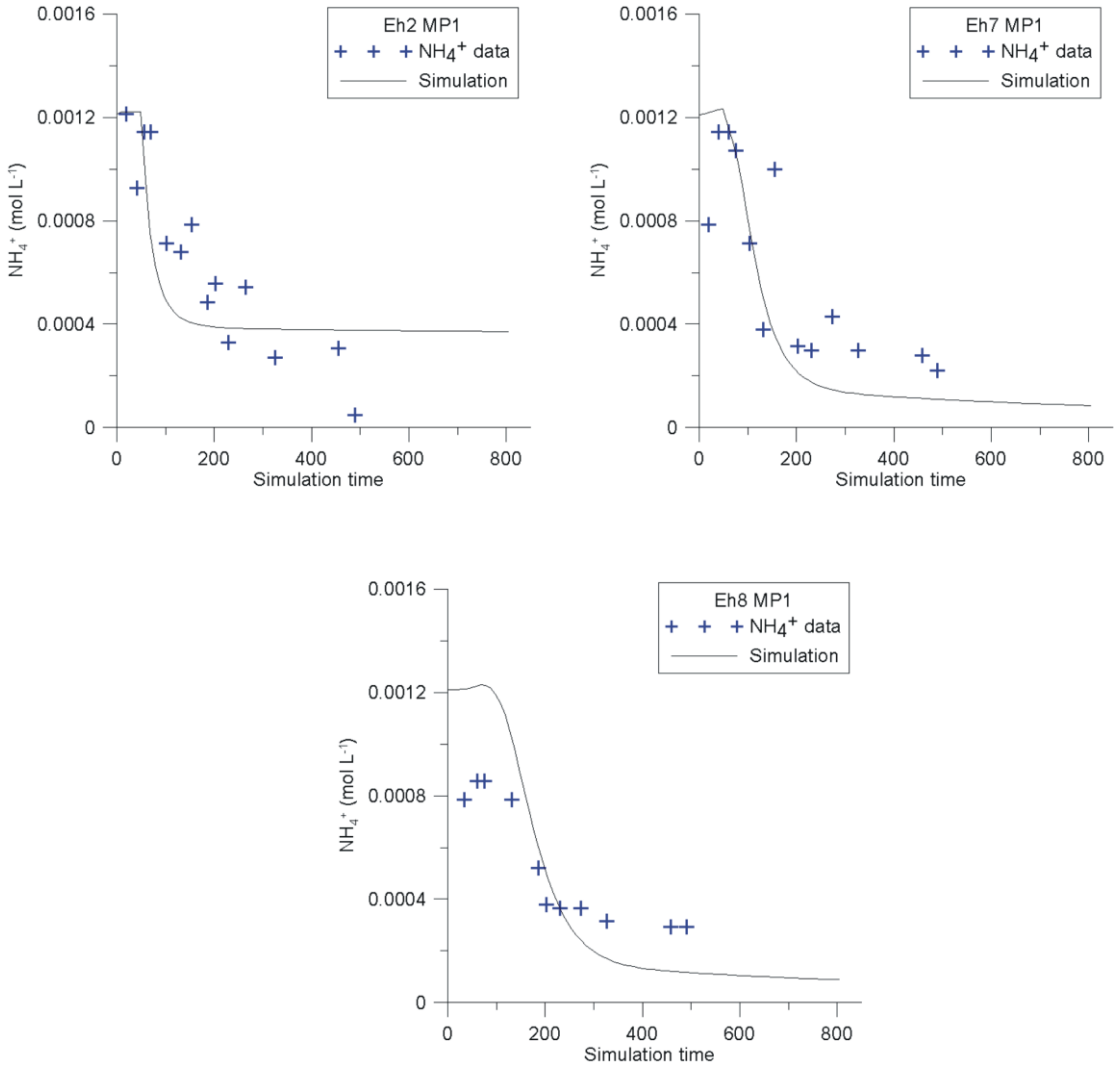

Figure 5.11 Measured and simulated NH_4^+ concentrations at the monitoring wells Eh2 MP1, Eh7 MP1 and Eh8 MP1.

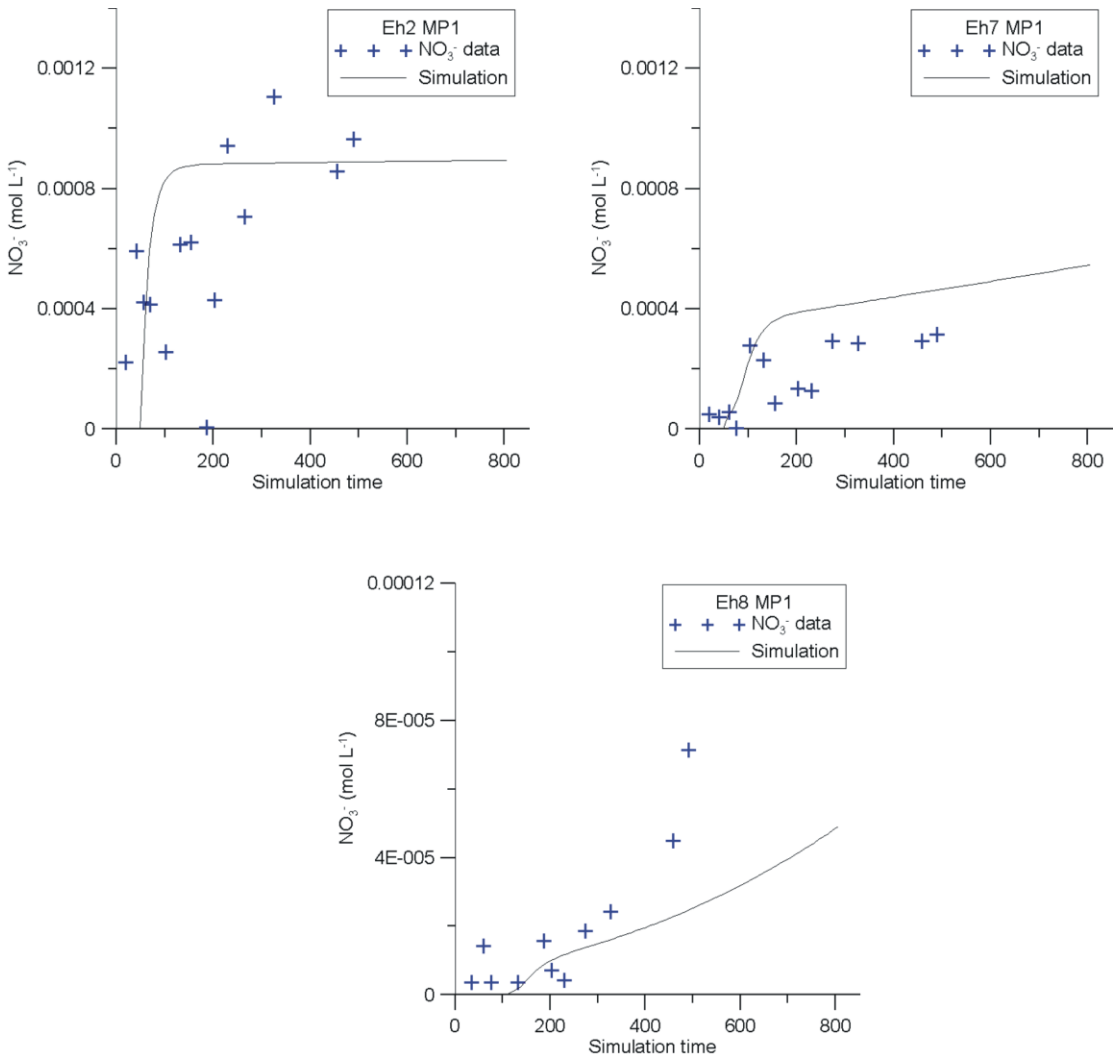

Figure 5.12 Measured and simulated NO_3^- concentrations at the monitoring wells Eh2 MP1, Eh7 MP1 and Eh8 MP1.

SO_4^{2-} and pH simulation

Simulated SO_4^{2-} concentrations show a slight increase at the injection transect due to the oxidation of pyrite. A larger increase of SO_4^{2-} is simulated at the downgradient monitoring wells Eh7 MP1 and Eh8 MP2 as a result of the autotrophic denitrification (Fig. 5.13). Measured SO_4^{2-} concentration fluctuates significantly and no clear increasing trends can be observed at the observation points. The assumed initial concentration of SO_4^{2-} is significantly lower than SO_4^{2-} concentration measured at the three monitoring wells. This phenomenon can be related to the effects of previous remediation activities that may have increased the concentration of SO_4^{2-} in groundwater. Fig. 5.13 also shows the values of pH at the three observation wells. The pH distribution is observed to be anticorrelated with the SO_4^{2-} concentration. An initial period of about 150-200 days during which pH shows a

decreasing trend can be observed. Following this period, pH reveals a variation of around ± 0.4 pH units. The model is able to partly reproduce the decrease of pH, while it fails to simulate the subsequent variation of the measured pH. Simulated pH values originate from the balance between the acidification due to pyrite oxidation and the calcite buffering.

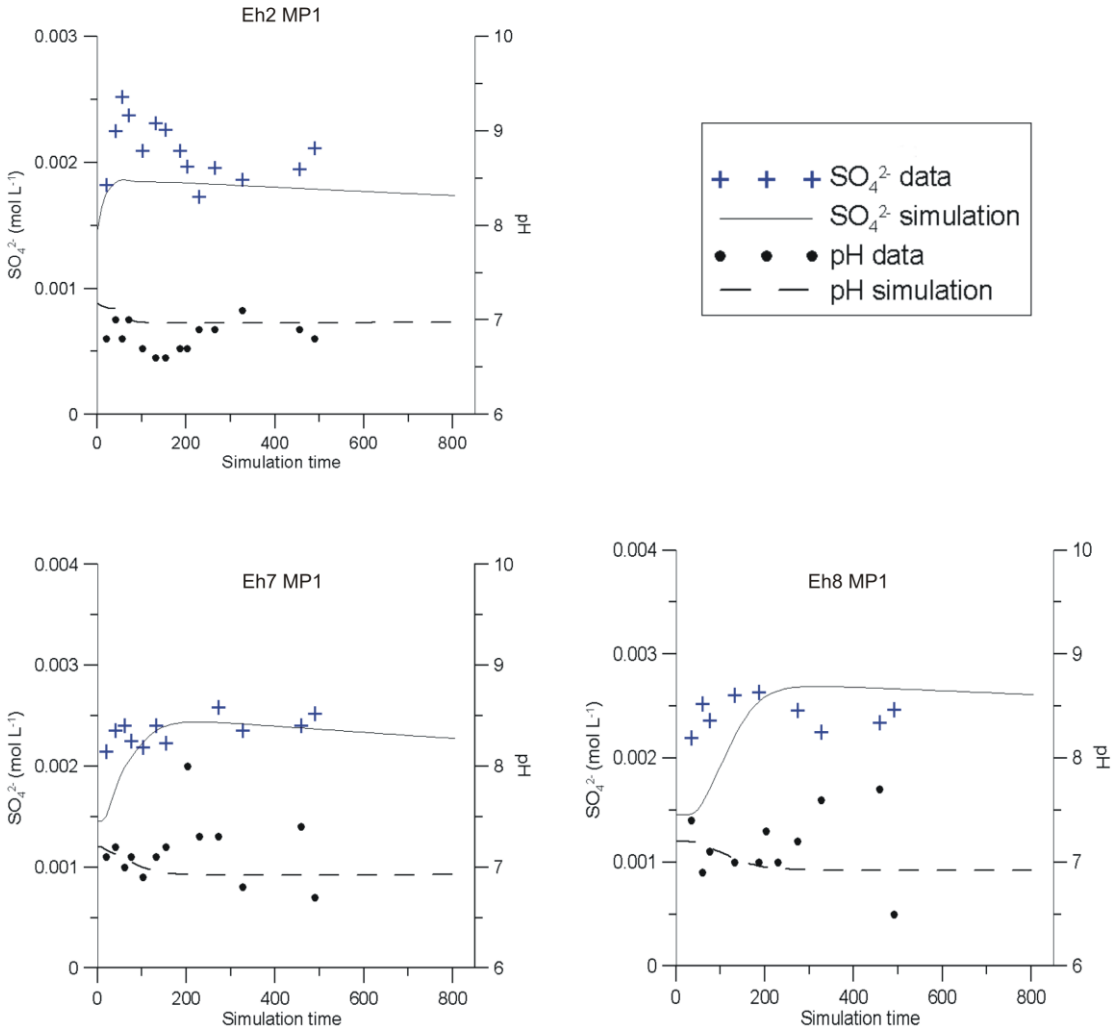

Figure 5.13 Measured and simulated SO_4^{2-} concentrations and pH at the monitoring wells Eh2 MP1, Eh7 MP1 and Eh8 MP1.

5.4.5 Model Interpretation

Reproducing dissolved O_2 concentration through the applied model is a difficult task. Although a large number of measured parameters could be reproduced by the model simulations, some inconsistencies remain which have not been solved so far. A major issue is the disagreement between the bad fit of simulated O_2 concentrations contrasting the

good fit of NO_3^-, NH_4^+ and p-TSA concentrations. How can the model reproduce concentrations of electron donors without using correct concentrations of the electron acceptor O_2? A number of reasons are assumed to be responsible for these disagreements such as the neglection of (i) 2-and 3D effects of the gas distribution, (ii) the formation of O_2 gas bubbles and its impact on the sediment permeability, (iii) the transient conditions of groundwater flow and gas injection, (iv) the heterogeneous sediment distribution or (v) the inhibition of microbial activity to elevated O_2 concentrations.

5.5 Suggestions to Optimize the IAS Remediation Measure for p-TSA

IAS systems have been in practice for several years (Ardito and Bullings, 1990) but many processes are still not well understood (Johnson et al., 2001) and therefore, in many sites the remediation technology failed to perform the expectations. At the study site, the resulting influences of the remediation technology on p-TSA concentration were unexpected and some factors can be evoked to explain the unsuccessful application of the IAS system.

5.5.1 Toxic high O_2 Concentration

As several authors report, high O_2 concentration can inhibit the microbial metabolism (Caldwell, 1965; Wszlelaki et al., 1999). The main explanation for this toxicity which gains widespread acceptance is the formation of superoxide radicals (O_2^-) that are destructive to some aspect of cell metabolism (Fridovich, 1995). Balcke et al. (2009) described how exposure of chlorobenzene-degrading microorganisms to O_2 concentration higher than 90 mg L^{-1} lead to minor degradation efficiency. Such microbial behaviour under high O_2 concentration was also shown by laboratory tests with soils and groundwater of the field site. Nitrification of NH_4^+ by bacteria was inhibited by O_2 concentration higher than 100 mg L^{-1} (Giese et al., unpublished). O_2 concentrations in the groundwater were often higher than 90 mg L^{-1} due to the injection of pure O_2 gas. Therefore, injection rates should be reduced to obtain lower dissolved O_2 concentrations. Alternatively to pure O_2 gas, air injections into the aquifer can be performed. However this possibility has to be

considered with care since incomplete nitrogen dissolution may interfere with an efficient groundwater aeration (Geistlinger et al., 2005; Balcke et al., 2008).

5.5.2 O_2 Gas Distribution

The success of gas injection for remediation strongly depends on the homogeneity of the oxygenated zone in the sediment. However, the gas distribution is controlled by the geology of the field site and by operational conditions such as injection pressure, operation mode, etc. The effect of injection rate is illustrated in Fig. 5.14 and shows that also at higher injection rates some zones of the aquifer could not be sufficiently aerated. Leeson et al. (2002), recommends a spacing of 4.5 m between injection wells in homogeneous and high permeable aquifers which is much smaller than the spacings, between 13 and 29 m, chosen at the field site.

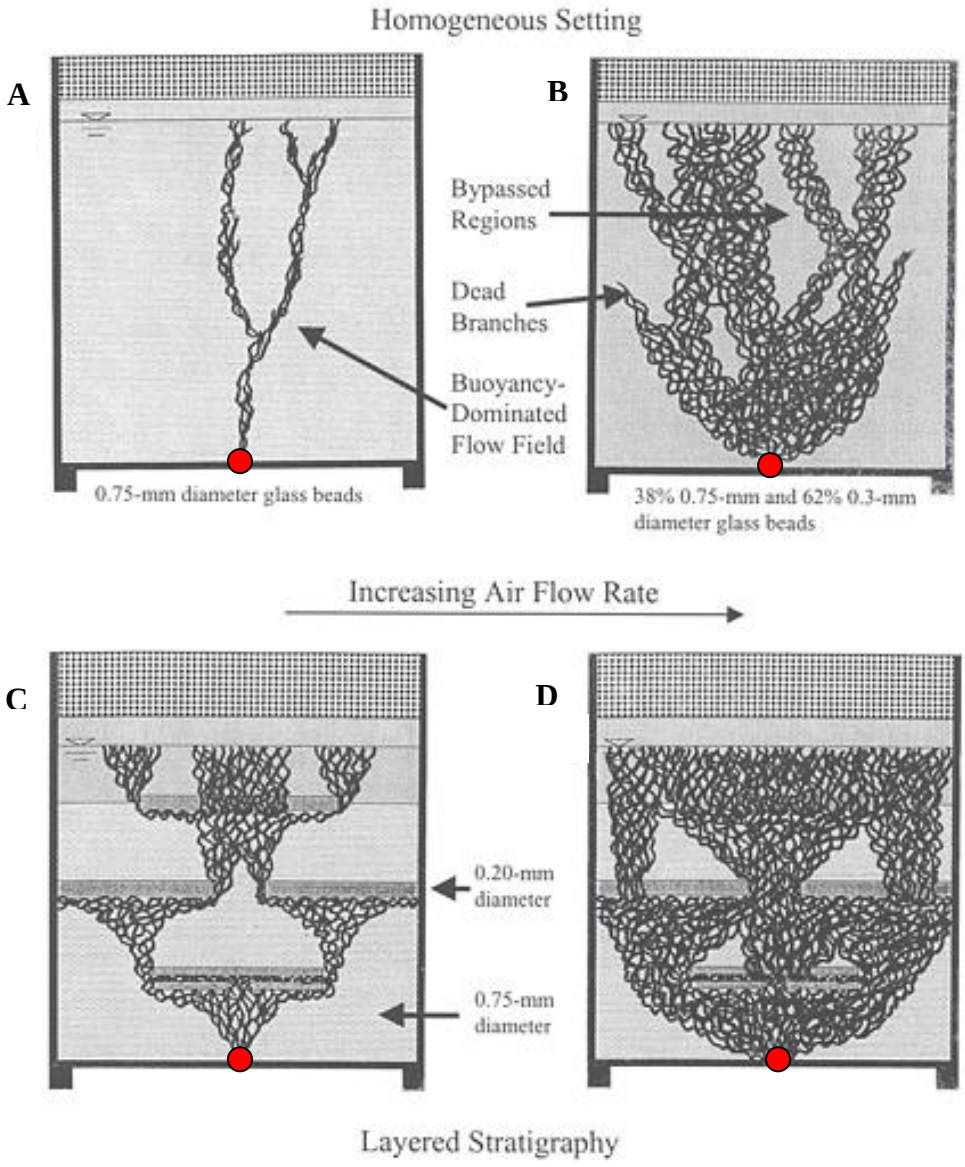

Figure 5.14 Effects of gas flow rate changes on gas distribution in two model hydrogeological settings (From Ji et al., 1993). The red circle represents the gas injection point.

5.5.3 Permeability Changes

Particle transport and the formation of gas bubbles may reduce the permeabilities and the groundwater flow through the oxidation barrier (Leeson et al., 2002). An option for reducing the possible impact of permeability reduction is to operate the IAS system in a pulsed mode, with the frequency of pulsing being linked to the groundwater flowrate and to the desired contaminant removal. However, as reported in Leeson et al. (2002), further studies of this topic are still needed.

5.5.4 Rise of the Water Table

Gas injection may lead to the vertical displacement of groundwater usually called “water table mounding” (Suthersan, 1999). A technical report on the operation of the IAS system at the study site written by the Fugro Consult GmbH Company (unpublished) described how in some points of the injection transect the water level during gas injection increased by 75 cm. The displacement of deeper and more contaminated groundwater towards the shallower portion of the aquifer can complicate the evaluation of the biodegradation rates and the comparison to groundwater collected at monitoring wells located downgradient. This can be observed at the monitoring well Eh2 (Fig. 5.15) where the Cl^- concentration of the unit OP resembled that of the MP unit indicating the rise of deeper groundwater due to gas injections. However, this phenomenon was only observed at this monitoring point.

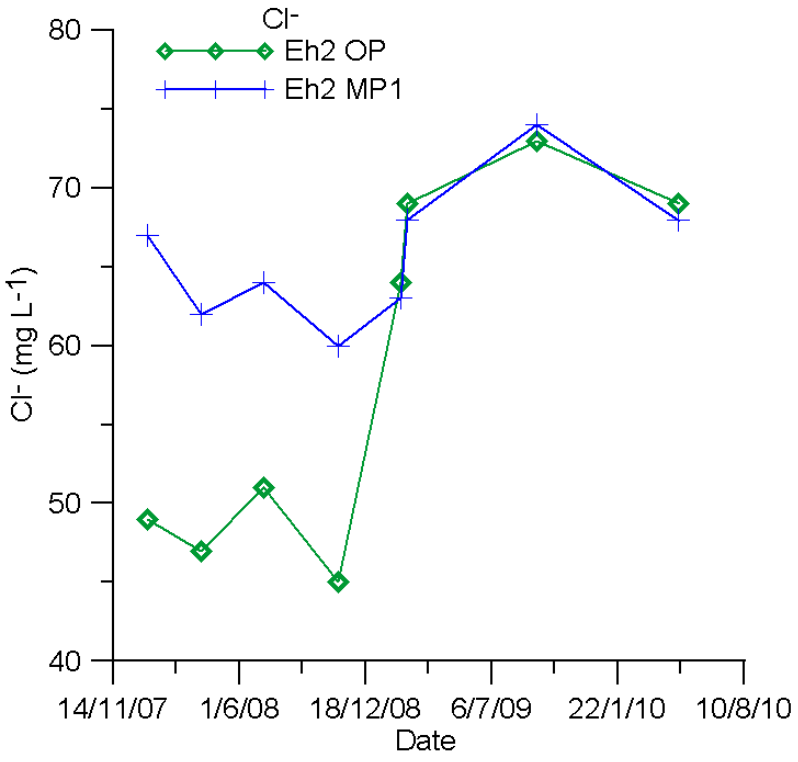

Figure 5.15 Cl^- concentration at the monitoring well Eh2 in the depositional sediment units OP and MP1.

5.5.5 Monitoring

As already mentioned, at the field site only two monitoring wells (H1 MP2 and H2 MP2, Fig. 5.2) were regularly sampled for p-TSA analysis, while p-TSA concentration was only occasionally measured at the other monitoring wells. As shown in Fig. 5.16, p-TSA concentration at the monitoring wells that were periodically sampled exhibit a strong variation. This was not observed in the other two monitoring points (Eh8 MP1 and Eh2 MP2, Fig 5.16, C and D) due to the scarcity of measurements which considerably limits the possibility of evaluating the efficiency of remediation.

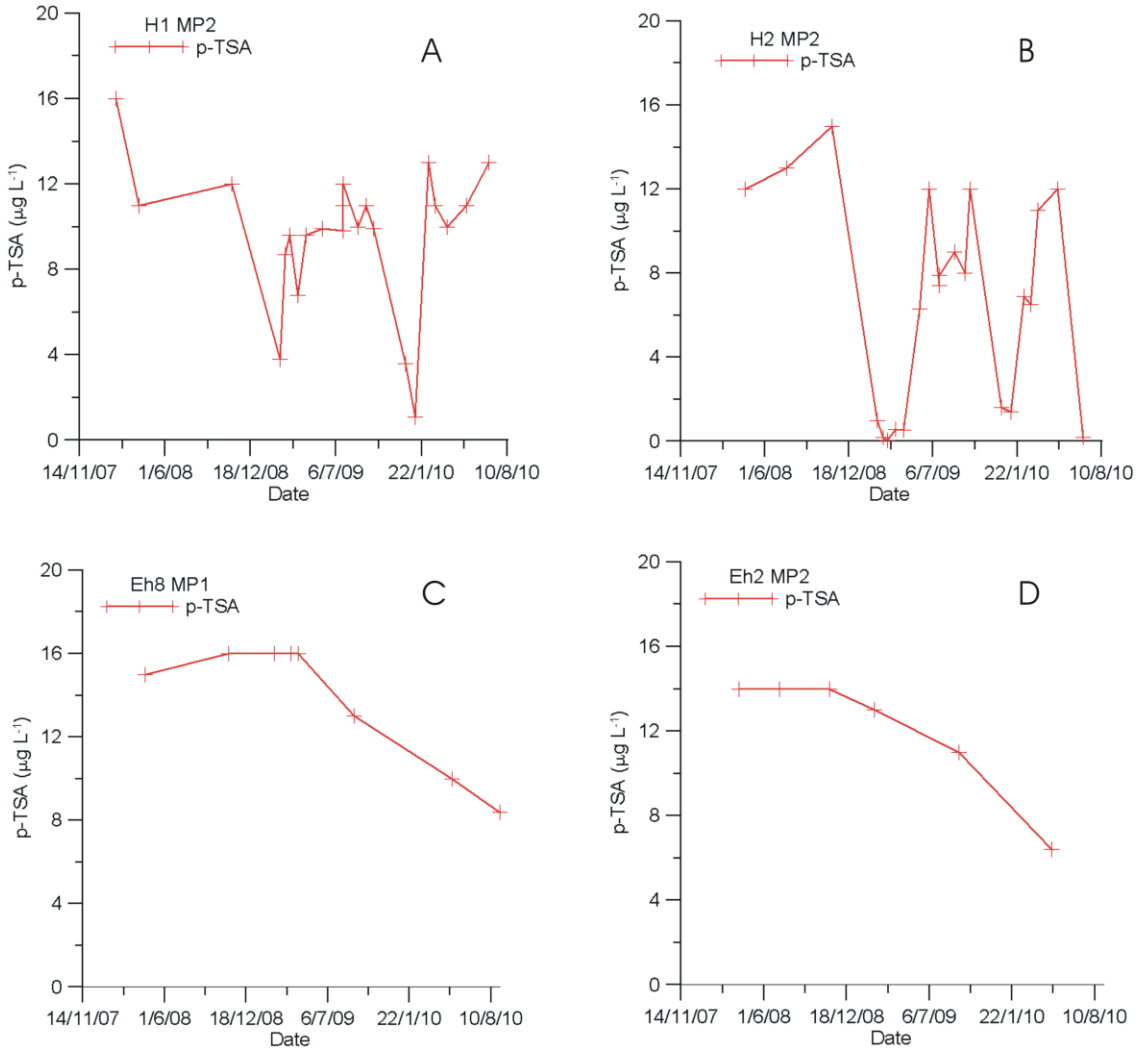

Figure 5.16 p-TSA concentration during O_2 gas sparging at: A) monitoring point H1 MP2; B) monitoring point H2 MP2; C) monitoring point Eh8 MP1; D) monitoring point Eh2 MP2.

5.5.6 Transient Flow Conditions

The flow field at the study site is extremely transient due to gas injections and to time variant abstraction rates at the well gallery A and B of the DWTP of Friedrichshagen. An abstraction well downgradient of the injection transect that constrains the groundwater to pass through the oxidation barrier and to capture the remediated groundwater is an important remediation element that should be considered when an IAS systems is applied. Transient flow conditions at the field site complicate the evaluation of the ongoing processes since groundwater flowing along different flow paths is collected at one monitoring well. An abstraction well with an appropriate pumping rate would minimize this problem. Moreover, the presence of an abstraction well forcing the groundwater to flow through the oxidation barrier would limit the lateral displacement of the groundwater due to the gas injections.

5.6 Conclusion and Outlook

During IAS operation, p-TSA and NH_4^+ were not sufficiently degraded and both compounds appeared to coexist with high concentrations of dissolved O_2. The inefficient degradation of p-TSA and NH_4^+ is mainly related to (i) inhomogeneous distribution of O_2 in the subsurface, (ii) the antiseptic effects of high O_2 concentrations and (iii) to permeability changes caused by the formation of gas bubbles. p-TSA and NH_4^+ degradation could be improved by increasing the number of injection wells to allow a more homogeneous distribution of O_2 in the groundwater. The generation of an induced hydraulic gradient through the construction of a pumping well would enhance the groundwater to flow through the oxidation barrier. Moreover, groundwater sampling should be intensified.

Modelling results show disagreement between observed and simulated dissolved O_2 concentrations. This incompatibility is due to (i) 2-and 3D effects controlling O_2 distribution, (ii) reduced microbial activity and (iii) transient flow conditions. In order to improve the simulation results, distribution of the gas bubbles and mass transfer kinetic between gas and groundwater should be considered in the model simulation. Adapted kinetics rates should be implemented to account the reduced microbial activity in the presence of high O_2 concentrations.

6 Combined Conclusions and Outlook

The present study presented a comprehensive investigation of para-toluenesulfonamide (p-TSA) behaviour (i) during drinking water treatment, (ii) under anoxic aquifer conditions and (iii) during the application of an in situ air sparging system (IAS). Field distribution of p-TSA was carefully studied in order to understand transport mechanisms that control its displacement in the aquifer. Through different methods applied at different scales a better understanding of the fate of p-TSA was achieved. In the following, the main results of the four sections covered by this study will be summarized. In addition, some suggestions for further investigations and open issues concerning p-TSA will be given in the outlook section.

6.1 Modelling of p-TSA Removal during Rapid Sand Filtration

- Degradation rate constants for p-TSA removal during rapid sand filtration range between 10^{-3} and 10^{-2} s^{-1}. These determinations were previously not available in the literature.
- Higher degradation rate constants close to the column inlet were observed. This can probably be related to a greater availability of nutrients that enhance microbial activity and microbial population.
- p-TSA degradation rate constants appear to be time variant depending on the change of the environmental conditions due to the transition between infiltration rates.
- Degradation parameters show only a minor variation when applying different infiltration rates. Therefore, an optimal infiltration rate for the removal of p-TSA during rapid sand filtration could not be defined.
- Michaelis Menten kinetics and first-order kinetics applied to reproduce experimental data reveal that Michaelis Menten kinetics is more appropriate to reproduce highly transient experimental conditions than the more simplistic linear approach.
- Some suggestions about possible improvements in the design of treatment plants for p-TSA removal are also given. First, oxic conditions are essential to maintain the observed high degradation rates. In order to avoid a variation of the degradation rate due to the adaption of microbes to new environmental conditions, the infiltration rate

should be kept constant. Finally, the filter length could be reduced to less than 1 m since the majority of p-TSA removal was observed to occur in the first 0.5 m of the column.

6.2 Investigation of p-TSA Redox Sensitivity with a Column Study and Numerical Modelling

- In the absence of O_2, p-TSA is not removed from the groundwater, confirming the observed persistence of p-TSA in the anoxic aquifer of the field site.
- Under oxic conditions, p-TSA is almost fully eliminated showing degradation rate constants increasing from 2.8E-06 to 6.15E-05 s^{-1}. As for the previous study, the time variation of the degradation rate constants could be related to the adaption of microbes to the changing redox conditions.
- The obtained degradation rate constants were far below those obtained during the rapid sand filtration experiment. The reason for this difference is related to the aquifer material used in the column experiment. This material is characterized by the presence of electron donors and by a different O_2 demand with respect to the silica sand used for rapid sand filtration.
- Results show that a remediation activity involving air/O_2 injection in the aquifer enhancing microbial activity is a suitable strategy for the removal of p-TSA.

6.3 Field Scale Studies and Modelling

- Cl^- and p-TSA show, at the field site, the same distribution pattern, indicating that p-TSA behaves as a tracer under anoxic conditions.
- High concentrations of p-TSA can still be encountered below the contamination source area as an effect of hydraulic retardation due to the presence of layers with a low permeability.
- The conservative transport behaviour of p-TSA at field scale was confirmed by a two-dimensional non reactive transport model.

- The dual-domain mass transfer approach was able to reproduce hydraulic retardation of p-TSA.
- The calibrated transport model was used for prognostic simulations yielding high p-TSA loads to be expected in the drinking water treatment plant for approximately 130 years.

6.4 Application of the IAS Technique

- The application of the in situ air sparging (IAS) system at the field site produced only limited affects on p-TSA and NH_4^+ remediation in groundwater. Although high dissolved O_2 concentrations were introduced at the injections transect, p-TSA degradation and nitrification only occurred in a few monitoring wells. At the field site, high dissolved O_2 concentrations (of about 90 mg L^{-1}) were observed together with high concentrations of p-TSA and NH_4^+.
- The reactive transport simulation was able to reproduce p-TSA, NH_4^+ and NO_3^- concentrations at the selected monitoring wells, whereas O_2 concentrations could not be fitted. This limits considerably the reliability of this initial modelling approach. The main limitations of the model are (i) the use of a 1D approach, (ii) the assumption of steady state flow conditions, (iii) disregarding of the gas phase and (iv) the toxic effect of elevated O_2 concentrations on microbial activity.
- Possible reasons for the unsuccessful application of the IAS system are the following:
    - Too high dissolved O_2 concentrations in some areas of the injection transect inhibit microbial activity;
    - The inhomogeneous distribution of the gas is responsible for insufficient O_2 supply to some areas of the oxidation barrier;
    - O_2 gas injection can reduce the aquifer permeability obstructing the groundwater flow through the oxidation barrier. Hence, the groundwater is forced to move laterally of the remediation site or below the injection areas without being remediated;
    - At the field site, the monitoring well system does not have a sufficient number of observation points. The evaluations of the IAS system based on small data suffers from large uncertainties;

- The gas injections cause local mounding of the water table therefore implying the mixing of groundwater with different contamination loads;
- Transient field conditions complicate the evaluation on the remediation activity.

6.5 Outlook

Until recently, very few studies addressed the microbiology controlling p-TSA degradation. Future research should focus on identifying the microbes responsible for p-TSA degradation and understanding their metabolism. These specific microbial data on growth and mortality rates could be incorporated in the simulations thus obtaining more reliable model approaches and management tools for remediation.

Another important scientific issue is the identification of intermediate compounds forming during p-TSA bio-degradation. The decomposition of a non toxic compound may generate products of environmental concern.

Future column studies can introduce improvements in the experimental set up. In the column experiment simulating O_2 aquifer injections (chapter 3), O_2 optodes measuring the O_2 propagation front inside the column could not be installed. Including this information would better constrain model results giving therefore more reliable estimates of p-TSA degradation rate constants under oxic conditions.

Future remediation measures require a refined dataset of p-TSA concentrations at the field site in space and time. These data are necessary to assess the reliability of reactive transport simulations.

Improvement of the IAS system operation could be achieved by undertaking a series of measures, such as the addition of injection and monitoring wells, the intensification of sampling campaigns and the generation of an hydraulic gradient that enhances the groundwater flow passing the oxidation barrier.

References

Abdel-Shafy, H., Guindi, K.A., Tawfik, N.S., 2008. Groundwater contamination as affected by long term sewage irrigation in Egypt. Efficient Management of Wastewater, 53-63.

Aivalioti, M.V., Gidarakos, E.L., 2008. In-well sparging efficiency in remediating the aquifer of a petroleum refinery site. J. Environ. Eng. Sci. 7, 71-82.

Amondham, W., Parkpian, P., Polprasert, C., Delaune, R.D., Jugsujinda, A., 2006. Paraquat adsorption, degradation, and remobilization in tropical soils of Thailand. J. of Environ. Sc. and Health part B-pesticides Food Contam.and Agricol. Waste 41 (5), 485-507.

Appello, C.A.J. and Postma D., 2007. Geochemistry, Groundwater and Pollution. A.A. Balkema Ed.; Amsterdam, The Netherlands.

Ardito, C.P., Billings, J.F., 1990. Alternative remediation strategies: The subsurface volatilization and ventilation system. In proceedings of the conference on petroleum hydrocarbons and organic chemicals in groundwater: prevention, detection and restoration, National Water Well Association, Dublin, Ohio, 281-296.

Ayotte, J.D., Argue, D.M., Mcgarry, F.J., Degnan, J.R., Hayes, L., Flanagan, S.M., Helsel, D.R., 2008. Methyl tert-butyl ether (MTBE) in public and private wells in new Hampshire: Occurrence, factor and possible implications. Environ. Sci. Technol. 42 (2), 677-684.

Balcke, G.U., Meenken, S., Hoefer, C, Oswald, S.E., 2007. Kinetic gas-water transfer and accumulation in porous media during pulsed oxygen sparging. Environ. Sci. Technol. 41, 4428-4434.

Balcke, G.U., Paschke, H., Vogt, C., Schirmer, M., 2009. Pulsed gas injection: a minimum effort approach for enhanced natural attenuation of chlorobenzene in contaminated groundwater. Environ. Pollution 157, 2011-2018.

Barry, D.A., Prommer, H., Miller, C.T., Engesgaard, P., Brun, A., Zheng, C., 2002. Modelling the fate of oxidisable organic contaminants in groundwater. Advances in Water Resources 25, 945-983.

Bass, D.H., Hastings, N.A., Brown, R.A., 2000. Performance of air sparging systems: a review of case studies. J. of Hazardous Mat. 72, 101-119.

Batt, A.L. and Aga, D.S., 2005. Simultaneous analysis of multiple classes of antibiotics by ion trap LC/MS/MS for assessing surface water and groundwater contamination. Anal. Chem. 77, 2940-2947.

Bechmann, W., Grunewald, K., 1995a. Organic pollutants in soils and substrates of the sewage farm area south of Berlin. Zeitschrift fur Pflanzenernahrung und Bodenkunde 158 (8), 543-548.

Bechmann, W., Grunewald, K., 1995b. PAH profiles in sewage farm substrates. Chemische Technik., 47 (1), 26-30.

Beljaars, P.R., Vandijk, R. and Brands, A., 1994. Determination of p-toluenesulfonamide in ice-cream by combination of continuous-flow and liquid-chromatography-summary of collaborative study. J. AOAC Int., 77 (3), 672-674.

Bengtsson, G. and Carlsson, C., 2001a. Contribution of suspended and sorbed groundwater bacteria to degradation of dissolved and sorbed aniline. Applied Microbiology and Biotechnology 57 (1-2), 234-241.

Bengtsson, G. and Carlsson, C., 2001b. Degradation of dissolved and sorbed 2,4-dichlorophenol in soil columns by suspended and sorbed bacteria. Biodegradation, 12 (6), 419-432.

Bennett G.D. and Zheng C.M., 2002. Applied contaminant transport modeling: Theory and practice. Wiley Interscience, 621, John Wiley and Sons., New York.

Berner, R.A., 1981. A new geochemical classification of sedimentary environments. Journal of Sedimentary Petrology, 51 (2), 359-365.

BIOXWAND, 2004. Forschungs-und Entwicklungsvorhaben “Bioxwand-Entwicklung und Erprobung einer Bio-Oxidationswand im Abstrom eines hoch mit Ammonium

kontaminierten Grundwasserleiters“, ein Projekt der Berliner Wasserbetriebe, gefördert durch das Bundesministerium für Bildung und Forschung im Rahmen des BMBF-Förderprogrammes “Umweltforschung und Umwelttechnik“, Projekttraeger für Wassertechnologie und Entsorgung Forschungszentrum Karlsruhe GmbH in der Helmholtz-Gesellschaft, Foerderkennzeichen 02WT 0091, February 2004. DGFZ, Dresden (in German, unpubl.).

Blume, H.P., Horn, R., Alaily, F., Jayakody, A.N., Meshref, H., 1980. Sand cambisol functioning as a filter through long-term irrigation with wastewater. Soil Sci. 130 (4), 186-192.

Borden, R.C., Bedient, P.B., 1986. Transport in dissolved hydrocarbons influenced by oxygen-limited biodegradation. 1. Theoretical development. Water Resour. Res. 22 (13), 1973-1982.

Borden, R.C., Goin, R.T., Kao, C.M., 1997. Control of BTEX migration using a biologically enhanced permeable barrier. Ground Water Monit. & Remediat. 17 (1), 70-80.

Bosma, T.N.P., Schnoor, J.L., Schraa, G., Zehnder, A.J.B., 1988. Simulation model for biotransformation of xenobiotics and chemotaxis in soil columns. J. Contam, Hydrol. 2, 225-236.

Bosma, T.N.P., Ballemans, E.M.W., Hoekstra, N.K., Welscher, R.A.G., Smeenk, J.G.M.M., Schraa, G., Zehnder, A.J.B., 1996. Biotransformation of organics in soil columns and an infiltration area. Ground Water 34, 49-56.

Bouwer, E.J., 1992. Environmental Microbiology. Mitchell R. ed, John Wiley & Sons.

Bouwer, E.J., Zehnder, J.B., 1993. Bioremediation of organic compounds – putting microbial metabolism to work. Trends Biotechnol. 11, 360-367.

Brown, R.A., Hicks, R.J., Hicks, P.M., 1994. Use of air sparging for in situ bioremediation. In: Air sparging for site remediation. R.E. Hinchee, Ed. Lewis, Publisher, Boca Raton, Fl., 38-55.

BWB (Berliner Wasserbetriebe), 1992: Analyse der zeitlichen und räumlichen Beschaffenheitsentwicklung des Grundwassers im Einzugsgebiet des Wasserwerks Berlin-Friedrichshagen im Auftrag der Berliner Wasserbetriebe. Gesellschaft für Umwelt- und Wirtschaftsgeologie, Berlin (unpublished).

BWB (Berliner Wasserbetriebe), 1995. Simulation der Grundwasserdynamik im Einzugsgebiet der Nordgalerien des Wasserwerkes Friedrichshagen unter Berücksichtigung geplanter Sanierungsmassnahmen. Im Auftrag der Berliner Wasserbetriebe. UWG Gesellschaft für Umwelt-und Wirtschaftsgeologie mbH Berlin. (Unpublished).

BWB (Berliner Wasserbetriebe), 2000. Forschungs- und Entwicklungsvorhaben "Entwicklung eines gekoppelten Nitrifikations-Denitrifikations-Verfahrens zur In-Situ-Reinigung stark Stickstoff belasteter Grundwasserleiters". Projektträger Wassertechnologie und Schlammbehandlung Forschungszentrum Karlsruhe GmbH, DGFZ Dresden.

BWB (Berliner Wasserbetriebe), 2007. http://www.bwb.de.

Caldwell, J., 1965. Effects of high partial pressures of oxygen on fungi and bacteria. Nature 206, 321-323.

Chapelle, F.H., 2001. Groundwater, Microbiology and Geochemistry. John Wiley & Sons, Inc.

Chapman, S.W., Byerley, B.T., Smyth, D.A., Mackay, D.M., 1997. A pilot test of passive oxygen release for enhancement of in situ bioremediation of BTEX-contaminated ground water. Ground Water Monit. & Remediat. 17 (2), 93-105.

Chiang, H.W., Kinzelbach, W., 2001. 3-D Groundwater modeling with PMWIN. Berlin, Germany: Springer.

Comsol Multiphisics, August 2006. Earth Science Module User's Guide. Version 3.3. © Copyright 1994-2006 by Comsol Ab..

Corapcioglu, M.Y. Hossain, M.A., Hossain, M.A., 1991. Methanogenic biotransformation of chlorinated hydrocarbons in ground water. Journal of Environmental Engineering-ASCE 117 (1), 47-65.

Daughton, C.G. and Ternes, T.A., 1999. Pharmaceuticals and personal care products in the environment: Agents of subtle change?. Environ. Health Persp., 107, 907-938.

Derksen, J.G.M., Rijs, G.B.J. and Jongbloed, R.H., 2004. Diffuse pollution of surface water by pharmaceutical products. Water Sci. Technol., 49 (3), 213-221.

Donaldson, J.H., Istok, J.D., O'Reilly, K.T., 1998. Dissolved gas transport in the presence of a trapped gas phase: experimental evaluation of a two-dimensional kinetic model. Ground Water 36, 133-142.

DVWK, 1992. Grundwasseruntersuchung und Probenahme 128. Regeln zur Wasserwirtschaft-Entnahme und Untersuchungsumfang von Grundwasserproben, pp. 36. (Groundwater investigation and sampling 128. Rules for water sampling and analysis of groundwater samples).

Engelmann, F., Remus, W., Roscher, C. and Voigt, I., 1992 (unpublished). Analyse der zeitlichen und räumlichen Beschaffenheitsentwicklung des Grundwassers im Einzugsgebiet der Nordgalerien des Wasserwerkes Berlin-Friedrichshagen. UWG GmbH Berlin, Berlin.

EPA (United States Environmental Protection Agency), 2000. The history of drinking water treatments. EPA-816-F-00-006. Available on internet at: http://www.epa.gov/ogwdw/consumer/pdf/hist.pdf

Espinoza, F.P., Minsker, B.S., Golberg, D.E., 2005. Adaptive hybrid genetic algorithm for groundwater remediation design. J. Water Resour. Plan Manage 131, 14-24.

Feehley, C.E., Zheng, C., Molz, F.J., 2000. A dual-domain mass transfer approach for modeling solute transport in heterogeneous aquifers: Application to the macrodispersion experiment (MADE) site. Water Resour. Res.

Fiorenza, S., Ward, C.H., 1992. Microbial adaptation to hydrogen peroxide and biodegradation of aromatic hydrocarbons. J. of Industrial Microbiology and Biotechnology 18, 140-151.

Frederikse, H.P.R. and Lide, D.R., 1997. Handbook of Chemistry and Physics. CRC Press, Boca Raton, Florida.

Fridovich, I., 1995. Superoxide radical and superoxide dismutases. Annual Review of Biochemistry, 64, 97-112.

Fry, V.A., Selker, J.S., Gorelick, S.M., 1997. Experimental investigations for trapping oxygen gas in saturated porous media for in situ bioremediation. Water Resour. Res. 33, 2687.

Gaikowski, M.P., Larson, W.J., Steuer, J.J. and Gingerich, W.H., 2004. Validation of two dilution models to predict chloramine-T concentrations in aquaculture facility effluent. Aquatic. Eng., 30 (3-4), 127-140.

Geistlinger, H., BeckmannA., Lazik, D., 2005. Mass transfer between a multicomponent trapped gas phase and a mobile water phase: experiment and theory. Water Resour. Res. 41. W11408, doi:10.1029/2004WR003885.

Gelhar, L.W., Mantoglou, A., Welty, C. and Rehfeldt, K.R., 1985. A review of field-scale physical solute transport processes in saturated and unsaturated porous media. Rep. EA-4190, Electro. Power Res. Ins., Palo Alto Calif.

Giese, R., Engelmann, F., Ehbrecht, H., unpublished. Implementation of an in situ bubble wall for oxidation and bioremediation of an aquifer contaminated by ammonium.

Goedeke, S., Vogt, C., Schirmer, M., 2008. Estimation of kinetic Monod parameters for anaerobic degradation of benzene in groundwater. Environmental Geology, 55 (2), 423-431.

Golden Software Inc., 2002. Surfer 8.

Grathwohl, P., 2006. Long-term behaviour of organic contaminants in soil and groundwater (in German). Grundwasser 11 (3), 157-163.

Groundwater Research Institute GmbH Dresden, 2000. Prozeßuntersuchungen in verschiedenen Maßstabsebenen zur gekoppelteten in-situ Nitrifikation/Denitrifikation als Sanierungstechnologie für einen stark stickstoffkontaminierten Grundwasserleiter. (in German, unpubl.)

Grummt, T., and Dieter, H.H., 2006. Investigation report on the compound p-TSA. (in German).German Federal Environmental Agency (UBA), Bad-Elster.

Grunewald, K., 1994. Investigations of soils in the large sewage farm areas south of Berlin. Zeitschrift fur Pflanzenernahrung und Bodenkunde, 157 (2), 125-130.

Grünheid, S., Amy, G., Jekel, M., 2005. Removal of bulk dissolved organic carbon (DOC) and trace organic compounds by bank filtration and artificial recharge. Water Res. 39, 3219-3228.

Guan, J., Aral, M.M., 1999. Optimal remediation with well locations and pumping rates selected as continuous decision variables. J. Hydrol. 221, 20-42.

Hamann, E., 2009. Reaktive Stofftransportmodellierung einer urbanen Grundwasserkontamination aus einem ehemaligen Rieselfeld. Doctoral thesis, Humboldt Universität Berlin.

Hamm, S.Y., Bidaux, P., 1996. Dual-porosity fractal models for transient flow analysis in fissured rocks. Water Resour. Res. 32 (9), 2733-2246.

Haneke, K.E., 2002. Toxicological summary for chloramine-T [127-65-1] and p-toluenesulfonamide [70-55-3]. Integrated Laboratory System, (http://ntpserver.niehs.nih.gov/ntp/htdocs/Chem_Background/ExsumPdf/ChloramineT.pdf), pp. 68.

Harris, J.O., Powell, M.D., Attard, M., Green, T.J., 2004. Efficacy of chloramine-T as a treatment for amoebic gill disease (AGD) in marine atlantic salmon (Salmo salar L.). Aquac. Res., 35 (15), 1448-1456.

Haselow, J.S., Greenkorn, R.A., 1991. An experimental investigation of the effect of idealized heterogeneity on the dispersion of miscible fluids. Water Resour. Res., 27 (9), 2473-2482.

Heberer, T., 1995. Identifizierung und quantifizierung von Pestizidrückstände und Umweltkontaminanten in Grund- und Oberflächenwasser mittels Kapillargaschromatographie - Massenspektrometrie. doctoral thesis, Technische Universität, Berlin, 381 pp.

Heberer, T., Stan, H.J. 1994. N-(phenylsulfonyl)-sarcosine a new contaminant in sewage farm ground-water. Fresen. Environ. Bull., 3 (10), 639-643.

Heberer, T., Stan, H.J., 1997. Determination of clofibric acid and N-(phenylsulfonyl)-sarcosine in sewage, river and drinking water. Int J Environ An Ch, 67 (1-4), 113-123.

Heberer, T., 2002a. Occurrence, fate and removal of pharmaceutical residues in the aquatic environment: a review of recent research data. Toxicol. Lett., 131 (1-2), 5-17.

Heberer, T., 2002b. Tracking persistent pharmaceutical residues from municipal sewage to drinking water. J. Hydrol., 266 (3-4), 175-189.

Heberer, T., Massmann, G., Fanck, B., Taute, T., Dünnbier, U., 2008. Behaviour and redox sensitivity of antimicrobial residues during bank filtration. Chemosphere 73, 451-460.

Hecht, H., Kölling, M., 2002. Investigation of pyrite weathering processes in the vadose zone using optical oxygen sensors. Environ. Geol. 42, 800-809.

Henze, M., Harremoes, P., Cour Jansen, P., Jes la Cour, J., Arvin, E., 1995. Wastewater treatment, biological and chemical processes. Springer, Heidelberg, ISBN : 978-3-540-42228-0.

Hoffmann, C., Renger, M., Hajnos, M.,Sokolowska, Z., Jozefaciuk, G., Marschner, B., 1999. Reactions of sewage farm soils to different irrigation solutions in a column experiment. 1. Solid phase physicochemical properties. Z. Pflanz Bodenkunde 162 (6), 653-659.

Hoffmann, C., Böken, H., Metz, R., Renger, M., 2000. Verwendung von Geschiebemergel-Aushub zur Sicherung schwermetallbelasteter. Großflächiger Altlastenstandorte, 24. Landesumweltamt Branderburg, Potsdam.

Höhener, P., Dakhel, N., Christophersen, M., Broholm, M., Kjeldsen, P., 2006. Biodegradation of hydrocarbons vapors: comparison of laboratory studies and field investigations in the vadose zone at the emplaced fuel source experiment, Airbase Værløse. J. of Contam. Hydrol. 88 (3-4), 337-358.

Holm, P.E., Nielsen, P.H., Albrechtsen, H.J., Christensen, T.H., 1992. Importance of unattached bacteria and bacteria attached to the sediment in determining potential for degradation of xenobiotic organic contaminant in an aerobic aquifer. Appl. Environ. Microbiol. 58 (9), 3020-3026.

Holocher, J., Peeters, F., Aeschbach-Hertig, W., Kinzelbach, W., Kipfer, R., 2003. Kinetic model of gas bubble dissolution in groundwater and its implications for the dissolved gas composition. Environ. Sci. Technol. 37, 1337.

Horner, C., 2005a. Erarbeitung von Planungsunterlagen für die Pilotanlage Machnow, IGB Institut für Gewaesseroekologie und Binnenfischerei im Forschungsverbung Berlin im Auftrag der Berliner Wasserbetriebe. Berlin. (in German, unpubl.).

Horner, C., 2005b. Erarbeitung von Planungsunterlagen für die Pilotanlage Machnow (Phase 2), IGB Institut für Gewaesseroekologie und Binnenfischerei im Forschungsverbung Berlin im Auftrag der Berliner Wasserbetriebe. Berlin. (in German, unpubl.).

Horner, C., Engelmann, F., Nützmann, 2009. Model based verification and prognosis of acidification and sulphate releasing processes downstream of a former sewage field in Berlin (Germany). J. Cont. Hydrol. 106, 83-98.

Howard, D., 2004. Pesticide adsorption and half-life. Utah State University Extension.

IAEA (International Atomic Energy Agency), 1998. Application of isotope techniques to investigated groundwater pollution. IAEA Tecdoc-1046, Vienna, 1998.

IUCLID (International Uniform Chemical Information Database). Available on internet at: http://www.epa.gov/HPV/pubs/summaries/ptoluene/c15409rr2.pdf

Ji, W., Dahmani, A., Ahlfeld, D., Lin, J.D., Hill, E., 1993. Laboratory study of air sparging: air flow visualization. Ground Water Monit. Remed. Fall. 115-126.

Johnson, P.C., Johnson, R., Bruce, C.L., Leeson, A., 2001. Advances in in situ air sparging. Bioremediation J. 5 (4), 251-266.

Johnston, C.D., Rayner, J.L., Patterson, B.M., Davis, G.B., 1998. Volatilisation and biodegradation during ari sparging of dissolved BTEX-contaminated groundwater. J. Cont. Hydrol. 33, 377-404.

Jørgensen, P.R., Helstrup, T., Urup, J., Seifert, D., 2004. Modeling of non-reactive solute transport in fracturated clayey till during variable flow rate and time. J. Cont. Hydrol.

Kim, Y., 2007. Aquatic toxicity of acetaminophen, carbamazepine, cimetidine, diltiazem and six major sulfonamides, and their potential ecological risk in Korea. Environ. Int., 33 (3), 370-375.

Kim, H.S., Jaffe, P.R., 2008. Degradation of toluene by a mixed population of archetypal aerobes, microaerophiles and denitrifiers: laboratory sand column experiment and multispecies biofilm model formulation. Biotechnology and Bioengineering 99 (2), 290-301.

Kinzelbach, W., Schafer, W., Herzer, J., 1991. Numerical modeling of natural and enhanced denitrification processes in aquifer. Water Resour. Res., 27 (6), 1123-1135.

Knudsen, J.B.S., Aagaard, P., Breedveld, G., 2000. A column study on reactive transport of dissolved jet-fuel in a sandy aquifer. 1. Biodegradation and mineralization kinetics of the organic solutes. Groundwater 2000, 175-176.

Leeson, A., Johnson, P.C., Johnson, R.L., Vogel, C.M., Hinchee, R.E., Marley, M., Peargin, T., Bruce, C.L., Amerson, I.L., Coonfare, C.T., Gillespie, R.D., McWhorter, D.B., 2002. Air sparging design paradigm. Available at: http://www.cluin.org/download/contaminantfocus/dnapl/Treatment_Technologies/Air_Sparg_paradigm.pdf

Li, P.J., Stagnitti, F., Xiong, X., Peterson, J., 2009. Temporal and spatial distribution patterns of heavy metals in soils at a long-standing sewage farm. Environ. Monit. And Ass. 149 (1-4), 275-282.

Lindsey, M.E., Meyer, M.T., Thurman, E.M., 2001. Analysis of trace levels of sulfonamide and tetracycline antimicrobials in groundwater and surface water using solid-phase extraction and liquid chromatography/mass spectrometry, Anal. Chem. 73 (19), 4640–4646.

Loss, R., Wollgast, J., Huber, T and Hanke, G., 2007. Polar herbicides, pharmaceutical products, perfluorooctanesulfate (PFOS), perfluorooctanoate (PFOA), and nonylphenol and its carboxylates and ethoxylates in surface and tap waters around Lake Maggiore in Northern Italy. Anal. Bioanal. Chem., 387 (4), 1469-1478.

Mackay, D. and Shiu W.Y., 1992. Illustrated handbook of physical-chemical properties and environmental fate of organic chemicals. Vol.II. Polynuclear aromatic hydrocarbons, polychlorinated dioxins and dibenzofurans. Lewis Publishers, Boca Raton, Florida.

Magga, Z., Tzovolou, D.N., Theodoropoulou, M.A., Dalkarani, T., Pikios, K., Tsakiroglou, C.D., 2008. Soil column experiments used as a means to assess transport, sorption and biodegradation of pesticides in groundwater. Journal of Environmental Science and Health part-B Pesticides Food Contaminants and Agricultural Waste, 43 (8), 732-741.

Marley, M.C., Hazebrouck, D.J., Walsh, M.T., 1992. The application of in situ air sparging as an innovative soils and groundwater remediation technology. Ground Water Monitoring Rev. 12 (2), 137-145.

Marquis, S.A., 1994. Bioplume II: A powerful tool for bioremediation design in alluvial and periglacial paleodepositional settings. In: Proceedings of the Eighth National Outdoor Action Conference and Exposition. Dublin, OH: Ground Water Publishing Company.

Maskey, S., Jonoski, A., Solomatine, D.P., 2002. Groundwater remediation strategy using global optimization algorithms, J. Water Res. Plan Manage 128, 431-440.

Massmann, G., Greskowiak, J., Dunnbier, U., Zuehlke, S., Knappe, A., Pekdeger, A., 2006. The impact of variable temperatures on the redox conditions and the behavior of pharmaceuticals residues during artificial recharge. J. Hydrol. 328, 141-156.

Massmann, G., Dünnbier, U., Heberer, T., Taute, T., 2008. Behaviour and redox sensitivity of pharmaceuticals residues during bank filtration- Investigation of phenanzone-type residues. Chemosphere, 71 (8), 1476-1485.

McDonald, M.G., Harbaugh, A.W., 1998. A modular three-dimensional finite-difference groundwater flow model. U.S. Geological Survey Techniques of Water Resources Investigations, Book 6, 586.

Meffe, R., Massmann, G., Kohfahl, C., Taute, T., Richter, D., Dünnbier, U., Pekdeger, A., (submitted 2010a). Investigating the redox sensitivity of para-toluenesulfonamide (p-TSA) with a column study. Submitted to Environmental Earth Sciences

Meffe, R., Kohfahl, C., Hamann, E., Massmann, G., Dünnbier, U., Pekdeger, A., (submitted 2010b). Fate of para-toluenesulfonamide (p-TSA) in groundwater under anoxic conditions: Modelling results from a field site in Berlin (Germany). Submitted to Science of the Total Environment.

Meffe, R., Kohfahl, C., Holzbecher, E., Massmann, G., Richter, D., Dünnbier, U., Pekdeger, A., 2010. Modelling the removal of p-TSA (para-toluenesulfonamide) during rapid sand filtration used for drinking water treatment. Water Res. 44 (1), 205-213.

Meinertz, J.R., Schmidt, L.J., Stehly, G.R. and Gingerich, W.H., 1999. Liquid chromatographic determination of para-toluenesulfonamide in edible fillet tissues from three species of fish. J. AOAC Int., 82 (5), 1064-1070.

Michaelis, L., Menten M.L., 1913. The kinetics of the invertase activity (in German). Biochem. Z., 49, 333-369.

Miotlinski, K., 2008. Coupled reactive transport modeling of redox processes in a nitrate-polluted sandy aquifer. Aquat. Geochem. 14, 117-131.

NIDESI, 2000. Forschungs-und Entwicklungvorhaben “Entwicklung eines gekoppelten Nitrifikations-Denitrifikations-Verfahrens zur In-Situ-Reinigung stark Stickstoff belasteter Grundwasserleiter“, Kurztitel „NIDESI“. Ein Projekt der Berliner Wasserbetriebe, gefoerdert durch den Bundesminister für Bildung und Forschung im Rahmen des BMBF-Foerderprogrammes „Umwelforschung und Umwelttechnik“

Projekttraeger Wassertechnologie und Schlammbehandlung Forschungszentrum Karlsruhe GmbH, DGFZ, Dresden (in German, unpubl.).

OECD (Organization of Economic Co-operation and Development), 1994. Screening information data set for high production volume chemicals. Vol.2, UNEP Chemicals, 28.

Oswald, S.E., Griepentrog, M., Schirmer, M., Balcke, G.U., 2008. Interplay between oxygen demand reactions and kinetic gas-water transfer in porous media. Water Reas. 42, 3579-3590.

Pang, L.P., Close, M., Flintoft, M., 2005. Degradation and sorption of atrazine, hexazinone and procymidone in coastal sand aquifer media. Pest Management Science, 61 (2), 133-143.

Park, J., Chen, M.J., Kukor, J.J., Abriola, L.M., 2001. Influence of substrate exposure history on biodegradation in a porous medium. J. of Contam. Hydrol. 51 (3-4), 233-256.

Parkhurst, D., Appelo, C.A.J., 1999. PHREEQC (version 2)- A computer programm for speciation, batch-reaction, one-dimensional transport, and inverse geochemical calculations. Water Resources Investigations Report99-4259. U.S. Geological Survey, Denver, CO.

Patterson, B.M., Franzmann, P.D., Davis, G.B., Elbers, J., Zappia, L.R., 2002. Using polymer mats to biodegrade atrazine in groundwater: laboratory experiments. J. Contam. Hydrol. 54, 195-213.

Pavelic, P., Nicholson, B., Dillon P.J., Barry, K., 2005. Fate of disinfection by-products in groundwater during aquifer storage and recovery with reclaimed water. J. Contam. Hydrol. 77, 119-141.

Pholchan, P., Jones, M., Donnelly, T., Sallis, P.J., 2008. Fate of estrogens during the biological treatment of synthetic wastewater in a nitrite-accumulating sequencing batch reactor. Environ. Sci. Technol. 42, 6141-6147.

Prommer, H., Stuyfzand, P.J., 2004. Identification of temperature dependent water quality changes during a deep well injection experiment in a pyritic aquifer. Environ. Sci. & Technol. 39, 2200-2209.

Reddy, K.R., Kosgi, S., Zhou, J., 1995. A review of in situ air sparging for the remediation of VOC-contaminated saturated soils and groundwater. Hazard. Waste Hazard. Mat. 12, 97-118.

Reineke, A.K., Preiss, A., Elend, M., Hollender, J., 2008. Detection of methylquinoline transformation products in microcosm experiments and in tar oil contaminated groundwater using LC-MNR. Chemosphere 70, 2118-2126.

Richter, D., Duennbier, U., Massmann, G., Pekdeger, A., 2007. Quantitative determination of three sulfonamides in environmental water samples using liquid chromatography coupled to electrospray tandem mass spectrometry. Journal of Chromatography A, 1157 (1-2), 115-121.

Richter, D., Massmann, G., Dünnbier, U., 2008a. Identification and significance of sulphonamides (p-TSA, o-TSA, BSA) in an urban water cycle (Berlin, Germany). Water Research, 42 (6-7), 1369-1378.

Richter, D., Massmann, G., Dünnbier, U., 2008b. Behaviour of sulfonamides (p-TSA, o-TSA, BSA) during drinking water treatment Chemosphere, 71 (8), 1574-1581.

Richter, D., Massmann, G., Taute, T., Dünnbier, U., 2009. Investigation of the fate of sulfonamides downgradient of a decommissioned sewage farm near Berlin, Germany, J. Contaminant Hydrology, 106, 183-194.

Rooklidge, S.J., Burns, E.R., Bolte, J.P., 2004. Modeling antimicrobial contaminant removal in slow sand filtration. Water Reasearch, 39 (2-3), 331-339.

Sabbagh, G.J., Fox, G.A., Ma, L., 2007. Modeling pesticide fate and nonideal transport from seed treated with a slow-release pesticide in a laboratory column. Transaction of the Asabe 50 (2), 523-532.

Salanitro, J.P., Johnson, P.C., Spinnler, G.E., Maner, P.M., Wisniewski, H.L., Bruce, C., 2000. Field-scale demonstration of enhanced MTBE bioremediation through aquifer bioaugmentation and oxygenation. Environ. Sci. Technol. 34 (19), 4152-4162.

Sato, T., Kimura, Y., Takamizawa, K., 2002. Modeling transport and biodegradation of PCE in sandy soil. 1st Conference on Brownfields Site: Assessment, Rehabilitation and Development. Brownfields Site:Assessment, Rehabilitation and Development, 515-524.

Schäfer, D., Schäfer, W., Kinzelbach, W., 1998. Simulation of processes related to biodegradation of aquifers 2. Structure of 3D transport model. J. Contam. Hydrol. 31, 167-186.

Schaffner, I.R., Juneau, A.J., 1995. In-situ air sparging without nutrient amendment: an effective bioremediation strategy for treating petroleum-contaminated groundwater systems, in proceedings, The Ninth National Outdoor Action Conference, National Ground Water Association, 101-115. Available online: http://www.bioremediationgroup.org/BioReferences/Tier1Papers/insitu.htm. Accessed: December 7, 2010.

Scheytt, T., Grams, S., Asbrand, M., 2000. Grundwasserströmung und Beschaffenheit unter dem Einfluss 100-jähriger Rieselfeldwirtschaft. Wasser and Boden.

Schenk, R., 1995. Zum aktuellen Stand der bodenkundlichen und hydrogeologischen Untersuchungen im Forschungsprojekt " Rieselfelder südlich Berlins", Landesumweltamt Brandenburg, Potsdam.

Schultz, H.D., Zabel, M.,Editors, 2006. Marine Geochemistry. Publisher Springer.

Schwab, A.P., Splichal, P.A., Banks, M.K., 2006. Persistence of atrazine and alachlor in ground water aquifers and soil. Water Air and Soil Pollut. 171, 203-235.

Schwarzenbach, R.P., Escher, B.I., Fenner, K., Hofstetter, T.B., Johnson, C.A., von Guten, U., Wehrli, B., 2006. The challenge of micropollutants in aquatic systems. Sci. 313, 1072-1077.

Serapiglia, S., 2002. Effect of physical parameters on the biodegradation of the ammonium contamination plume at the Osterhofen site: two and three dimensional simulations. Ph.D. dissertation, Department of Applied Environmental Geology, University of Tuebingen.

Sensatec, 2009. Zum Stand der Arbeiten and der Piloranlage Krummendammer Heide. Annual Report (in German).

Senstadt, 2007. Environmental Atlas. New Groundwater Formation. Urban and Environmental Information System (UEIS). Berlin Department for Urban Development. http://www. Stadtentwicklung.berlin.de/umwelt/umweltatlas/karten/pdf/e02_17_2005.pdf

Siebe, C., Fisher, W.R. 1996. Effect of long-term irrigation with untreated sewage effluents on soil properties and heavy metal adsorption of Leptosols and Vertisols in Central Mexico. Zeitschrift für Pflanzenernahrung und Bodenkunde 159 (4), 357-364.

Smail, D.A., Grant, R., Simpson, D., Bain, N., and Hastings, T.S., 2004. Disinfectants against cultured Infectious Salmon Anaemia (ISA) virus: the virucidal effect of three iodophors, chloramines-T, chlorine dioxide and peracetic acid/hydrogen peroxide/acetic acid mixture. Aquaculture, 240 (1-4), 29-38.

Stempvoort, D.R.V., Armstrong, J., Mayer, B., 2007. Microbial reduction of sulfate injected to gas condensate plumes in cold water. J. Contam. Hydrol. 92 (3-4), 184-207.

Soares, A., Guieysse, B., Jefferson, B., Cartmell, E., Lester, J.N., 2008. Nonylphenol in the environment: a critical review on occurrence, fate, toxicity and treatment in wastewaters. Environ. Intern. 34 (7), 1033-1049.

Suthersan, S.S., 1999. In situ air sparging. Remediation engineering: design concepts. Ed. Suthan S. Suthersan, CRC Press LLC, Boca Raton.

Ternes, T.A., Joss, A., Siegrist, H., 2004. Scrutinizing pharmaceuticals and personal care products in wastewater treatment. Environ. Sci. Technol. 38, 392A-399A.

Ternes, T., 2007. Occurrence of micropollutants in the aquatic environment: a new challenge for water management. Water Sci. Technol. 55 (12), 327-332.

Toride, N., Leij, F.J., van Genuchten, M.Th., 1999. The CXTFIT code for estimating transport parameters from laboratory or field tracer experiments. U.S. Salinity Lab., Agric. Res. Service, US Dep. Of Agric., Research Report No. 137, Riverside, CA.

Tsai, Y.J., 2008. Air distribution and size changes in the remediated zone after air sparging for soil particle movement. J. Hazard. Mat. 158, 438-444.

Tuxen, N., Reitzel, L.A., Albrechtsen, H.J., Bjerg, P.L., 2006. Oxygen-enhanced biodegradation of phenoxy acids in ground water at contaminated site. Ground Water 44, 256-265.

Ulrich G.A., Suflita, J., 2002. Enhancement of microbial sulfate reduction for the remediation of hydrocarbon contaminated aquifer-a laboratory and field scale project-final report executive summary, Epa agreement number: R827015-01-0, University of Oklahoma, Tulsa. Available at: http://ipec.utulsa.edu/14.d/14_FinalRev.pdf.

van Genuchten, M.Th., Wierenga, P.J., 1977. Mass transport studies in sorbing porous media .2 Experimental evaluation with tritrium (^3H_2O). Soil Science Society of America Journal 41, 272-278.

van Haperen, A.M., van Velde, J.W., van Ginkel, C.G., 2001. biodegradation of p-toluenesulphonamide by a Pseudomona sp. FEMS Microbiology Letters 204, 299-304.

Vulava, V.M., Perry, E.B., Romanek, C.S., Seaman, J.C., 2002. Dissolved gases as partitioning tracer for determination of hydrogeological parameters. Environ. Sci. Technol. 36 (2), 254-262.

Wilson, R.D., Mackay, D.M., Scow, K.M., 2002. In situ MTBE biodegradation supported by diffusive oxygen release. Environ. Sci. Technol. 36 (2), 190-199.

Wszlaki, A., Shimshon, B.Y., Mitcham, B., 1999. Do high oxygen atmospheres control postharvest decay of fruits and vegetables? Perishables handling Quaterly Issue 99, 22-25.

Wu-Seng, L., 1993. Water quality modeling. CRC Press, Inc.

Xu, J., Wu., L., Chang, A., Zhang, Y., 2010. Impact of long-term reclaimed wastewater irrigation on agricultural soils: a preliminary assessment. J. Hazard. Mater. 183 (1-3), 780-786.

Yu. J.T., Bouwer, E.J., Coelhan, M., 2006. Occurrence and biodegradability studies of selected pharmaceuticals and personal care products in sewage effluent. Agricultural Water Management, 82 (1-2), 72-80.

Zheng, C., Wang, P.P., 1999. MT3DMS: A modular three-dimensional multispecies transport model for simulation of advection, dispersion, and chemical reactions of contaminations in groundwater system; documentation and user's guide SERDP-99-1. U.S. Army Corps of Engineers, Washington, DC.

Appendix

A1

```
TITLE Equilibrate infilling solution Analysis EH1 MP1 of Feb 09

SOLUTION_MASTER_SPECIES
    Paratol         Paratol           0     171.212         171.212
    Amm             AmmH+             0     Amm             14.0067

SOLUTION_SPECIES
H2O + 0.01e- = H2O-0.01
    log_k     -9
Paratol = Paratol
    log_k     0
AmmH+ = AmmH+
    log_k     0
    -gamma    2.5 0
AmmH+ = Amm + H+
    log_k     -9.252
    delta_h   12.48 kcal
    -analytical_expression 0.6322 -0.001225 -2835.76 0 0
AmmH+ + SO4-2 = AmmHSO4-
    log_k     1.11

EXCHANGE_SPECIES
X- = X-
log_k 0.0
AmmH+ + X- = AmmHX
log_k 0.6
-gamma 2.5  0.0
delta_h  -2.4   # Laudelout et al., 1968

SOLUTION  1
units   mg/l
Temp        10.0
pH          7.7
pe          2
Amm         17.1
N(5)        0
Ca          135
C(4)        5.6  mmol/l
Mg          13.2
Na          45
K           15
S(6)        140  as SO4-2
Cl          75    charge
Fe          5
Mn          0.63
Paratol     11 ug/l

EQUILIBRIUM_PHASES 1
    Calcite   0 1.56
    CO2(g)    -1.84 10
    Fe(OH)3(a) 0 0
    Pyrolusite 0 0
    Rhodochrosite 0 0
```

```
EXCHANGE  1
X  0.1100E-01
-equilibrate with solution 1

SELECTED_OUTPUT
    -file                 Equi_infilling_solution.dat
    -high_precision       true
    -reset                false
    -ph                   true
    -pe                   true
    -totals               Ca  Mg  Na  K  Fe(2)  Fe(3)  Mn
                          S(6)  S(-2)  C(4)  O(0)  N(5)  N(3)  Cl
                          Amm
    -molalities           HCO3-
    -equilibrium_phases   Fe(OH)3(a)  Pyrolusite  Rhodochrosite  Calcite


END
```

A2

```
##############
#DATABASE D:\Program Files\USGS\Phreeqc Interactive 2.15.0\phreeqc.dat
##############
TITLE modeling the application of the IAS system
******************
SOLUTION_MASTER_SPECIES
    Paratol        Paratol          0     171.212         171.212
    Amm            AmmH+            0     Amm             14.0067
    Orgc           Orgc             0.0   Orgc            30.0

SOLUTION_SPECIES
H2O + 0.01e- = H2O-0.01
    log_k     -9
Paratol = Paratol
    log_k     0
AmmH+ = AmmH+
    log_k     0
    -gamma    2.5 0
AmmH+ = Amm + H+
    log_k     -9.252
    delta_h   12.48 kcal
    -analytical_expression 0.6322 -0.001225 -2835.76 0 0
AmmH+ + SO4-2 = AmmHSO4-
    log_k     1.11
Orgc=Orgc
     log_k     0


EXCHANGE_SPECIES
X- = X-
log_k 0.0
AmmH+ + X- = AmmHX
log_k 0.6
-gamma 2.5  0.0
delta_h  -2.4   # Laudelout et al., 1968

SOLUTION  0 Infilling solution (equilibrated)
units   mg/l
Temp        10.0
pH          7.7
pe          2
Amm         17.1
N(5)        0
Ca          135
C(4)        5.6  mmol/l
Mg          13.2
Na          45
K           15
S(6)        140    as SO4-2
Cl          75 charge
Fe          5.0
Mn          0.63
Paratol     14 ug/l
Orgc         5.2
END

USE solution 0
```

```
EQUILIBRIUM_PHASES 0
Calcite 0 1.56
Pyrolusite 0  0
Fe(OH)3(a) 0  0
Rhodochrosite 0  0
CO2(g) -1.84 10

EXCHANGE  0
X  0.1100E-01
-equilibrate with solution 0

END

SOLUTION  1-41 aquifer intial solution (same of infilling solution)
units   mg/l
Temp        10.0
pH          7.7
pe          2.0
Amm         17.1
N(5)        0
Ca          135
C(4)        5.6      mmol/l
Mg          13.2
Na          45
K           15
S(6)        140.0      as SO4-2
Cl          75  charge
Fe          5.0
Mn          0.63
Paratol     14 ug/l
Orgc         5.2

EQUILIBRIUM_PHASES 1-41
Calcite 0 1.56
Pyrolusite 0  0
Fe(OH)3(a) 0  0
Rhodochrosite 0  0
CO2(g) -1.84 10

EXCHANGE  1-41
X  0.1100E-01
-equilibrate with solution 1
Save Solution 1-41
End

EQUILIBRIUM_PHASES 1
O2(g) -0.2
Calcite 0 1.56
EQUILIBRIUM_PHASES 2-41
Calcite 0 1.56

EXCHANGE  1-41
X  0.1100E-01
-equilibrate with solution 1


RATES


Paratol
-start
```

```
10 s = TOT("Paratol")
20 mo2=TOT("O(0)")
30 IF(mo2 < 1e-7) THEN GOTO 110
35 if(mo2>1e-7 and total_time=0) then t1=0
40 if(mo2=1e-7)then t1=total_time
45 if(mo2>1e-7 and 0<total_time<=32*86400) then v_max=parm(1)
50 if(mo2>1e-7 and total_time>32*86400) then v_max=parm(2)
55 k_ms = PARM(3)
60 k_mo2 = PARM(4)
70 f1 = s/(k_ms+s)
80 f2 = mo2/(k_mo2+mo2)
90 rate = v_max*f1*f2
100 moles = rate*TIME
110 SAVE moles
-end


Amm
-start
40 ammon=TOT("Amm")
50 mo2= Tot("O(0)")
60 if(mo2>1e-7 and total_time=0) then t1=0
65 if(mo2=1e-7) then t1=total_time
70 if(mo2>1e-7 and total_time >t1+50*86400) then k_nitr=parm(1)
75 if (ammon<1e-7) then goto 130
80 if (mo2<1e-7) then goto 130
90 f1=ammon/(parm(2)+ammon)
100 f2=mo2/(parm(3)+mo2)
110 rate=k_nitr*f1*f2
120 moles=rate*time
130 save moles
-end

    Pyrite
-start
1 rem parm(1) = log10(A/V, 1/dm)    parm(2) = exp for (m/m0)
2 rem parm(3) = exp for O2          parm(4) = exp for H+  parm(5) =f2
10 if (m <= 0) then goto 200    # moles of reactant
20 ox = mol("O2")
30 nox = parm(5)*mol("NO3-")
40 if (ox <1e-7) then goto 130
50 logox=1e-10
60 if (ox>=1e-7) then logox =log10(ox)
70 if (si("Pyrite") >= 0) then goto 200
80  rate  =  -10.19  +  parm(1)  +  parm(3)*logox  +  parm(4)*lm("H+")+  \
parm(2)*log10(m/m0)
90 moles= 10^rate * time
100 if (moles > m) then moles = m
110 if (moles >= (mol("O2")/3.5)) then moles = mol("O2")/3.5
120 goto 200
130 if (nox< 1e-7) then goto 200
140 logox=1e-10
150 if (nox>=1e-7) then logox = log10(nox)
160 if (si("Pyrite") >= 0) then goto 200
170  rate  =  -10.19  +  parm(1)  +  parm(3)*logox  +  parm(4)*lm("H+")+  \
parm(2)*log10(m/m0)
175 moles= 10^rate * time
180 if (moles > m) then moles = m
190 if (moles >=(mol("NO3-")/3.0)) then moles =mol("NO3-")/3.0
200 save moles
-end
```

```
Orgc
  -start
   10 m_orgc=tot("Orgc")
   20 if (m_orgc <= 0) then goto 1000
   30 mo2=tot("O(0)")
   35 if mo2<=1e-10 then mo2=1e-10
   40 mno3=TOT("N(5)")
   45 if mno3<1e-10 then mno3=1e-10
   70 monox=mo2/(1e-6 +mo2)
   80 monno3=mno3/(1e-6 +mno3)
   120 inho2=1e-6/(1e-6 +mo2)
   160 rate = (parm(1)/86400)*monox+(parm(2)/86400)*inho2
   200 moles = rate * m_orgc * time
   210 if (moles > m_orgc) then moles = m_orgc
   1000 save moles
  -end


  Orgc_sed
-start
20  m_Orgc= TOT("Orgc")
21  mOrgc_sed= TOT("Orgc_sed")
25  mSolub_Orgc= parm(1)
30  diss_rate_const= parm(2)
35  if (m<=1e-6) then goto 200
40  rate = (diss_rate_const/86400) * (mSolub_Orgc - mOrgc)
70  moles = rate * m * time
80  if (moles > m) then moles = m
200 save moles
-end

END

KINETICS 1-41
Amm
    -formula  AmmH+  -1 O2  -2 NO3-  1
    -m        1
    -m0       1
    -parms    0.5e-009 1e-006 1e-006
    -tol      1e-008
Paratol
    -formula  Paratol  -1
    -m        1
    -m0       1
    -parms    0.38e-14 0.42e-013 1.75e-009 3e-006
    -tol      1e-008
Pyrite
    -formula  FeS2  1
    -m        0.01372
    -m0       0.01372
    -parms    1 0.67 0.5 -0.11 1
    -tol      1e-008
Orgc_sed
    -formula  Orgc  1
    -m        0.1468
    -m0       0.1468
    -parms    0.0005 1e-005
    -tol      1e-008
Orgc
    -formula  Orgc  -1 CH2O  1
```

```
    -m        0.000173
    -m0       0.000173
    -parms    0.0001 0.0001
    -tol      1e-008

-steps       1
-step_divide 1
-runge_kutta 3
-bad_step_max 500



TRANSPORT
    -cells                 41
    -shifts                82
    -time_step             847141.46 # 9.8 days
    -flow_direction        forward
    -boundary_conditions   flux flux
    -lengths               1*1.0 40*5.0
    -dispersivities        5.0
    -diffusion_coefficient 1.0e-9
    -warnings              false
    -print_cells           1-41
    -print_frequency       1
    -punch_cells           1-41
    -punch_frequency       1


SELECTED_OUTPUT
    -file                  Calcite_equi.xls
    -ph                    true
    -pe                    true
    -totals                Amm  C(4)  Fe(2)  N(3)  N(5)  N(0)  O(0)
                           Orgc  Paratol  S(-2)  S(6)  Ca
    -molalities            NO3-  O2  HCO3-
    -saturation_indices    N2(g)  CO2(g)  Calcite  Pyrite
                           Pyrochroite  Rhodochrosite  Fe(OH)3(a)
    -gases                 N2(g)
    -kinetic_reactants     Orgc_sed  Orgc  Pyrite
```

Acknowledgement

I want to thank the persons that made the development of this work possible and supported me during these long three years.

A special thank to PD. Dr. Claus Kohfahl who supported and supervised my work with valuable advices and illuminating discussions. Sincere thanks to Prof. Dr. Gudrun Massmann of the Carl von Ossietzky University of Oldenburg for her determinant contribution to this work and for being a constant source of encouragement. I also wish to thank both of them for the careful evaluation of this thesis.

I wish to express my gratitude to Prof. Dr. Asaf Pekdeger for his constructive comments during numerous discussions.

I carried out this work with the help of many people who shared with me their knowledge and their time. I would like to thank Dr. Doreen Richter of the Water Technology Center of Karlsruhe for assisting me with her experience on the subject of this thesis. I kindly thank Dr. Uwe Dünnbier of the Berlin Water Company for the interesting discussions and the valuable support. Sincere thanks to PD. Dr. Ekkehard Holzbecher of the Georg-August University of Göttingen for help in the modelling during the first part of this work. I would also like to thank Dr. Christoph Horner of the Liebniz Institute of Freshwater Ecology and Inland Fisheries of Berlin for assistance in the modelling described in chapter 5. Many thanks also to Mr. Peter Schmolke for kindly providing me with field site data. Thanks to Stephanie Warbein for her help during the column tracer test described in chapter 3.

The members of the hydrogeology working group of the Free University of Berlin constantly supported me during my work. Thanks to Dr. Thomas Taute for help in laboratory work during the column experiment and for discussions about the interpretation of data. Thanks to Dr. Enrico Hamann for the patient support and the excellent collaboration. I gratefully aknowledge Christian Menz and Liisa Paul for help in setting up the laboratory equipment. I would like to thank Gunnar Lorenzen and Christoph Sprenger for their constant encouragement to continue despite the difficulties and for their friendship that made me feel home. I thank also Ulrike Hass for help in the German translations and for the nice time spent together talking about the project and not only about that. And of course, thanks to the other members of the hydrogeology working group that created a nice

working atmosphere even during the unfriendly German winter, therefore thanks to: Johannes Birner, Andreas Winkler, Andrea Knappe, Victoria Burke, Ahmed Al-ameri, Fabien Magrí, Matthias Ricking, Ulrike Maiwald, Martin Recker, Lutz Thomas, Torsten Liedholz, Elke Heyde, Birgit Kuhlbarsch, Dietrich Lange and Achim Bartels.

My greatest thanks to Gregorio who constantly encouraged me with his extraordinary pacience, willingness and devotion.

Curriculum Vitae

For reasons of data protection,
the curriculum vitae is not included in the online version